Jour. Fac. Sci., Hokkaido Univ., Ser. IV,
vol. 17, no. 4, Aug., 1977, pp.629-694.

METAMORPHISM OF THE SAMBAGAWA AND CHICHIBU BELTS IN THE OSHIKA DISTRICT, NAGANO PREFECTURE, CENTRAL JAPAN

by

Teruo Watanabe

(with 28 text-figures, 15 tables and 4 plates)

(Contribution from the Department of Geology and Mineralogy,
Faculty of Science, Hokkaido University, No. 1493)

Abstract

Geology, structure, and metamorphism of the Sambagawa and Chichibu Belts in the Oshika district, central Japan, are studied. Both belts have suffered the Sambagawa metamorphism, resulting in mineral assemblages of high-pressure and low-temperature type.

The Sambagawa Belt is composed of various schists and greenstones with ultramafic rocks and dykes. Mafic schists in the western part of the Sambagawa Belt are considered to have been derived from reworked hyalocastite* On the other hand, mafic rocks in the eastern part of the belt have been derived mainly from pillow lava and primary hyaloclastite. The Chichibu Belt is composed of some schists and weakly metamorphosed rocks. Mafic rocks in the Chichibu Belt are meta-basalt or diabase, and primary or reworked hyaloclastite. The meta-basalts in the Chichibu Belt are higher in alkali content than those in the Sambagawa Belt.

Four folding stages are recognized in both belts. The main recrystallization occurred during the first stage of folding and retrogressive recrystallization partially proceeded during the second stage of folding. The first stage of the Sambagawa metamorphism is considered to have occurred before the diastrophism between Late Triassic and Early Jurassic.

Three zones (Zones I, II, and III) are discriminated from the Chichibu to the Sambagawa Belts. Zone II is distinguished from Zone I by the first appearance of Na-amphibole around relict clinopyroxene. Zone III is characterized by disappearance of contact paragenesis of pumpellyite – epidote. Mineral assemblages in Zone I are pumpellyite – actionolite schist facies and those in Zones II and III are transitional between the glaucophane schist facies, greenschist facies, and pumpellyite – actinolite schist facies. In the mafic rocks, appearance of Na-amphibole is controlled by Fe_2O_3/FeO ratio and MgO, whereas that of pumpellyite depends on MgO/CaO ratio besides Fe_2O_3/FeO ratio. Therefore, the above minerals can not be used as an index mineral of metamorphic zoning, without taking the bulk composition of host rock into account. The composition of actinolite with prograde metamorphism increases in Na_2O and Al_2O_3 content; that of core epidote increases in Al_2O_3 content. The analysis of mineral assemblages in mutual contact and recent data of experimental petrology suggest that the Sambagawa metamorphism occurred at 300 – 350°C and at pressures of 5 – 6 kb.

* Definition and classification of hyaloclastites in this paper are based on the proposal by Kawachi, Landis and Watanabe (1976).

Introduction

The Sambagawa and Chichibu metamorphic rocks occur in two parallel-striking belts running through Honshu, Shikoku, and Kyushu, southwest Japan, and the Chichibu Belt is distributed on the outer side (the Pacific ocean side) of the Sambagawa Belt. It has been widely recognized that the Sambagawa metamorphism characterized by high pressure – low temperature mineral assemblages, extends from the Sambagawa Belt towards the Chichibu Belt, though the two belts may be separated by a major fault (Research Group for Crystalline Schist of the Southwest Japan, 1953; Ishii et al. 1953; Seki, 1958, etc.).

The area of the present study, Oshika district, Shimoina-gun, Nagano prefecture, (35°35′N, 138°5′E), covers the northeastern portion of these two belts (Fig.1). The geological structure and metamorphism in this district are discussed on the basis of the data of geology, petrography, composition of minerals, and the analyses of mineral paragenesis.

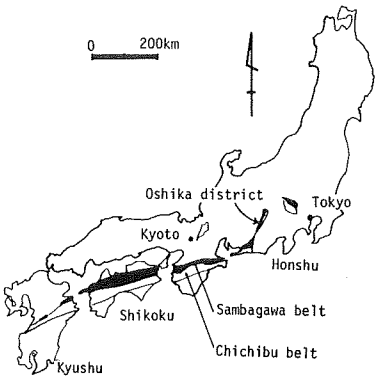

Fig. 1 Distribution of the Sambagawa and Chichibu Belts and position of the Oshika district.

Outline of Geology

The Sambagawa and Chichibu Belts run parallel in roughly N-S belts as shown in Fig.2. The boundary between the Sambagawa and Chichibu Belts has

Fig. 2 Geologic map and profile of the Sambagawa and Chichibu Belts in the Oshika district. Unshaded parts in the Sambagawa Belt show landslide deposits. 1: pelitic schists or semi-schists with minor siliceous and mafic rocks. 2: mafic schists or greenstones. 3: siliceous schists or meta-cherts with minor pelitic and mafic rocks. 4: limestones with minor pelitic, siliceous, and mafic rocks. 5: psammitic schists or semi-schists. 6: intercalation of siliceous and pelitic rocks. 6: intercalation of siliceous and pelitic rocks. 7: green-hornblende gabbros or hornblendites. 8: ultramafic rocks and associated gabbros. 9: pyroxene gabbros. 10. kaersutite gabbro. 11: Todai formation and similar rocks.

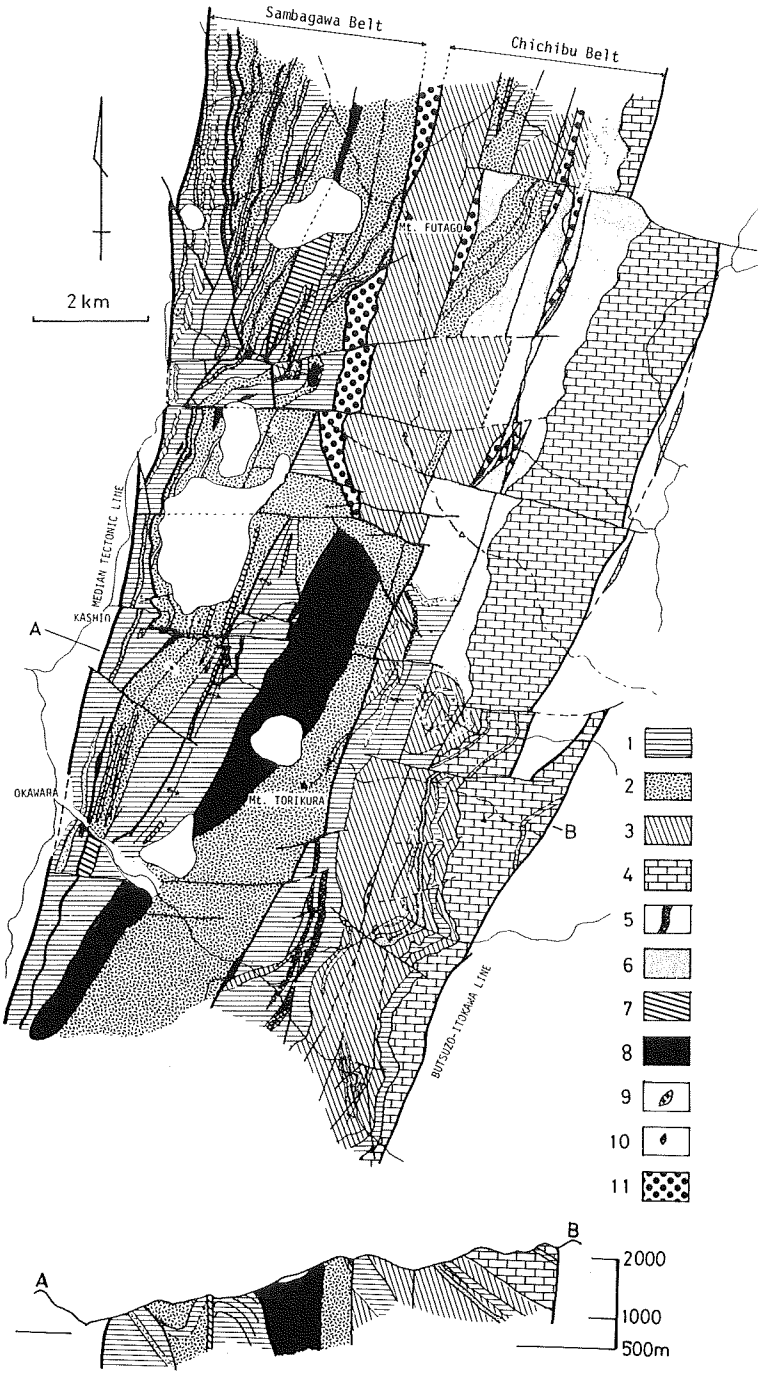
Sambagawa Belt
Chichibu Belt
Mt. FUTAGO
2 km
MEDIAN TECTONIC LINE
KASHIN
A
OKAWARA
Mt. TORIKURA
B
BUTSUZO-ITOSAWA LINE
1
2
3
4
5
6
7
8
9
10
11
A
B
2000
1000
500m

been considered to be the Todai Tectonic Zone (Matsushima et al., 1957; Watanabe, 1970). To the west of the Sambagawa Belt, the Ryoke Metamorphic Belt of high temperature – low pressure type is situated. The boundary between the Ryoke and the Sambagawa Belts is a fault, the Median Tectonic Line.

To the east of the Chichibu Belt, the Shimanto Belt is situated. The boundary between both belts is marked by a major fault, the Butsuzo-Itokawa Tectonic Line.

The Sambagawa Belt consists mainly of crystalline schists on the western side and of massive greenstones on the eastern side. The greenstones are correlated with the Mikabu green rocks occurring elsewhere in Kanto Mountains and southwest Japan. No fossils have been found in the rocks of the Sambagawa Belt of the Oshika district. It is generally believed, however, that most of the rocks of the belt are derived from Upper Paleozoic formations.

Rocks of the Chichibu Belt, which are divided into several blocks by NS and EW trending faults, consist of weakly metamorphosed mafic volcanogenic rocks, gabbro, keratophyre, pelitic and psammitic rocks, cherts and limestones. *Neoschwagerina* sp. and *Parafusulina* sp. have been reported from the Chichibu Belt near Wada, to the 25 km south of the Oshika district (Nagano Prefectural Geological Society, 1962). The occurrence of *Neoschwagerina* was also reported from a limestone boulder which is believed to have been derived from the Chichibu Belt in Shiokawa of the Oshika district (Kobayashi, 1973, p.210). Recently Triassic conodonts were found in rocks of the Chichibu Belt near Wada (Sakamoto, 1976). Therefore, the Chichibu Belt contains Permian and Triassic formations, though their relation is not clear.

In the Todai Tectonic Zone between the Sambagawa and Chichibu Belts, the Early Cretaceous Todai formation outcrops (Matsushima et al., 1957; Maeda and Kitamura, 1965; Watanabe, 1970). Moreover, in a narrow fault zone in the Chichibu Belt, there are the rocks which closely resemble to the lowest conglomerate of the Todai Formation (Maeda and Kitamura, 1965) or sandstone and slate of the Shimanto Belt. These rocks do not seen to have suffered the Sambagawa metamorphism. The Shimanto Belt, to the east of the Chichibu Belt, is composed of Upper Mesozoic – Paleogene Tertiary rocks.

Sambagawa Belt

This belt is divided into several blocks by three N-S trending faults, i.e. the Ohana-zawa fault and its southern extension, the Komotate-zawa fault and Inogaya-zawa fault, and a E-W trending fault south of Kuro-kawa. These blocks are called the Ohana-zawa, Tebiraki-zawa, Shin'nagi-zawa, Nashihara, and

Torikura-yama blocks (Fig.3). Although stratigraphical relationship among these blocks is not clear, the difference of assemblage of lithofacies among them is suggested that these blocks derived from different basins of nearly the same age.

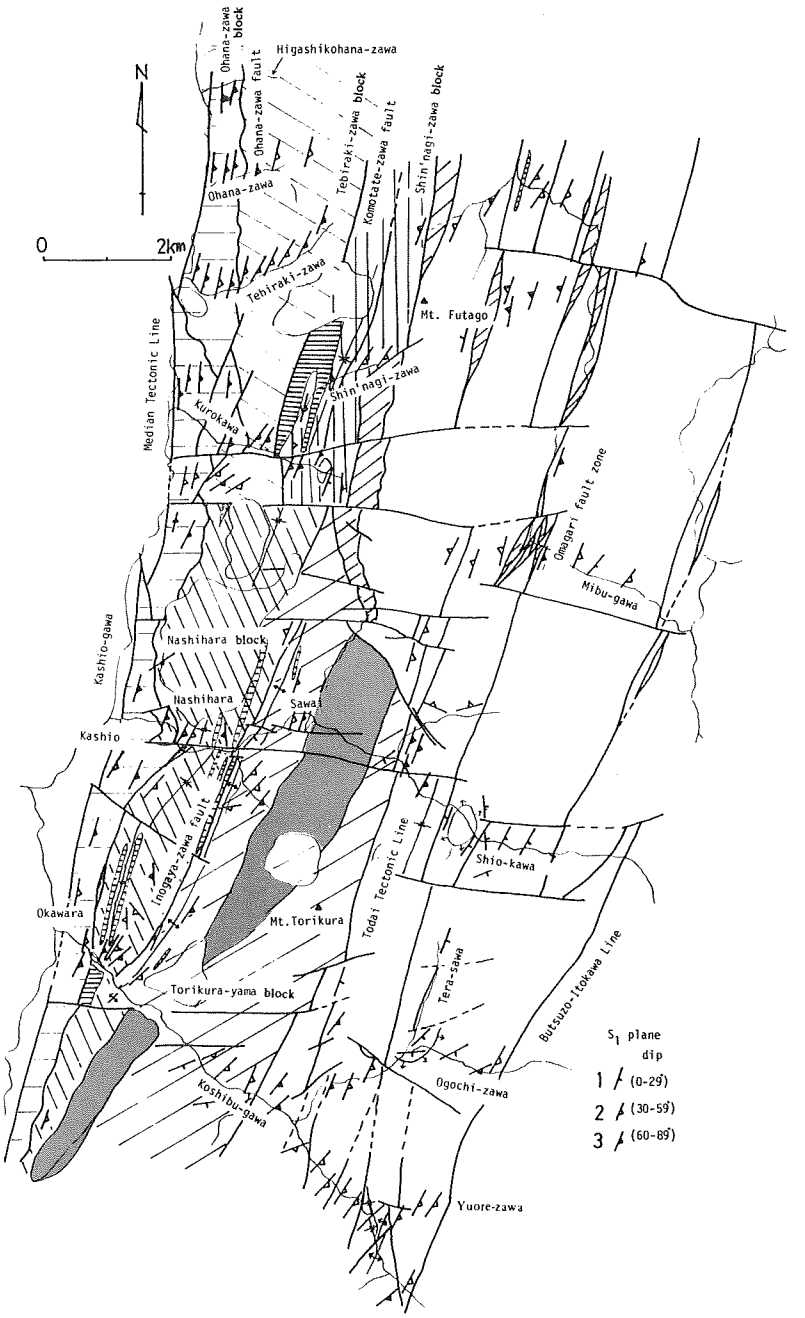

Fig. 3 Tectonic map of the Sambagawa and Chichibu Belts in the Oshika district.

Ohana-zawa block

This block is situated in the Western part of the Sambagawa Belt and composed of various schists. Most predominant lithofacies is pelitic, while mafic and acid volcanogenic, siliceous, psammitic, and calcareous schists are minor. Foliated serpentinites and small metamorphosed mafic intrusive bodies also occur is several places. Albite porphyroblasts up to 0.5 mm across, develop in all types of schists in a narrow zone (less than 100 m) immediately to the east of the Median Tectonic Line. These spotted schists are conformably overlain by non-spotted schists.

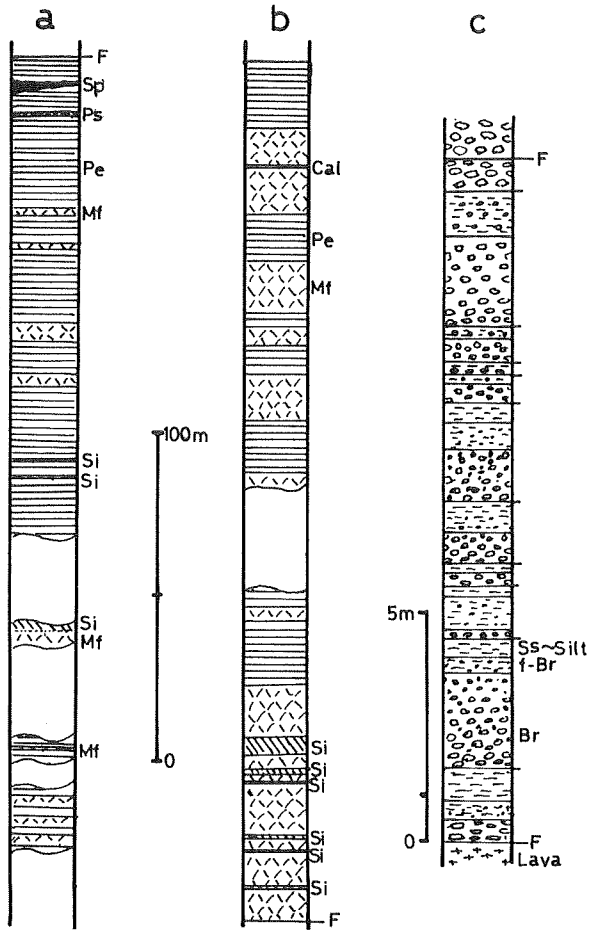

Fig. 4 Columnar sections of the formations of the Sambagawa Belt in Ohana-zawa (a), Tebiraki-zawa (b) blocks, and of cycles of sedimentation from hyaloclastic breccia to hyaloclastic siltstone at Sawai (c). F: fault, Sp: serpentinite, Ps: psammitic schist, Pe: pelitic schist, Mf: mafic schist, Si: siliceous schist, Cal: calcareous schist, Br: hyaloclastic breccia, f-Br: fine hyaloclastic breccia, Ss – Silt: hyaloclastic sandstone – hyaloclastic siltstone.

A representative columnar section in this block is shown in Fig.4a. The total thickness of the schists is about 260 m at the Ohana-zawa.

The foliated structure (S_1 plane) is parallel to the different lithofacies (= bedding plane) and well developed in mafic and pelitic schists. The foliation plane trends N-S – N30°E and dips 40° – 70° to the east. Isoclinal and tight folds as defined by Fleuty (1964) develop everywhere, and axial planes of these folds generally dip to the east. On the surface of S_1 planes, micro-corrugations and micro-folds are present and these lineations direct to N10°E – N30°E. Along the Median Tectonic Line mylonitic schists with scattered silicic layers are observed. Along the Ohana-zawa fault which is the eastern margin of this block, accordion folds are observed in pelitic schists.

Tebiraki-zawa block

The Tebiraki-zawa block is located on the north-eastern side of the Ohana-zawa block. This block is composed mainly of mafic and pelitic schists associated with minor siliceous and calcareous schists and small bodies of serpentinite and metapyroxenite. Most predominant mafic schists are finely laminated and are often intercalated with thin siliceous and calcareous schists, Some of them are micaceous blueschists. A representative stratigraphical sequence of the Tebiraki-zawa block is shown in Fig.4b. The foliation planes trend mainly N20°E – N40°E, dipping 50° – 70° to the east. As this NNE foliation direction is obliquely cut by the NS trending Ohana-zawa fault plane as shown in Fig.3, the missing horizons cut off by the fault become larger southward. The thickness of the schists is about 860 m at Tebiraki-zawa.

At the southernmost part of the block, the axial plane cleavage (S_2) of the finely laminated schist is nearly flat and the enveloping surface of S_1 is almost vertical (Plate la). This structure suggests that a part of this block correspond to an overturned limb of recumbent fold.

Shin'nagi-zawa block

This block is situated on the eastern side of the Tebiraki-zawa block. The western part of this block is occupied by complex bodies of wehrlitic serpentinite, hornblendite, and hornblende gabbro. On the east side of the ultramafic and mafic rocks, massive greenstones with pillow and hyaloclastic structures predominantly occur (Plate Ib). Several thin basaltic dykes are found in close-packed pillow lava. Some mafic schistose rocks are intercalated in the massive greenstones, and they are considered to have been derived from hyaloclastic sandstone and siltstone. The metamorphosed pillow lava and hyaloclastite preserve the original texture. The pillow lavas show diabasic or basaltic textures in the cores, and glassy or variolitic textures on the margins.

Dendritic clinopyroxene is also observed in the marginal part. The varioles attain several centimeters in diameter, and the vesicles of the pillow lavas are always less than 2 mm in diameter. Glass shard texture is observed in the hyaloclastite. These features of greenstones are also common in the Nashihara and Torikura-yama blocks. In such massive meta-hyaloclastic rocks, hematite schist and micaceous blueschist are intercalated. Pelitic schist and minor siliceous and psammitic schists also occur in this block. Some of the siliceous schists contain a few sodic amphiboles. Clinopyroxene gabbro and small serpentinite bodies are found in several places.

Anticlinal and synclinal structures are observed in this block, and the directions of these axes are about N20°E. In the greenstones of the Koseto-gorge, the northern extension of the greenstones of this zone, the thickness is over 650 m (Watanabe, Yuasa, and Makimoto, 1976).

Nashihara block

This block is situated on the eastern side of the Ohana-zawa block and on the southern side of the Tebiraki-zawa and Shin'nagi-zawa blocks. Massive greenstones associated with hornblendite, hornblende gabbro, and serpentinite are predominantly distributed in this block. Serpentinite intruding along an E-W fault at Shio-kawa is accompanied by an altered zone (talc zone?) which grades into the surrounding pelitic schists (Plate Ic). Minor pelitic and siliceous schists are also present. More than ten cycles of sedimentation from the hyaloclastic breccia to hyaloclastic siltstone are observed in an outcrop. (Fig.4c). "Pillow tongues" (Moore, 1975) are also observed. Mafic dykes which intruded subparallel to the lave flow planes are generally well recrystallized, but sometimes contain relict clinopyroxene and brown kaersutitic amphibole (TiO_2 = 3.9%).

A syncline striking about N15°E characterizes the structure of this block, and weakly metamorphosed hornblendite and hornblende gabbro have intruded parallel to the axis.

Torikura-yama block

This block is situated on the east side of the Nashihara block. In the western part of this block, pelitic schists are predominant, intercalated with thin psammitic, siliceous, and mafic and acid volcanogenic schists. An anticline trending nearly N30°E is present. At the Inogaya-zawa, a clinopyroxene gabbro has intruded into the axial part of the anticline. Talc schist is found near the anticline axis. A few dykes of hornblendite and hornblende gabbro also occur in this part. In small acidic differentiated facies of the hornblendite, sodic ferrohedenbergite is found (No.11 in Table 1).

Table 1 Chemical compositions of relict clinopyroxene and amphibole. (Analyst Y. Kawachi and T. Watanabe)

Sample No.	1 72612	2 101705	3 72813	4 80905	5 92416	6 50801	7 7072808	8 81906	9 90504	10 90310	11 72404	12 101402	13 72404	14 82407	15 72723	16 92416
SiO_2	50.74	50.70	50.60	50.38	50.28	48.97	48.60	48.40	47.90	47.10	45.86	52.05	38.30	40.88	45.65	45.25
TiO_2	0.89	0.58	0.61	1.17	0.89	0.64	0.79	1.41	1.12	2.00	3.33	0.00	6.43	5.20	3.68	2.12
Al_2O_3	2.18	2.64	2.45	4.43	4.88	5.09	4.30	4.23	5.47	4.47	6.77	2.02	13.60	11.43	7.67	8.70
FeO*	9.88	7.09	7.87	8.82	6.32	5.95	6.67	10.70	9.58	7.76	6.86	25.86	11.40	14.87	10.43	14.44
MnO	0.29	n.d.	n.d.	0.13	0.10	0.05	0.14	0.11	0.27	0.10	0.00	0.32	0.06	0.34	0.15	0.16
MgO	15.08	16.60	16.30	13.47	15.01	17.11	17.00	14.50	14.40	16.00	13.84	1.92	12.70	10.49	15.38	13.96
CaO	19.92	22.40	22.30	21.20	21.84	21.55	21.40	20.80	20.50	21.80	22.92	13.72	12.80	11.94	9.87	10.77
Na_2O	0.33	n.d.	n.d.	0.49	0.27	0.69	0.28	0.32	0.52	0.34	0.46	3.45	2.07	2.43	3.78	2.65
K_2O	0.01	n.d.	n.d.	0.01	0.02	0.01	0.01	0.00	0.01	0.00	0.00	0.00	0.79	0.65	0.37	0.13
$H_2O(+)$	-	-	-	-	-	-	-	-	-	-	-	-	2.01***	2.00	2.04	2.04
Total	99.32	100.01	100.13	100.10	99.61	100.06	99.19	100.47	99.77	99.57	100.04	99.34	98.05 (100.16)****	100.23	99.02	100.22
Si	1.91	1.88	1.88	1.88	1.86	1.82	1.82	1.82	1.80	1.78	1.72	2.08	5.67	6.12	6.70	6.66
Al^{IV}	0.09	0.12	0.11	0.12	0.14	0.18	0.18	0.18	0.20	0.20	0.28	-	2.33	1.88	1.30	1.34
	2.00	2.00	1.99	2.00	2.00	2.00	2.00	2.00	2.00	1.98	2.00	2.08	8.00	8.00	8.00	8.00
Al^{VI}	0.01	-	-	0.07	0.08	0.04	0.01	0.01	0.05	-	0.02	0.09	0.06	0.13	0.03	0.17
Ti	0.03	0.02	0.02	0.03	0.03	0.02	0.02	0.04	0.03	0.06	0.09	0.00	0.72	0.59	0.41	0.24
Fe	0.31	0.22	0.25	0.28	0.20	0.18	0.21	0.34	0.30	0.24	0.22	0.86	1.42	1.86	1.28	1.78
Mn	0.01	-	-	-.00	0.00	0.00	0.00	0.00	0.01	0.00	0.00	0.01	0.01	0.04	0.02	0.02
Mg	0.85	0.92	0.90	0.75	0.83	0.94	0.95	0.81	0.81	0.90	0.78	0.11	2.81	2.34	3.37	3.06
Ca	0.80	0.89	0.89	0.85	0.87	0.86	0.86	0.84	0.83	0.88	0.92	0.59	2.03	1.91	1.55	1.70
Na	0.02	-	-	0.04	0.02	0.03	0.02	0.02	0.04	0.02	0.00	0.23	0.60	0.70	1.08	0.76
K	0.00	-	-	0.00	0.00	0.00	0.00	0.00	0.00	0.00	0.00	0.00	0.15	0.12	0.07	0.03
	2.03	2.05	2.06	2.02	2.03	2.07	2.07	2.06	2.07	2.10	2.03	1.89	7.99	7.59	7.79	7.76
Al_z**	5	6	6	6	7	9	9	9	10	10	14					

* Total Fe as FeO

** $Al_z = Al^{IV} \times 100/2$

*** not determined but calculated on the basis of mineral formula

**** Total Fe as Fe_2O_3

In the eastern part of this block, massive greenstones and isolated ultramafic masses associated with gabbro are widely exposed (Shimazu, 1956; Iizumi, 1968, 1972). The ultramafic masses are emplaced on the western margin of the greenstones. A few other gabbroic dykes intruded in the eastern side of the greenstones. A clinopyroxene gabbro includes some xenolithic blocks of metamorphosed coarse gabbro containing Na-amphibole, epidote, chlorite, actionolite and minor amounts of relict clinopyroxene. Shear zones with talc rarely develop in the massive greenstones. The greenstones seem to trend in a NE direction and gently dip to the east. In the greenstones of the Torikura-yama block, typical pillow structure is rather scarcely developed, while fine grained, compact hyaloclastite is predominant. Doleritic fragments besides basaltic ones are found in the hyaloclastic breccia. The total thickness is over 1000 m.

Chichibu Belt

In the Chichibu Belt, the directions of the foliation planes are variable and the dips are gentle, compared with those of the Sambagawa Belt. Generally, the upper horizon of the Chichibu Belt is distributed on the eastern side. On the basis of structural features, the Chichibu Belt in this district is divided into the following three areas, i.e. Mibu-gawa area, Shio-kawa area, and Koshibu-gawa area from north to south.

Mibu-gawa area

The Omagari fault zone runs nearly in a N-S direction along the Mibu-gawa. In the western side of this fault zone, the strata trend N5°E – N40°E and dip 40° – 70° to the west. The lower horizon on this side is composed mostly of greenstones, in which graded meta-hyaloclastite characteristically occurs with minor chert and pelitic schists. The upper horizon consists mostly of chert with greenstones of hyaloclastite origin and pelitic schists. On the eastern side of the Omagari fault zone, the strata dip to the east, trending N20°E – N30°E in strike. The rocks near the fault zone are steeply dipping slate and chert. Thick limestones associated with minor hyaloclastic and siliceous rocks are to the east, dipping 30° to the east.

In the Omagari fault zone, fine conglomerate, sandstone, slate and siliceous rocks occur. They closely resemble in appearance those of the lowest part of the Todai Formation and Shimanto Belt. The southern extension of this fault zone is recognized as a fault in both areas of the Shio-kawa and Koshibu-gawa.

Shio-kawa area

This area is divided into three sub-areas by two N-S trending faults. The

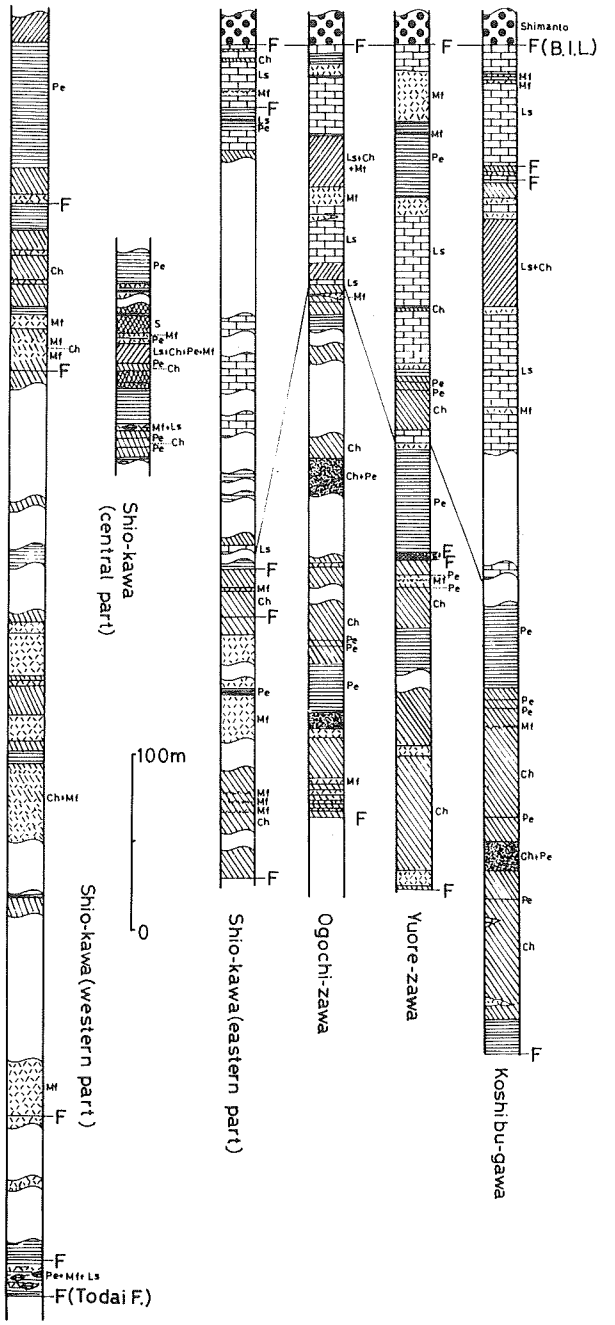

Fig. 5 Columnar sections of the formations of the Chichibu Belt in Shio-kawa and the eastern parts of Ogochi-zawa, Yuore-zawa, and Koshibu-gawa. F: fault, Todai F: Todai fault, B.I.L.: Butsuzo-Itokawa Line, Pe: pelitic rock, Ch: chert, Mf: mafic rocks, Ls: limestone, S: sandstone, Blank columnar parts show lack of outcrops.

western part has a synclinal structure, while the central part shows a dome structure. The eastern part shows a homoclinal structure dipping to the east. In the western part, pelitic, siliceous and mafic schists derived from hyaloclastite and lava, occur with minor psammitic schists. In the central part mafic hyaloclastic rocks decrease in amount. In the eastern part, limestones and siliceous schists with minor mafic and pelitic rocks are developed. *Neoschwagerina* sp. was discovered by Iwai et al. from a limestone boulder (Kobayashi, 1973; p.210). Columnar sections in the three sub-area, i.e. western, central and eastern parts, are shown in Fig.5 and their thicknesses are over 720 m, 115 m, and 470 m, respectively.

Koshibu-gawa area

This area essentially shows a monoclinal structure which trends mainly N10°E – N40°E, and dips 20° – 70° to the east. Many N-S trending faults are developed and small scale synclinal and anticlinal structures are seen in the eastern part of this area. A half dome structure plunging to the south is present near the confluence of Ogochi-zawa and Tera-sawa. The western part is composed of pelitic, psammitic and siliceous rocks and mafic metahyaloclastites. The central part is composed mainly of siliceous and pelitic rocks with minor psammitic rocks, karatophyre, gabbro, and mafic hyaloclastite. The eastern part consists of limestones with minor siliceous, pelitic, and mafic rocks. Columnar sections in the central and western parts are shown in Fig.5. The thicknesses of both strata in the central and eastern parts are over 300 m.

Todai Tectonic Zone

The Todai Formation occurs in this zone and is composed of conglomerate, sandstone, and slate. The total thickness of the formation in this district is estimated as 150 m. This formation is correlated with the Lower Cretaceous Arita series (Minato et al., 1965). Granitic boulders often occur in the conglomerate of this formation. The granitic boulders are considered to have been derived from the granite of shallow facies of the Ryoke Belt (Kano, 1961). Fragments of micaceous schist besides slate, chert and sandstone, are found in the conglomerate in the western part of the Todai Formation at Koseto-Gorge, north of this district. This micaceous schist has a mineral assemblage of quartz – alibite – white mica and is considered to have been derived from the Sambagawa Belt. The conglomeratic formation was discriminated as the Shobera Formation from the Todai Formation (Matsushima, 1973).

Origin of Mafic Volcanogenic Rocks and Submarine Volcanism

Foliated mafic schist in the Sambagawa Belt

Mafic rocks in the Ohana-zawa and Tebiraki-zawa blocks are well foliated schist. The foliated schists are thought to be of reworked hyaloclastite origin (Watanabe and Kawachi, in press) as discussed in central Shikoku (Kawachi, Landis and Watanabe, 1973 and 1976; Watanabe and Kawachi, 1975). Various foliations of different modal composition are recognized in the mafic schists. The representative foliated structure is an alternation of thin mafic and silicic layers. When calcite is abundantly contained in the silicic layer, the layer becomes coarse, up to 5 mm in thickness. When a considerable amount of epidote porphyroblast and/or ferrostilpnomelane is contained, the silicic layer becomes pale greenish yellow and/or dark brown in colour. Sedimentary units in the piles of the thick mafic schists are recognized by the boundaries between different foliated structures (Plate IId) and the presence of thin bands of siliceous schist (Plate IIe). The thickness of each sedimentary unit is generally several ~ fifty cm.

In the mafic schist with fine silicic layers, micro-grading structures up to 1.5 cm in thickness are sometimes observed. An example is shown by change of grain size of relict clinopyroxene and its alteration products (Plate IIIa). Other structures similar to grading are also recognized by change in modal composition of metamorphic minerals such as quartz, albite, actinolite and epidote as shown in Plates IIIb and c. Micro-rythmic alternation in mafic schist is also observed. Dark brown ~ opaque lamina often develop in the foliated mafic schists. These lamina are extremely mafic in composition and often show high TiO_2 content (Table 2). Some of them resemble amphibole in composition.

Table 2 Chemical compositions of brown ~ opaque parts in mafic schist (sample No.71907).

No.	1	2	3	4	5	6	7	8
SiO_2	28.93	30.30	45.78	48.87	50.93	51.14	51.97	52.09
TiO_2	12.30	10.92	0.06	8.42	4.88	2.07	0.76	0.60
Al_2O_3	11.33	13.17	8.92	11.70	9.50	18.10	3.95	3.62
FeO	11.88	13.19	13.94	7.06	6.65	7.04	10.83	11.13
MnO	0.20	0.15	0.20	0.10	0.11	0.12	0.17	0.20
MgO	12.65	13.93	12.88	8.48	8.47	7.43	16.74	16.33
CaO	10.35	7.78	12.19	10.52	14.59	5.02	11.26	12.02
Na_2O	0.14	0.12	1.45	4.03	2.30	5.79	0.85	1.08
K_2O	0.04	0.03	0.18	0.06	0.10	0.02	0.13	0.12
Total	87.82*	89.69	95.90	99.24	97.53	96.73	96.86	97.19

* Lacking of total value is assumed to be mainly $H_2O(+)$. Beam size of EPMA is about ten microns in the analysis.

Table 3 Bulk chemical compositions of mafic rocks and micaceous greenschists.

Sample No.	1 73102	2 72404	3 82912	4 72812	5 72805	6 72726	7 90310	8 93007	9 Shioyu	10 101602	11 5080101
SiO_2	44.02	45.34	45.70	42.20	46.95	46.75	44.16	41.94	43.82	41.03	42.73
TiO_2	2.84	2.82	1.62	1.20	1.46	1.10	1.03	0.60	2.50	0.47	1.19
Al_2O_3	18.12	17.78	17.04	17.44	16.79	15.67	7.92	11.53	16.00	17.51	9.52
Fe_2O_3	2.12	3.31	2.72	6.61	4.47	5.25	3.55	4.13	1.50	2.04	7.22
FeO	8.69	8.56	7.89	6.82	7.67	8.28	9.08	6.84	8.80	11.01	7.03
MnO	0.14	0.11	0.27	0.10	0.11	0.13	0.14	n.d.	0.12	n.d.	n.d.
MgO	5.47	4.45	5.75	6.83	6.09	6.67	17.69	13.61	8.36	9.21	14.62
CaO	7.30	7.38	11.46	13.75	9.94	9.95	10.95	13.92	11.76	9.65	11.25
Na_2O	3.69	5.25	3.40	2.20	3.36	3.06	0.53	1.13	4.81	2.54	1.45
K_2O	1.59	1.26	0.90	0.14	0.24	0.42	0.28	0.15	0.88	0.40	0.14
P_2O_5	0.16	0.19	0.11	0.08	0.04	0.05	0.09	n.d.	0.07	n.d.	n.d.
$H_2O(+)$	5.18	3.35	2.64	2.01	2.78	2.76	3.80	5.51	1.12	5.35	4.77
$H_2O(-)$	0.40	0.09	0.22	0.09	0.14	0.23	0.24	0.11	0.02	0.20	0.14
Total	99.72	99.89	99.72	99.47	100.04	100.32	99.46	99.47	99.76	99.41	100.06

Sample No.	12 82011	13 82227	14 82225	15 82217	16 72601	17 51111	18 90404	19 53101	20 72810 III	21 72810 III
SiO_2	48.54	45.14	46.30	43.01	47.08	47.11	63.65	60.18	49.10	41.67
TiO_2	0.70	1.53	0.82	1.01	0.73	1.16	0.40	0.81		
Al_2O_3	15.21	14.45	11.98	16.83	15.47	17.59	13.90	12.49		
Fe_2O_3	3.85	5.55	6.56	3.18	1.57	4.38	2.31	3.34		
FeO	7.66	8.87	7.25	9.73	8.55	6.21	5.10	5.31		
MnO	n.d.	0.21	n.d.	0.13	0.06	0.12	0.36	0.17		
MgO	6.91	7.81	12.00	9.76	12.59	7.33	3.62	4.08		
CaO	8.36	8.04	7.99	7.32	5.91	3.78	5.33	3.91		
Na_2O	3.44	2.56	2.73	2.29	2.91	5.07	2.17	2.30	4.54	3.40
K_2O	0.03	0.37	0.90	0.72	0.13	3.31	1.12	2.83	0.08	0.11
P_2O_5	n.d.	0.17	n.d.	0.13	0.04	0.04	0.09	0.08		
$H_2O(+)$	4.42	4.26	2.99	4.79	4.59	2.96	1.19	3.64	2.96	5.59
$H_2O(-)$	0.10	0.16	0.14	0.12	0.36	0.36	0.08	0.06	0.10	0.22
Total	99.22	99.12	99.66	99.02	99.99	99.42	99.32	99.20		

1 Calcite-quartz-albite-chlorite semi-schist (Yuore-zawa, Zone I)
2 Titanaugite-kaersutite meta-gabbro (Ogochi-zawa, Zone I)
3 Quartz-albite-epidote-actinolite-chlorite rock (relic Ca-pyroxene) (Shio-kawa, Zone I)
4 Quartz-albite-Na-amphibole-chlorite-epidote-actinolite rock (Koshibu-gawa, Zone II)
5 Pumpellyite-quartz-albite-actinolite-epidote-chlorite rock (Koshibu-gawa, Zone II)
6 Epidote-chlorite-actinolite rock (Koshibu-gawa, Zone II)
7 Chlorite-actinolite rock (relic Ca-pyroxene) (Shio-kawa, Zone II)
8 Chlorite-actinolite rock (relic Ca-pyroxene (Kuro-kawa, Zone III)
9 Jadeite-pumpellyite bearing meta-diabase (Shio-kawa, Zone II)
10 Epidote-chlorite-actinolite rock (relic Ca-pyroxene) vein Part: chlorite-pumpellyite-aegirine-augite-albite (Nashihara, Zone II)
11 Na-amphibole-aegirine-augite-chlorite-epidote-actinolite rock (relic Ca-pyroxene) (Shio-kawa, Zone II)
12 Calcite-quartz-albite-pumpellyite-chlorite-actinolite schist (Kuro-kawa, Zone III)
13 Quartz-calcite-albite-Na-amphibole-chlorite-epidote-actinolite schist (Tebiraki-zawa, Zone III)
14 Quartz-albite-chlorite-epidote-actinolite schist (Tebiraki-zawa, Zone III)
15 Quartz-albite-calcite-Na-amphibole-chlorite-epidote-actinolite schist (Tebiraki-zawa, Zone III)
16 Calcite-quartz-albite-epidote-actinolite-chlorite schist (Koshibu-gawa, Zone III)
17 Quartz-albite-calcite-white mica-Na-amphibole schist (Ito-zawa, Ichinose) collected by Y.Kawachi
18 Garnet-quartz-calcite-chlorite-epidote-albite-white mica-actinolite schist (Kuro-kawa, Zone III)
19 Actinolite calcite-quartz-epidote-chlorite-albite-white mica (Mizoguchi, Ichinose)
20 Epidote actinolite-chlorite rock (relic clino-pyroxene) (Aoki, Zone II)
21 ditto.

The grain size of metamorphic minerals in these schists is fine compared with that in the schists having abundant silicic layers.

Blueschists associated with hematite schist and siliceous schist are sometimes contained in the well foliated mafic schists. The blueschist contains sometimes a considerable amount of white mica and its bulk composition is markedly different from other mafic schists (No.17 in Table 3). $Na_2O + K_2O$ is very high and CaO is low, and Fe_2O_3/FeO is relatively high. In other cases, bulk composition of the blueschist in Kami-Ina, north of the Oshika district, is similar to the radiolarian mudstone with Cyprus umber (Watanabe, Yuasa and Makimoto, 1976). The radiolarian mudstone and umber in Cyprus are interpreted as precipitates in late stages of submarine volcanism (Robertson and Hudson, 1973). Accordingly, the above blueschists having unique bulk chemical composition may have been derived from similar precipitates.

Greenstones of the Sambagawa Belt

Bulk compositions are listed in Table 3 and are shown in a diagram of $Na_2O - H_2O(+)$ for testing the secondary change in chemical composition (Fig.6a). Recently Na_2O enrichment accompanied by increasing $H_2O(+)$ content in meta-basalt is recognized during zeolite facies metamorphism in the ocean floor (Miyashiro et al. 1971). Analytical data are not in harmony with such Na_2O enrichment, but Na_2O decreases with increase of $H_2O(+)$. This variation is similar to that in chemical composition from the core to margin of pillow lava (Nos.20 and 21 in Table 2 and Vallance, 1965). In the $SiO_2 - H_2O(+)$ diagram (Fig.6b) a similar chemical variation is recognized for the pillow lava and the greenstones of this district. Although the bulk chemical compositions are secondly changed, the greenstones can be classified into three groups based on their alkali contents, i.e. high, intermediate and low alkalic groups (Fig.7). The high alkalic group is plotted in the alkalic rock field in $Na_2O+K_2O - SiO_2$ diagram. The intermediate alkalic group falls in the field of high alkali tholeiite ~ alkalic rock. The low alkalic group from the lower horizon of the Nashihara block correspond to picritic basalt. In the MgO $-FeO+Fe_2O_3 - Na_2O+K_2O$ diagram (Fig.8), the low alkali group is plotted in the similar field of the Mikabu greenstones of the Kanto Mountains (Uchida, 1967) and in the iron-rich side of those of eastern Shikoku (Iwasaki, 1969). Most of the lavas in the Oshika district fall on the alkali-rich side as compared with the Mikabu greenstones of western Shikoku (Suzuki et al., 1971 and 1972).

In the greenstones in this district, relict minerals such as Ca-pyroxene and kaersutitic amphibole are found (Table 1). On the basis of Maruyama's classification (1976), the chemical compositions of relict Ca-pyroxenes are

plotted in Si-Al and Si-Ti diagrams (Fig.9). Most of the relict Ca-pyroxenes in the greenstones are plotted in the field of alkalic basalt, while those of the gabbro intruded in later stage are, with some expections, in the field of tholeiitic basalt. The occurrence of kaersutitic amphibole also suggests that the greenstones have alkalic affinity.

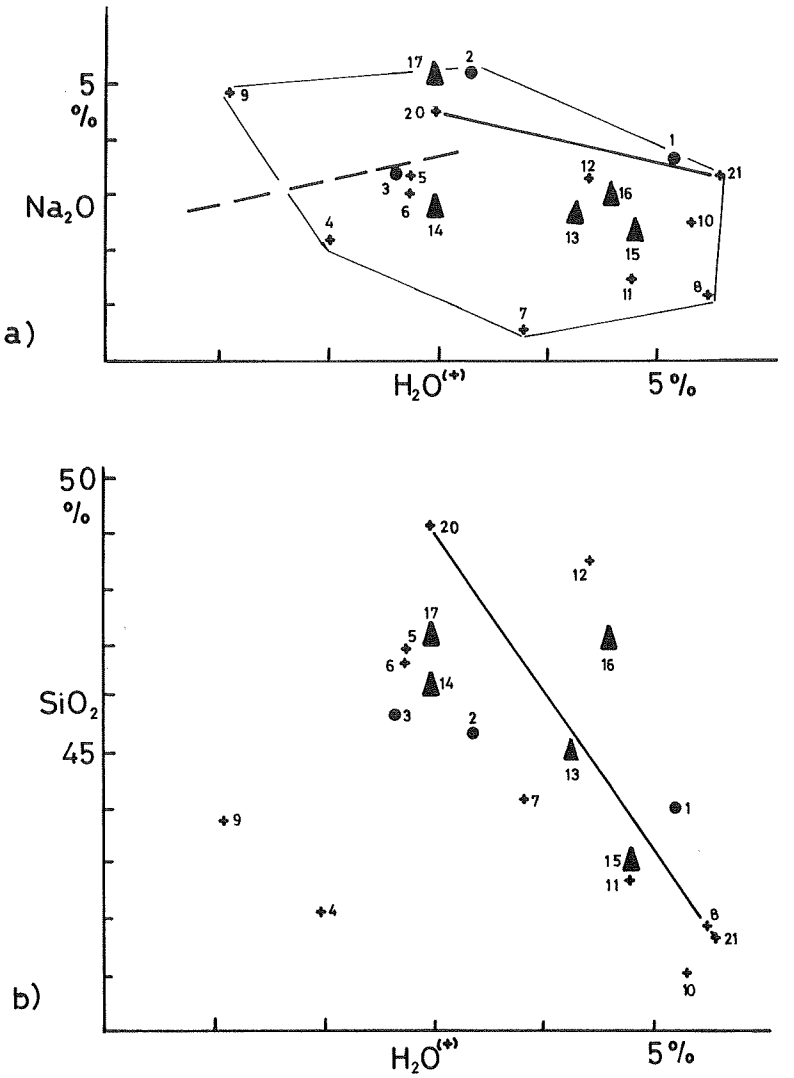

Fig. 6 $Na_2O - H_2O(+)$ diagram (a) and $SiO_2 - H_2O(+)$ diagram (b) for the mafic rocks. solid circle: Zone I, cross: Zone II, solid triangle: Zone III. Numbers correspond to those in Table 3. A broken line shows the variation trend of chemical composition during the zeolite facies metamorphism in the ocean floor (Miyashiro et al., 1971).

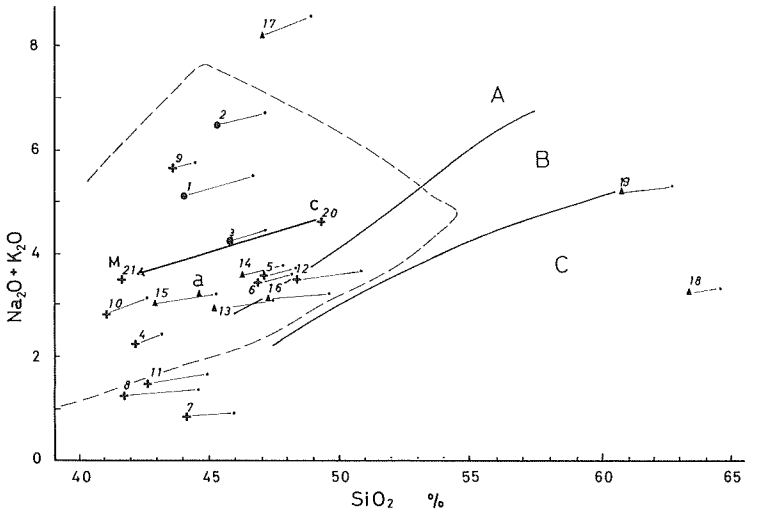

Fig. 7 Na_2O+K_2O – SiO_2 diagram for the mafic rocks and the micaceous greenschists in the Oshika district. Compositional range of mafic schist in the Sambagawa Metamorphic Belt is also shown by the area enclosed by the broken line (Kawachi, 1970) A: alkali rock series, B: high alumina series, C: tholeiite series (Kuno, 1968). M ——C : compositional change of a pillow lava from core to margin (Okawara). a: data by partial analysis. Small solid circles show the chemical composition calculated as anhydrous. solid circle: Zone I, cross: Zone II solid triangle: Zone III Numbers correspond to those in Table 3.

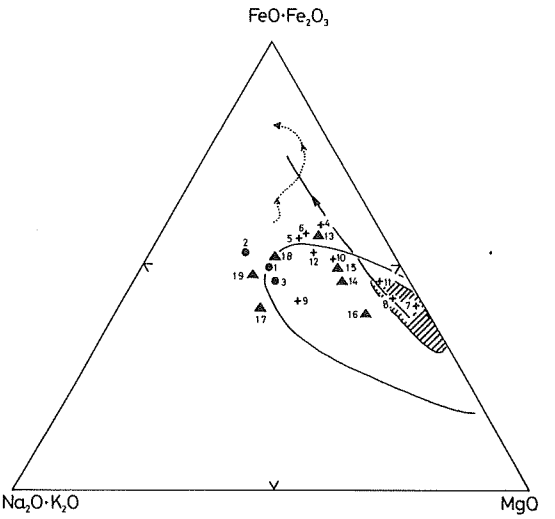

Fig. 8 MgO – $FeO+Fe_2O_3$ – Na_2O+K_2O diagram for the mafic rocks and the micaceous greenschists. solid line with arrow: trend of the Mikabu greenstones of Tomisuyama (Suzuki et al., 1971). dotted line with arrow: trend of the layered gabbroid mass in the Mikabu greenstones of Okuki (Suzuki et al., 1972). enclosed area by solid line: the Mikabu greenstones in eastern Shikoku (Iwasaki, 1969). hatched area: the Mikabu greenstones in the Kanto mountains (Uchida, 1967). Numbers and symbols are the same as in Fig.7.

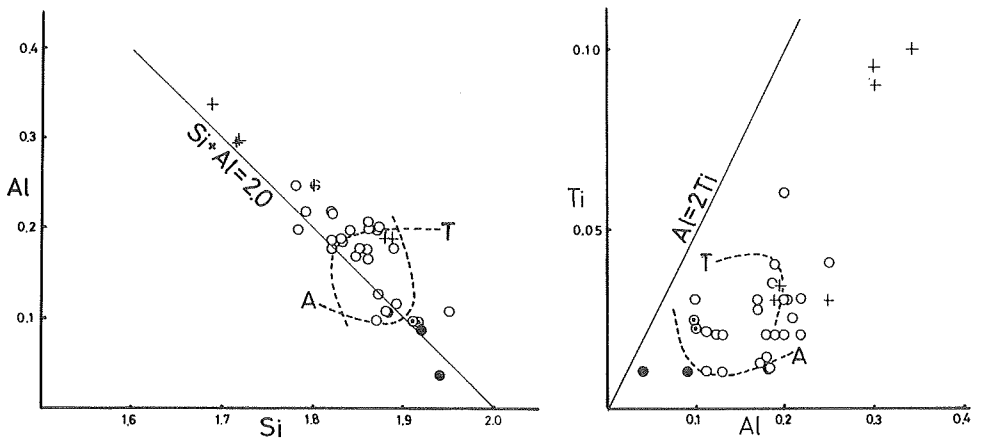

Fig. 9 Left: Al-Si diagram for relict clinopyroxene. The higher Al side of the broken line A is the field of alkali basalt and the lower Al side of the line T is the field of tholeiite. Right: Ti-Al diagram for relict clinopyroxene. The higher Ti side of the broken line A is the field of alkali basalt and the lower Ti side of the line T is that of tholeiite (proposed by Maruyama, 1976). cross: clinopyroxene in the greenstones in the Chichibu Belt, open circle: clinopyroxene in the greenstones in the Sambagawa Belt, solid circle: clinopyroxene in the gabbro of later intrusion in the Sambagawa Belt, circle with a dot: clinopyroxene in the gabbroic xenolith in the Torikura-yama block. Data from Kawachi and Watanabe (1972) is also used in this figure.

Greenstones of the Chichibu Belt

The amount of volcanogenic rocks in this belt is small compared with that in the Sambagawa Belt, though they become more common towards the west. Characteristic rocks of them are reworked fine-grained hyaloclastites occurring as thin beds intercalated in pelitic rocks. Thick greenstones composed mainly of lava and hyaloclastic breccia are also found in several places. The size of vesicles in the basaltic rocks is generally small, less than 2.5 mm in diameter.

Bulk compositions of basaltic lava and gabbro are plotted in the field of alkalic basalt (Fig.8). The basaltic rocks of the Chichibu Belt are more alkalic than those of greenstones of the Sambagawa Belt in the Oshika district. Fine-grained hyaloclastite also has similar chemical composition. Kaersutite and titanaugite often occur in the Chichibu Belt (Table 1).

Mesoscopic and Microscopic Structure

Planar structure, mesoscopic fold structure and lineation are well developed in the rocks of this district, especially in the schists of the Sambagawa Belt.

Planar structure

S_1 : Distinguished as alternating foliation planes, such as micaceous and quartz-feldspathic layers in pelitic schist (Fig.10a). The thickness of each layer is generally several millimeters in pelitic schists and the plane parallel to the bedding plane. Slaty cleavage in the Chichibu Belt is generally parallel to this plane.

S_2 : Generally oblique to the S_1 plane at a high angle. Spacing of the S_2 planes is less than one centimeter (Fig.10a). These planes are well developed in the pelitic and minor mafic schists, though in psammitic schists and limestones they are hardly observed. Oblique two directional fracture cleavage planes are often observed (Watanabe and Kwanke, 1974). Therefore the S_2 plane is considered to have been formed by at least two stages of deformation. The early plane is weakly fissile compared with the later one.

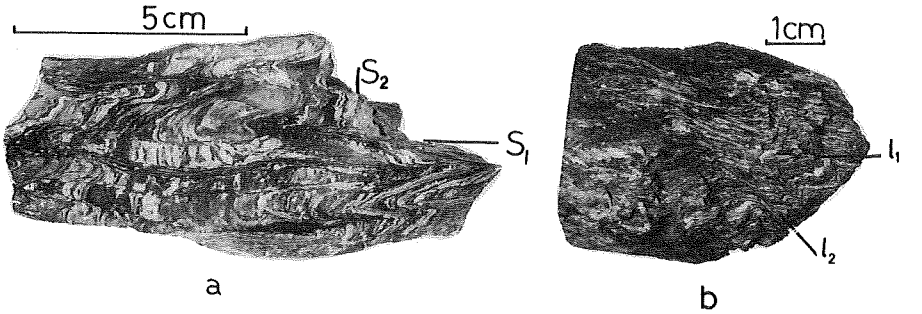

Fig. 10a A model showing the relationship to the S_1 and S_2 planes.
10b A sample showing intersection of lineations (l_1 and l_2) in a pelitic schist from the Ohana-zawa.

Fold structure

F_1 folds: Within the S_1 plane very small isoclinal folds or rootless intrafolial folds (Turner and Weiss, 1963) are well developed in pelitic schists and a few mafic schists. Axial plane cleavage and the limbs of F_1 folds are parallel to the S_1 plane. The F_1 fold represents the earliest stage of folding in the rocks of the Sambagawa Belt. Types of folds described as "isoclinal fold" (Hide, 1961), "Type 1 fold" (Oyagi, 1964), and "B_1 fold" (Hara, 1966) in other areas of the Sambagawa Belt, correspond to F_1 folds. The wave length of the F_1 fold varies from several centimeters to 1 mm or less. The F_1 folds can be classified into two types i.e. F_1-a and F_1-b. The mineral aggregates are partially discordant with the F_1 folds in F_1-a (Plate IIId) and concordant with the F_1 folds in F_1-b (Plate IVa-c). In the axial part of the F_1-b folds there are many varieties in shape and size of quartz grains, quartz fabrics, and arrangement of mica or

amphibole. Accordingly, the F_1-b folds can be further classfied into three subtypes, i.e. F_1-b1, F_1-b2, and F_1-b3 (Watanabe, 1974).

In the axial part of the F_1-b1 folds (Plate IVa) the direction of elongation of amphibole and white mica coincides with that of the axial planes of the F_1 folds. Elongated quartz grains are also arranged in the same direction, and the shape of individual quartz grains is somewhat lobate. In the axial part of the F_1-b2 folds (Plate IVb) the dimensional orientation of white mica is the same as in the F_1-bl folds, but quartz grains are granular and polygonal in habit. In the axial part of the F_1-b3 folds (Plate Vc) elongated micas are arranged parallel to the F_1 folds and quartz grains are granular and polygonal. Intermediate fold subtypes between these three subtypes are also present. Coexistence of two fold types in a thin section is sometimes observed (cf Plate IV in Watanabe, 1975). The genesis of F_1-a folds seems to be rather different from F_1-b folds, as both wave length and amplitude of F_1-a type folds are considerably larger than those of F_1-b folds. Hitherto, F_1-a folds have been found only in the Chichibu Belt.

F_2 folds: This type of fold usually accompanies S_2 planes and is considered to have formed after the formation of F_1 folds which bend the axial planes and axes of the F_1 folds. F_2 folds can be subdivided into two types, i.e. $F_{2\text{-}1}$ and $F_{2\text{-}2}$ in order of formation. The lineation associated with $F_{2\text{-}1}$ folds is cut by the lineation associated with $F_{2\text{-}2}$ folds.

F_3 folds: The axial angle of this type of fold is usually acute and cleavage develops in the fold axis. This fold type resembles the accordion fold (de Sitter, 1956); its wave length is 5 – 10 cm. It is widely developed in pelitic schists on the west side of the Ohana-zawa Fault and on the east side of the Inogaya-zawa Fault. Since these folds bend the axis of the F_2 folds they are considered to have formed subsequent to the F_2 folds.

F_4 folds: Small kink folds rarely developed in some of the pelitic and mafic schists. The direction of the F_4 fold axes is different from that of the F_3 folds (cf. Fig.17b in Watanabe, 1970). This fold represents the latest folding stage.

Lineation

Lineations can be classified into two types in this area.

l_1: A lineation parallel to the direction of the axial planes of F_1 folds, represented by streaks, weak corrugations, and rarely micro-fold axes.

l_2: A lineation parallel to the axial plane of F_2 folds, represented by corrugations and micro-fold axes.

An example in which both l_1 and l_2 intersect each other is shown in Fig.10b. Both lineations are clearly recognized in the Higashikohana-zawa section where l_1 dips to the south and l_2 to the north (cf. Fig.15 in Watanabe

and Kwanke, 1974).

Quartz fabrics of F_1-b folds

F_1-b1 type (Plate IVa): Needle-like minerals in Plate IVa are sodic amphibole, other minerals are quartz. The quartz grains are mostly 0.015 – 0.03 mm in diameter of longest direction in a-c plane, though porphyroblastic coarse quartz grains up to 0.08 mm across are sometimes observed in a fine-grained quartz matrix. Most of the quartz grains show wavy extinction. Deformation lamellae are rarely found in porphyroblastic quartz grains. The optical axes of quartz (Fig.11a) are arranged in or near the a-c plane, but not near the area of the tectonic a-axis.

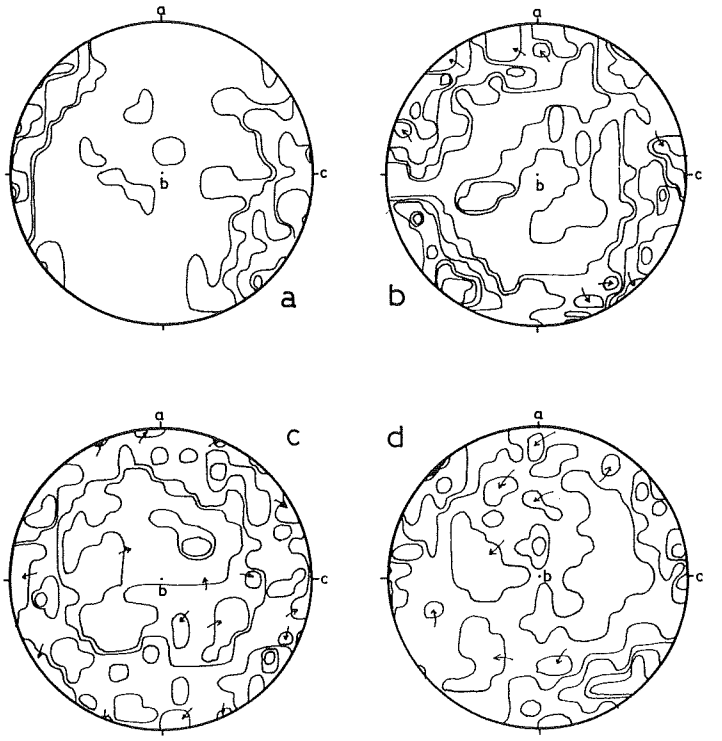

Fig. 11 Quartz fabric diagrams in the axial part of F_1 and F_2 folds.
a): F_1-b1 fold. Contours. 2-4-6-8-10% (100 points) lower Hemisphere (L.H.)
b): F_1-b2 fold. Contours, 1-2-3-4-5% (200 points, L.H.)
c): F_1-b3 fold. Contours. 1-2-3-4-5% (200 points, L.H.)
d): F_2 fold. Contours. 1-2-3-4-5% (100 points, L.H.)

F_1-b2 type (Plate IVb): Elongated minerals in Plate IVb are white mica, other minerals are quartz and a minor amount of ablite. The grain size of quartz in this type (0.03 – 0.07 mm) is coarser than that of the F_1-b3 type.

Quartz grains are slightly elongated along the axial plane. One directional arrangement of white mica is not so notable as in the F_1-b1 type. The optical axes of quartz (Fig.11b) are mainly concentrated in an imperfect girdle perpendicular to the b-axis.

F_1-b3 type (Plate IVc): Constituent minerals in Plate IVc are the same as above. The quartz grains are coarser than in the F_1-b1 and F_1-b2 types (0.06 – 0.08 mm) and their shape is nearly equigranular. The optical axes of quartz (Fig.11c) are scattered as compared with those of other F_1-b type folds.

Genesis of F_1-b folds in pelitic schist

Metamorphic minerals occurring in harmony with F_1-b folds, indicate that deformation and recrystallization is considered to have proceeded simultaneously during F_1-b folding. Distribution of each fold type is not always related to the metamorphic grade (Fig.12a). Two types of F_1-b fold occur even in one thin section. Accordingly, the difference in the quartz fabrics for each fold type must be independent of the metamorphic grade. Quartz fabrics are controlled not only by temperature and confining pressure, but also by strain ratio and strain rate (Green et al., 1970; Suzuki, 1970; Hara, 1971; 1974; Hara and Paulitsch, 1971; Yamazaki et al. 1971; Kumazawa et al. 1971). The fabric pattern of quartz in the F_1-b1 folds resembles that of the rapid strain rate as studied by Green et al. (1970) and that of mylonite (e.g. Sander, 1966). Therefore, the F_1-b1 folds are assumed to have formed at the rapid strain rate.

Green et al. (1970), Griggs et al. (1960) and Carter et al. (1970) demostrated that grain size and shape of quartz or calcite are controlled by the amount of H_2O during recrystallization. In this connection the fact that quartz grains in F_1-b2 and F_1-b3 folds are coarse and equigranular compared with those of F_1-b1, may be interpreted in terms of different amounts of H_2O or other fluid phases during recrystallization. The quartz grains elongated along the axial planes of F_1-b folds are interpreted to have been formed under compression perpendicular to the axial planes of F_1-b folds (= S_1 plane) (see Spry, 1969, p.159).

As F_1-b folds develop within the foliation of pelitic schist, these folds have a close genetic relation to the formation of foliation planes. Kojima and Hide (1958) and Kojima (1950) considered that the foliation of schists of the Sambagawa Belt corresponds to the lamination of the original rocks though modfied by metamorphic differentiation. For the most of the foliations this interpretation is valid except for the foliation of pelitic schist with microfold structures such as F_1-b folds. On the other hand, Nakayama (1960) interpreted that the foliated structure was formed due to differential movement by horizontal tension. However, Nakayama did not mention the formation of the

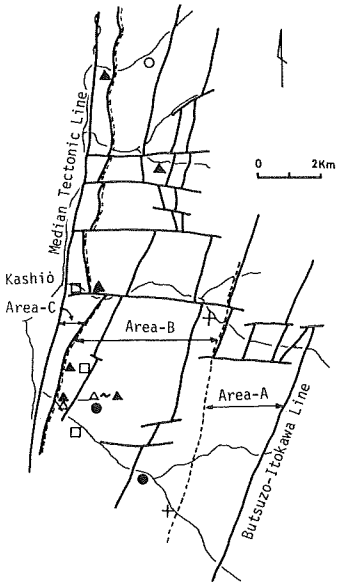

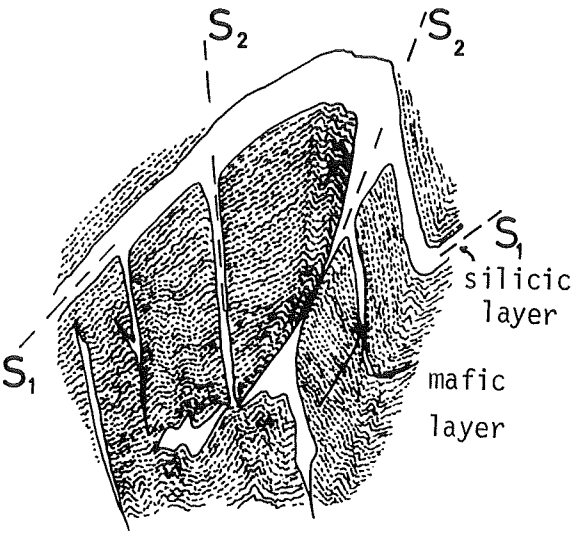

Fig. 12a (Left): Localities of representative F_1 and F_2 folds and structural zoning by F_2 fold of the Sambagawa and Chichibu Belts. Boundaries between three zones are shown by broken lines. cross: F_1-a fold, open triangle: F_1-b1 fold solid triangle: F_1-b2 fold, open square: F_1-b3 fold. open circle: $F_{2\text{-}1}$ fold, solid cricle: $F_{2\text{-}2}$ fold

Fig. 12b (Right): $F_{2\text{-}1}$ fold in a mafic schist from Tebiraki-zawa. A sample showing arrangement of silicic layers in the direction of S_2 plane.

micro-folds such as the F_1-b folds.

The F_1-b folds were formed under compression perpendicular to the S_1-plane. Compression perpendicular to bedding planes would shorten the thickness of strata as observed by concentric folded quartz veins in semi-schists of the Shimanto Belt, say 16 – 60% (Kawachi and Kwanke, 1968). The amount of shortening is generally larger in slate than in sandstone. For the metamorphic rocks in the Oshika district, the amount of shortening is difficult to measure due to flow fold under the higher grade metamorphism, but is estimated to be larger than in the Shimanto Belt. Especially, in the pelitic rocks, plastic flow along the bedding planes is considered to have occurred, inferred from the features of F_1-b folds such as flow folds and torn-off fold limbs (cf. Plate IV in Watanabe, 1975). In an experiment with polygonal ice, plastic flow due to compression was reported by Matsuda and Kizaki (1971). In the pelitic rocks which are mainly composed of quartz and mica, the difference of their ductilities might cause differential flow at the time of plastic flow and result in the separation of micaceous and quartzose parts. The differential

movement between two layers of probably somewhat irregular and bended form, is considered to cause formation of F_1-b folds. The strain rate of each F_1-b folding was not necessary uniform. Micro-shear planes might have been produced in the plane where strain rate was large, and these shear planes were passageways for the fluid phase.

Recrystallization related to F_2 folds

During F_2 folding rearrangement of mica and carbonaceous matter is generally recognized along the axial planes of F_2 folds. However, calcitic layers branching from S_1 foliated layers in mafic schists have recrystallized along the axial planes of F_2 folds in some cases (Fig.12b). The calcitic layers are composed of calcite, quartz, albite, chlorite, and white mica. The F_2 folds are associated with weak fissile S_2 cleavage planes and weak micro-corrugation, indicating characteristic features of $F_{2\text{-}1}$ folds. Partial recrystallization of calcite, quartz and ablite have also occurred during $F_{2\text{-}2}$ folding (Watanabe, 1974). According to Griggs et al. (1960), calcite or marble yields to plastic flow at low temperature and confining pressure compared with other rocks or minerals. Therefore, the calcitic layers along the axial plane cleavage of F_2 folds are considered to have formed under the retrogressive condition.

In the axial part of an F_2 fold, optical axes of quartz disperse and are somewhat concentrated around the b-axis compared with those of F_1 folds (Fig.11d).

Time sequence of deformation and zonation by fold structure

In other regions of the Sambagawa belt, multiple deformation has been also reported (e.g. Nakayama, 1950, 1952, 1960; Kojima, 1951; Kojima and Hide, 1958; Kojima and Suzuki, 1958; Hide, 1961, 1972; Oyagi, 1964; Hara, 1966). Hide (1972) especially established five phases of folding including three major ones.

The time sequence of deformation and its relation to recrystallization in this district are summarized in Table 4. F_2 folds characteristically develop in the area where pelitic schists are predominant, whereas F_3 folds occur along the Ohana-zawa and the Inogaya-zawa faults. The open and gentle folds (Fleuty, 1964) present in the central and eastern parts of the Chichibu belt (Area A in Fig.12a). The open fold is predominant in the Tebiraki-zawa, Shin'nagi-zawa, Nashihara, Torikura-yama blocks, and the western part of the Chichibu Belt (Area B). In the Ohana-zawa block, the western margin of the Sambagawa Belt, the close fold (Fleuty, 1964) develops predominantly (Area C). The boundaries between three areas (broken lines in Fig.12) are not always clear but rather gradational. The angle between limbs of folds becomes less

towards the western part of this district. This suggests that stress has increased from east to west during the formation of F_2 folds. Similar zonation of folding is found in the Tenryu district, Sambagawa Belt (Ishikawa, 1971).

Table 4 Time sequence of deformation and its relation to recrystallization.

Sequence of deformation ⟶				
F_1 fold	F_{2-1} fold	F_{2-2} fold	F_3 fold	F_4 fold
recrystal-lization in whole	partial recrystal-lization (calcite, quartz albite, chlorite, white mica)	partial recrystal-lization (calcite, quartz)	with faulting	

Metamorphic zoning

Throughout the Sambagawa and Chichibu Belts in the Oshika district, siliceous, calcareous and pelitic rocks are completely recrystallized. Some blastoporphyritic grains such as feldspar and quartz occur in the psammitic rocks of the low grade area. Volcanogenic and intrusive rocks sometimes preserve the original texture and relict minerals. Mineral assemblages of siliceous, psammitic, and pelitic rocks are rather simple compared with those of the mafic rocks. Quartz, albite, white mica, calcite, and chlorite occur in all these rocks. Stilpnomelane is sometimes found in various rock types. Carbonaceous materials, however, occur only in pelitic schists. Tourmaline and green mica occur in psammitic and pelitic schists in the Ohana-zawa block and the western part of the Tebiraki-zawa block. Near the Median Tectonic Line, garnet occur in siliceous schists and micaceous greenschists.

Various mineral assemblages are observed in the mafic schists consisting of actionolite, pumpellyite, chlorite, epidote, calcite, Na-amphibole, Na-pyroxene, stilpnomelane, sphene, white mica, tourmaline, quartz, and albite. Among them, epidote, actinolite, chlorite, calcite, quartz, and albite occur in most mafic schists. Lawsonite, prehnite and zeolite are not found in this district (Fig.13).

The following metamorphic zones can be established:

Zone I: the presence of pumpellyite and absence of Na-amphibole.

Zone II: the presence of Na-amphibole and contact mineral paragenesis of pumpellyite and epidote.

Zone III: the absence of contact mineral paragenesis of pumpellyite and epidote. Occurrence of pumpellyite is rare.

The distribution of each zone, the range of presence of the minerals, are shown in Fig.14. Optical properties of epidote, actinolite and chlorite in each zone are shown in Fig.15.

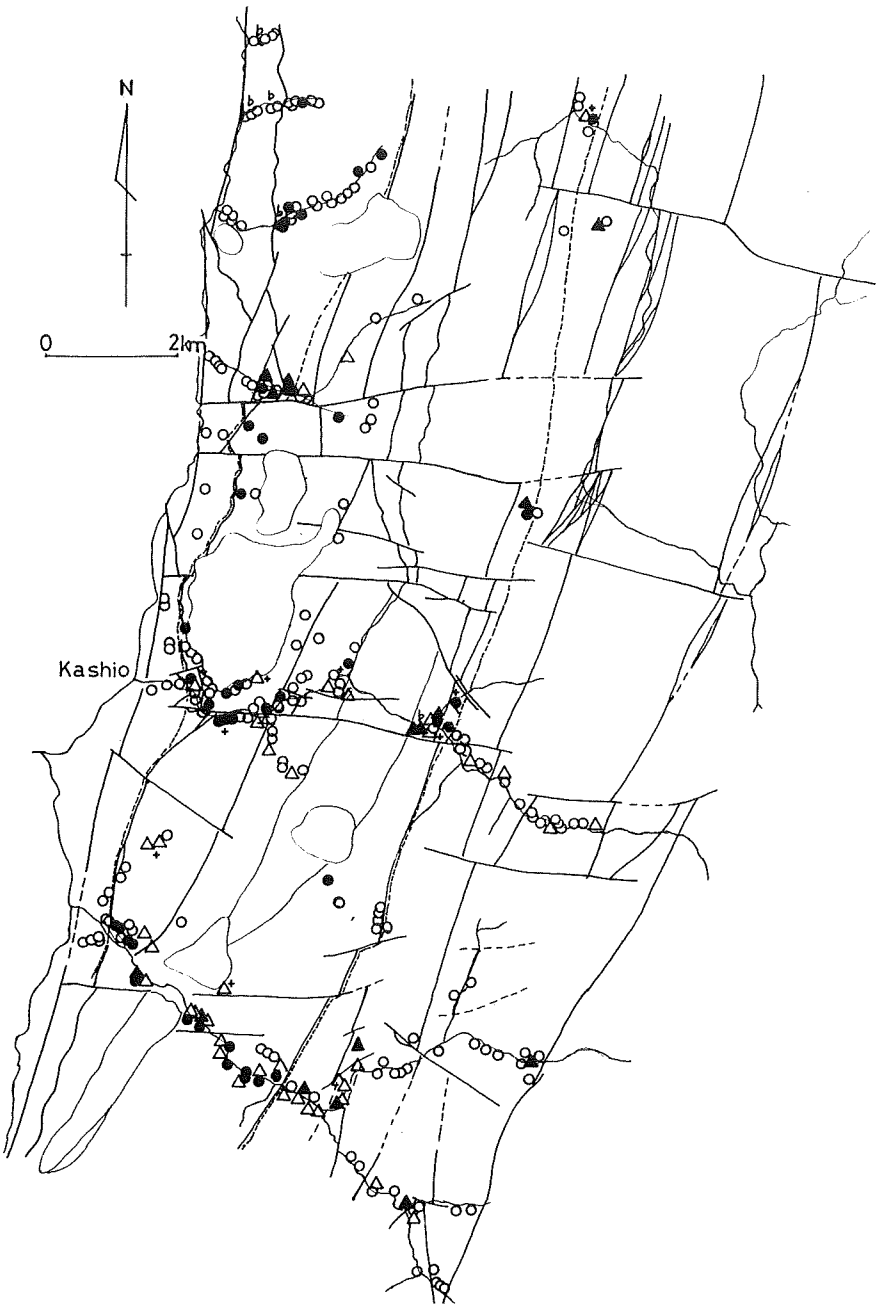

Fig. 13 Distribution map of some metamorphic minerals in the mafic rocks. solid circle: Na-amphibole, cross: Na-pyroxene (including vein minerals), open triangle: pumpellyite with epidote, solid triangle: pumpellyite without epidote, b mark: green biotite (including vein minerals), open circle: absence of the above minerals (mainly epidote – chlorite – actinolite assemblage)

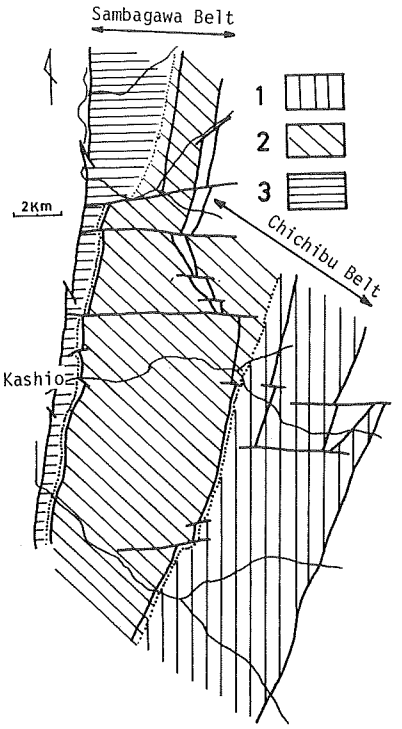

Zone	I	II	III
actinolite			
pumpellyite			--
Na-amphibole			?
Na-pyroxene		- - - -	
chlorite			
epidote			
calcite			
albite			
quartz			
sphene			
stilpnomelane	- - - -	- - - -	- - - -
white mica	- - - -	- - - -	- - - -

Fig. 14 Distribution map of the three metamorphic zones. (1: Zone I, 2: Zone II, 3: Zone III) and Range of presence of the metamorphic minerals in the mafic rocks (excluding Na-pyroxene and biotite in veins).

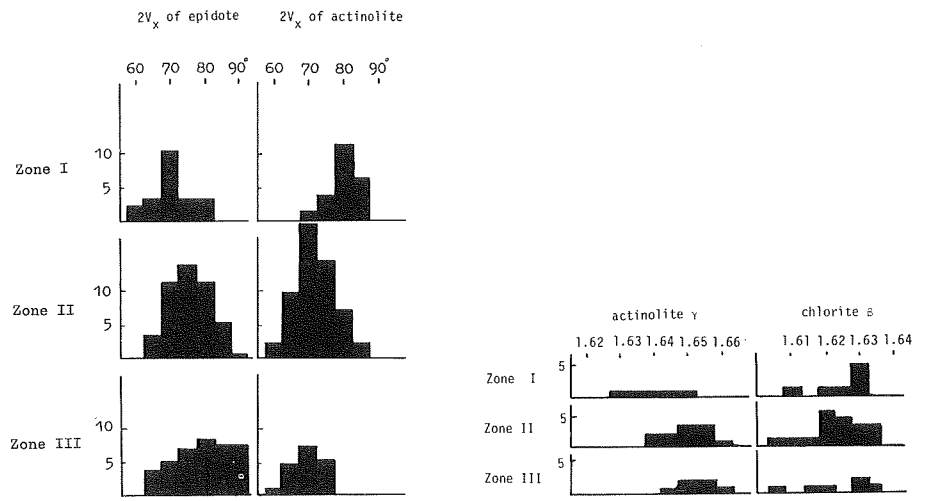

Fig. 15 Optical properties of epidote, actinolite, and chlorite in the mafic rocks. Ordinate shows number of measured minerals.

Zone I

The metamorphic minerals are generally fine grained except those occurring in vesicles of lavas, veins, and calcitic pools. The different grade of recrystallization due to differences in the original rocks is very distinct. For example, in most lavas the original texture and minerals are preserved, whereas, rocks derived from fine-grained hyaloclastite have been completely recrystallized, and aggregations of coarser metamorphic minerals such as chlorite and calcite occur along the schistosity. Silicic layers in meta-hyaloclastite are completely recrystallized even in the lowest metamorphic grade and contain coarser quartz, albite, calcite, chlorite, and pumplellyite. In meta-lavas, coarse grains of chlorite, calcite, pumpellyite and albite occur in vesicles and veins. Actinolite mainly occurs around relict Ca-pyroxene. In some cases, coarse actinolite and albite occur along micro-shear zones in the lavas. Fluid phases have been easily transported through vesicles, veins, micro-shear zones and a part of the fine-grained hyaloclastite. Contact paragenesis of pumpellyite and actinolite is not observed in the lower half part of the Koshibu-gawa area in this zone.

Contact mineral parageneses (Kawachi and Watanabe, 1974) of Zone 1 are follows:

pumpellyite – chlorite
pumpellyite – chlorite – epidote
actinolite – pumpellyite
actinolite – pumpellyite – calcite
actinolite – calcite
actinolite – chlorite – epidote
epidote – chlorite
epidote – calcite – chlorite
epidote – actinolite – pumpellyite
chlorite – calcite
actinolite – chlorite
actinolite – chlorite – pumpellyite
epidote – pumpellyite – calcite
epidote – actinolite – calcite
phengite – calcite
phengite – epidote – chlorite
stilpnomelane – calcite
stilpnomelane – chlorite
stilpnomelane – epidote – calcite

Quartz, albite, and sphene occur in all the rocks. The above paragenesis are plotted in the tetrahedron of Fig.16a except epidote – calcite – chlorite. The presence of the epidote – calcite – chlorite assemblage may be due to the difference of mole fraction of CO_2 (X_{CO_2}) in the fluid phase. An idealized reaction producing the epidote – calcite – chlorite assemblage under isochemical conditions is shown as follows:

$$100\,\underset{\text{Pumpellyite}}{Ca_4Mg(Al_{4.5}Fe^{3+}_{0.5})Si_6O_{23}(OH)_3} + 106\underset{\text{actinolite}}{Ca_2Mg_5Si_8O_{22}(OH)_2} + 512CO_2$$
$$= 50\underset{\text{epidote}}{Ca_2(Al_2Fe^{3+})Si_3O_{12}(OH)} + 70\underset{\text{chlorite}}{(Mg_9Al_3)(Si_6Al_2)O_{20}(OH)_{16}}$$
$$+ \underset{\text{calcite}}{512CaCO_3} + \underset{\text{quartz}}{878SiO_2} + 329H_2O$$

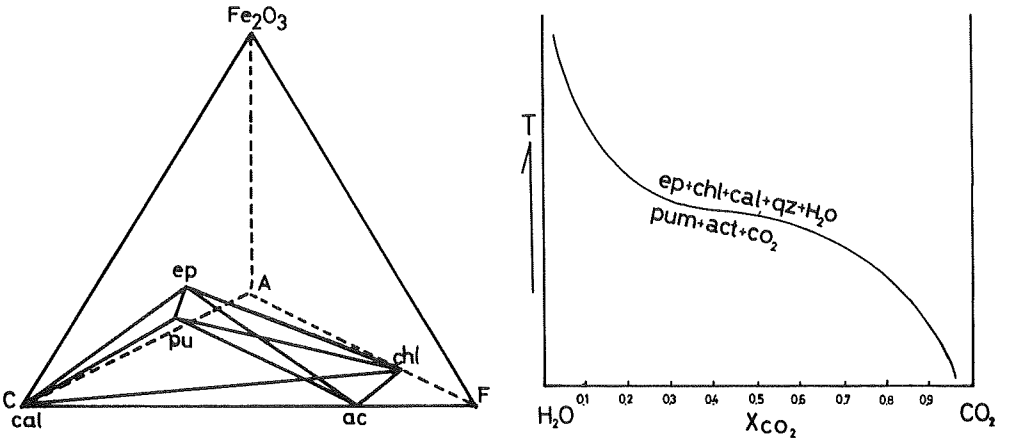

Fig. 16a (Left): Tetrahedron showing the mineral paragenesis in Zone I, except epidote – chlorite – calcite assemblage and stilpnomelane bearing assembalge. Stilpnomelane is neglected due to its changeable Fe_2O_3 content in the tetrahedron.

Fig. 16b (Right): X_{CO_2}-T diagram of an univariant reaction (pumpellyite + chlorite + CO_2 = epidote + chlorite + calcite + quartz + H_2O) at constant pressure. .

Dependence of X_{CO_2} is shown in Fig.16b.

In the high grade part of Zone I, pumpellyite with low FeO (3 – 4%) occurs between chlorite and pumpellyite with high FeO (7 – 8%) as a narrow zone (2 – 30 microns).

Zone II

Most of the greenstones contain relict minerals of Ca-pyroxene and a small amount of brown amphibole. Therefore, it is difficult to decide stable assemblages associated with excess quartz. Na-amphibole is generally observed around some Ca-pyroxenes. Actinolite mantling the Na-amphibole is often present. The contact of Na-amphibole and quartz, however, has been found in the rocks containing relict minerals. Moreover, the presence of Na-amphibole is largely dependent on bulk composition as mentioned later. Therefore, the boundary between Zones I and II is somewhat obscure. However the higher-grade side (western) from the point of the first appearance of Na-amphibole is treated as Zone II. Actinolite mantling relict clinopyroxene is smaller in amount in Zone I than Zone II. Na-amphibole seems to be formed when relict clinopyroxene considerably decomposed. This suggests that Na was supplied from relict clinopyroxene. In Zone II, Ca-pyroxene is almost mantled by calcic and/or sodic amphibole, and the contact of epidote with relict Ca-pyroxene is not observed. Therefore, the following reaction is assumed to indicate the transformation from Zone I to Zone II in the case of presence of large amounts of calcite and quartz.

$$\underset{\text{diopside}}{94CaMgSi_2O_6} + 10\underset{\text{epidote}}{Ca_2(Al_2Fe^{3+})Si_3O_{12}(OH)} + 10\underset{\text{albite}}{NaAlSi_3O_8} + 104CO_2 + 53H_2O$$
$$= \underset{\text{magnesio-riebeckite}}{5Na_2Mg_3Fe_2^{3+}Si_8O_{22}(OH)_2} + 5\underset{\text{tremolite}}{Ca_2Mg_5Si_8O_{22}(OH)_2} + 6\underset{\text{chlorite}}{(Mg_9Al_3)(Si_6Al_2)O_{22}(OH)_{16}}$$
$$+ \underset{\text{calcite}}{104CaCO_3} + \underset{\text{quartz}}{132SiO_2}$$

Here, pure compounds are assumed for convenience of calculation.

The following mineral assemblages are observed in the rocks containing quartz and albite in Zone II.

pumpellyite – epidote
pumpellyite – epidote – chlorite
pumpellyite – calcite
pumpellyite – actinolite
pumpellyite – actinolite – chlorite
actinolite – chlorite – epidote
actinolite – chlorite
actinolite – chlorite – calcite
actinolite – epidote
actinolite – epidote – chlorite
epidote – chlorite – calcite
Na-amphibole – phengite – calcite

In the rocks free from quartz:

Na-amphibole – actinolite – (±chlorite)
Na-amphibole – aegirine-augite (±chlorite)
Na-amphibole – epidote – (±chlorite)
aegirine-augite – chlorite
jadeite – pumpellyite

In this zone, pumpellyite completely replaces plagioclase phenocrysts. A subcalcic amphibole rich in FeO occurs around kaersutitic amphibole. Green biotite – pyrite veins and aegirine-augite bearing albititic veins are sometimes found in the greenstones. An aegirine-augite assemblage has been described as an indicator of Na-metasomatism (Watanabe, 1975). They are not found in the higher grade area. Similar occurrences were reported from other districts in the Sambagawa metamorphic terrain (Horikoshi, 1934; Nakayama, 1960).

Jadeite occurs in a large meta-hornblende diabase boulder near Shioyu, which has probably been derived from the Manshio stream, east of Kashio. Brown amphibole ($2V_z$ = 75° – 77°) occurs as a relict in this diabase, preserving ophitic texture, and its margin has changed to bluish green hornblende. The pseudomorph after plagioclase is completely replaced by minute grains of impure jadeite, pumpellyite, etc.

Zone III

In this zone, the occurrence of relict minerals is very rare. The following mineral assemblages are observed in the rocks containing quartz, albite, sphene, and sometimes tourmaline:

pumpellyite – chlorite
pumpellyite – actinolite
Na-amphibole – chlorite – calcite
Na-amphibole – chlorite
epidote – chlorite – calcite
epidote – calcite
epidote – stilpnomelane
epidote – chlorite – stilpnomelane

Na-amphibole – actinolite
Na-amphibole – actinolite – epidote
Na-amphibole – actinolite – chlorite
Na-amphibole – calcite
epidote – actinolite – chlorite
epidote – actinolite
epidote – chlorite
epidote – calcite
epidote – chlorite – phengite
epidote – chlorite – green biotite
actinolite – chlorite
actinolite – chlorite – calcite
actinolite – calcite
actinolite – epidote – calcite
chlorite – calcite
chlorite – stilpnomelane
stilpnomelane – phengite – chlorite
stilpnomelane – calcite
phengite – chlorite – calcite
phengite – calcite
green biotite – chlorite

Pumpellyite never occurs in contact with epidote in Zone III. The chemical composition of epidote increases slightly in clinozoisite molecule as mentioned later. The following reaction expected from Zone II to Zone III.

$$90\underset{\text{pistasite}}{Ca_2(Al_2Fe^{3+})Si_3O_{12}(OH)} + 52\underset{\text{pumpellyite}}{Ca_4MgAl_5Si_6O_{23}(OH)_3}$$
$$+ 2\underset{\text{chlorite}}{(Mg_9Al_3)(Si_6O_2)(OH)_{20}} + 58SiO_2$$
$$= 180\underset{\text{clinozoisitic epidote}}{Ca_2(Al_{2.5}Fe^{3+}_{0.5})Si_3O_{12}(OH)} + 14\underset{\text{actinolite}}{Ca_2Mg_5Si_8O_{22}(OH)_2} + 35H_2O$$

Banno (1964) has pointed out that the rocks carrying pumpellyite have a considerably low FeO_2O_3/FeO. Nakajima (1975) also stated that Fe_2O_3/FeO of host rocks influenced to the decomposition of pumpellyite. However, not only Fe_2O_3/FeO, but MgO/CaO is effective for the presence of pumpellyite (Fig.17).

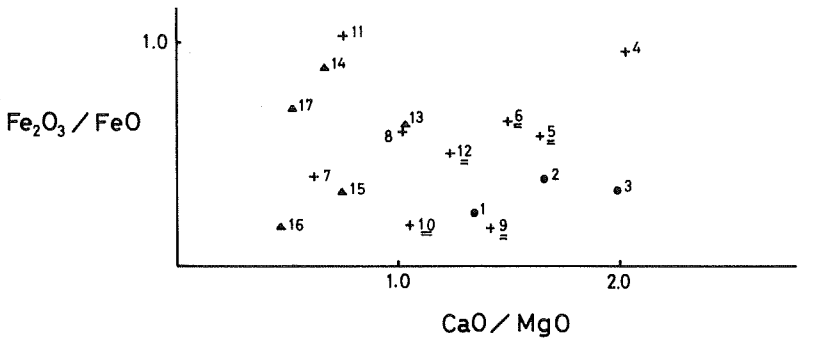

Fig. 17 Fe_2O_3/FeO – CaO/MgO diagram for the mafic rocks. Symbols and Numbers are the same as in Fig.7. Samples of No. 5, 6, 9, 10 and 12 contain pumpellyite in Zone II.

Na-amphibole does not occur in most parts of the Ohana-zawa blocks but is present in the Tebiraki-zawa block. The Na-amphibole generally occurs in the

mafic rocks with high Fe_2O_3/FeO in the Sambagawa Belt, Shikoku, and in the Sangun Metamorphic Belt (Ernst, et al. 1970; Nishimura, 1971). The rocks carrying a large amount of Na-amphibole from the Oshika district fall on the high Fe_2O_3 side of the Fe_2O_3/FeO – Na_2O/CaO diagram (Fig.18). The same tendency is recognized in data from other regions in the Sambagawa Belt (cf. Fig.1 in Watanabe and Kawachi, 1975). The occurrence of a small amount of Na-amphibole may depend on heterogeneity of Fe_2O_3/FeO in the rocks. Consequently, absence of the Na-amphibole in the Ohana-zawa block is due to the low Fe_2O_3/FeO.

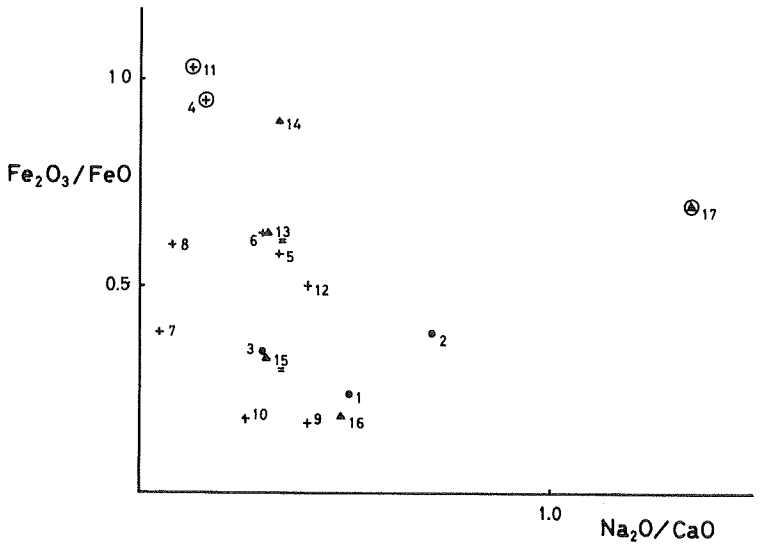

Fig. 18 Fe_2O_3/FeO – Na_2O/CaO diagram for the mafic rocks. Numbers correspond to those in Table 1. Rocks carrying Na-amphibole are Nos. 4, 11, 17, 13 and 15, but amounts of Na-amphibole in the rocks of No. 13 and 15 are very minor, i.e. 0.8% and 0.2% model amount, respectively.

Not only Fe_2O_3/FeO but also other components have an effect on the presence of Na-amphibole. Sample No.14 (82225) in Fig.24 is a Na-amphibole-free rock with a high Fe_2O_3/FeO and is rich in MgO. This rock contains large amounts of epidote and only a small amount of chlorite (Table 5) indicating that most of the Fe^{3+} was consumed to form epidote. Not enough Fe^{3+} remained to form the Na-amphibole and MgO was incorporated in actinolite. Consequently, Na-amphibole might not be formed in the magnesian schist.

The occurrence of Na-amphibole in some mafic schist is very characteristic. Namely, in the mafic schists intercalated with silicic layers, the Na-amphibole occurs mainly along the layer boundary, although some Na-amphibole appears in the silicic layers. Other mafic minerals such as actinolite, epidote and

chlorite, however, do not show a similar occurrence to the Na-amphibole, although they form the mafic layers, with minor amounts of sphene. Occurrence of the Na-amphibole along the layer boundary has a relation to its original laminated structure and mechanism of recrystallizon (a king of small scale metamorphic differentiation).

Table 5 Modal compositions of some mafic rocks and their MgO weight per cent.

Sample number	72601 (No.16)	101602 (No.10)	82217 (No.15)	90310 (No. 7)	82225 (No.14)
chlorite	17.7	40.2	17.9	13.2	7.0
actinolite	61.5	2.5	35.0	56.5	43.7
epidote	4.0	11.1	7.0	-	25.7
pumpellyite	-	0.73	-	-	-
calcite	0.9	-	5.7	-	-
quartz+albite	9.9	5.8	21.7	5	10.5
sphene (leucoxene)	6.0	5.6	11.7		13.1
mica	+	-	0.8	-	
others	0	34.1 (r-cpx)	0.2	25.3 (r-cpx)	
Total	100.0	100.0	100.0	100.0	100.0
Mgo (%)	12.59	9.21	9.76	17.69	12.00

Metamorphic minerals

Chemical compositions of metamorphic minerals were analyzed by the micro-probe analyzer (JXA-5A) of the Geological Survey of Japan. EPMA equipment of Kanazawa University and the Government Industrial Development Laboratory, Hokkaido, was also used for some of the analyses. Operation of the JXA-5A is computerized (Kawachi and Okumura, 1972; Okumura, Soya and Kawachi, 1974; Okumura and Soya, 1976). Correction of data was done by the method of Sweatman and Long (1969) and Bence and Albee (1968).

Analysis of an albite crystal from the Ohana-zawa block was done five times for the determination of reproducibility by the EPMA analysis. The result is as follows:

SiO_2: 68.38–69.70%
Al_2O_3: 19.13–19.50%
MnO: 0.0–0.02%
CaO: 0.03–0.08%
K_2O: 0.05–0.07%
TiO_2: 0.0–0.06%
FeO: 0.10–0.23%
MgO: 0.0–0.02%
Na_2O: 11.66–12.28%

For olivine the following result was obtained:

SiO_2: 38.98–39.53%
MnO: 0.41–0.48%
FeO: 17.52–18.36%
MgO: 42.91–43.51%

Table 6 Chemical compositions of albite and garnet.

	albite	garnet
No.	1 100605 (Zone III)	2 90404 (Zone III)
SiO_2	69.01	37.60
TiO_2	0.05	0.15
Al_2O_3	19.13	20.42
FeO	0.15	23.14
MnO	0.02	7.84
MgO	0.00	0.73
CaO	0.03	9.80
Na_2O	11.66	0.05
K_2O	0.06	0.01
Total	100.11	99.74
Si	6.02	6.049
Al^{IV}	-	-
	6.02	6.049
Al^{VI}	1.96	3.873
Ti	0.00	0.018
Fe^{2+}	0.01	3.113
Mn	0.00	1.068
Mg	0.00	0.175
Ca	0.003	1.689
Na	1.97	0.015
K	0.01	0.002
	3.953	9.953

Table 7 Chemical compositions of Na-pyroxene.

	1	2	3	4	5	6
	90208	101602	101602	5080101	90508	Shioyu
SiO_2	51.62	52.40	52.50	53.0	55.36	59.20
TiO_2	0.00	n.d.	0.15	0.4	0.06	0.00
Al_2O_3	0.47	2.24	3.98	4.0	3.05	19.98
Fe_2O_3	18.56*	19.74	18.11	22.1	0.00	5.45
FeO	0.00	0.00	0.00	0.0	9.46	0.00
MnO	0.48	0.00	0.26	0.1	0.52	0.00
MgO	8.77	6.73	6.08	4.2	9.32	0.00
CaO	17.01	11.72	10.75	5.5	18.30	0.97
Na_2O	3.94	7.30	8.56	10.2	3.08	13.51
K_2O	0.00	n.d.	0.00	0.1	0.00	0.00
Total	100.85	100.13	100.39	99.6	99.15	99.11
Si	1.92	1.95	1.95	1.98	2.061	2.041
Al^{IV}	0.02	0.05	0.05	0.02	-	0.000
	1.94	2.00	2.00	2.00	2.061	2.041
Al^{VI}	0.00	0.05	0.12	0.16	0.133	0.812
Fe^{3+}	0.52	0.56	0.50	0.62	0.000	0.141
Ti	0.00	0.00	0.01	0.01	0.010	0.000
Fe^{2+}	0.000	0.00	0.00	0.00	0.294	0.000
Mn	0.00	0.00	0.01	0.00	0.016	0.000
Mg	0.49	0.38	0.34	0.24	0.519	0.000
Ca	0.68	0.47	0.43	0.22	0.730	0.035
Na	0.29	0.53	0.61	0.74	0.222	0.903
K	0.00	0.00	0.00	0.00	0.000	0.000
	2.00	1.99	2.02	1.99	1.924	1.891

* Total Fe is estiminated as Fe_2O_3 in Aegirine-augite and jadeite, as FeO in sodic-augite.

Table 8 Chemical compositions of white mica.

	1	3	4	5
	80801	90404	82003	71915
SiO_2	54.48	52.14	52.13	51.14
TiO_2	0.07	0.12	0.05	0.24
Al_2O_3	24.51	26.75	24.30	26.09
Fe_2O_3	4.96	3.82	5.55	5.98
FeO	0.00	0.00	0.00	0.00
MnO	0.03	0.00	0.06	0.01
MgO	2.84	2.70	3.44	3.01
CaO	0.03	0.02	0.28	0.01
Na_2O	0.03	0.29	0.00	0.25
K_2O	9.17	10.30	10.35	9.42
H_2O (+)	4.58*	4.59	4.51	4.53
Total	100.70	100.73	100.67	100.68
Si	7.126	6.869	6.922	6.766
Al^{IV}	0.874	1.131	1.078	1.234
	8.000	8.000	8.000	8.000
Al^{VI}	2.906	3.029	2.726	2.834
Fe^{3+}	0.487	0.375	0.555	0.595
Ti	0.006	0.011	0.004	0.023
Fe^{2+}	0.000	0.000	0.000	0.000
Mn	0.003	0.000	0.006	0.001
Mg	0.553	0.525	0.680	0.593
	3.959	3.940	3.971	4.046
Ca	0.004	0.002	0.039	0.001
Na	0.007	0.073	0.000	0.064
K	1.530	1.736	1.753	1.590
	1.541	1.811	1.792	1.655

* not determined but calculated on the basis of mineral formula

Albite (No.1 in Table 6)

Albite in the westernmost part of the Ohana-zawa block is porphyroblastic. and includes epidote, sphene, and quartz in mafic schists and folded carbonaceous materials in pelitic schists.

Garnet (No.2 in Table 6)

The garnet in albite porphyroblasts is rich in CaO and MnO. In this albite porphyroblast, few epidote grains are included, although other albite porphyroblasts include many epidote grains.

Na-pyroxene (Table 7)

Chemical compositions of the Na-pyroxene are represented in a triangular diagram (Fig.19), in which the Al content was treated as proportional to the molecular ratio of jadeite/(aegirine + Ca-pyroxene) and Na content to that of (jadeite + aegirine)/Ca-pyroxene. One of Na-pyroxenes is impure jadeite and others are aegirine-augite and sodic augite.

The chemical composition of the rock containing jadeite is characterized by high Na_2O, and high Al_2O_3/Fe_2O_3 and low Fe_2O_3/FeO (Table 3, No.9). Seki (1959, 1960a,b), Seki et al. (1960) and Seki and Shido (1959) have reported jadeites from the Shibukawa district and the Kanto Mountains. Only one chemical analysis is available of these jadeites; it is included in a meta-gabbro

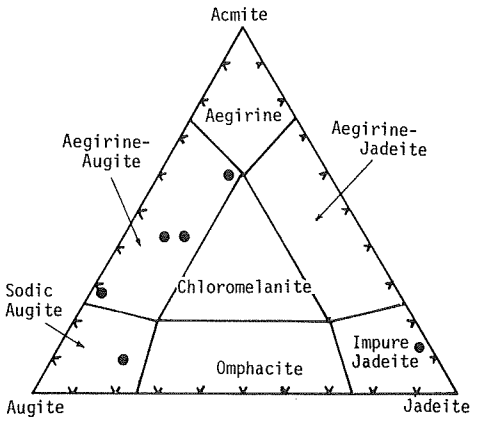

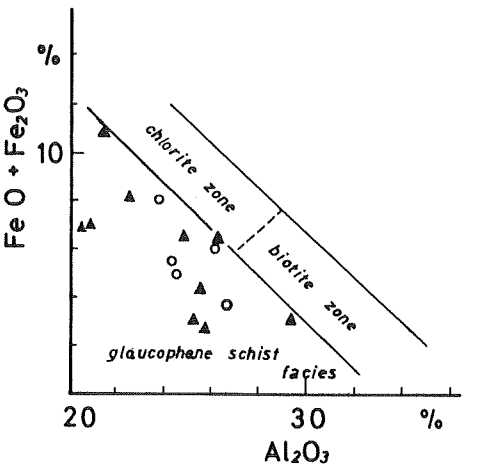

Fig. 19 (Left): Diagram showing composition of Na-pyroxene in the Oshika district. Name of Na-pyroxene is based on the classification by Essene and Fyfe (1967).

Fig. 20 (Right): $FeO+Fe_2O_3-Al_2O_3$ diagram of white mica. Facies boundaries were given by Miyashiro (1973). open circle: this paper, solid triangle: Miyashiro (1973b).

surrounded by serpentinite in the Shibukawa district (Seki, 1959). It is uncertain, however, whether these jadeites co-exist with quartz or not. No occurrence of jadeite in contact with quartz has been reported in the Sambagawa belt. Detailed description of the aegirine-augite in this district is given elswhere (Watanabe, 1975).

White mica (Table 8)

The analyzed specimens are phengite and their composition is not homogeneous. These phengites are plotted in the field of the glaucophane schist facies (Fig.20). Compositional change with increasing metamprphic grade is not recognized in this district.

Chlorite (Table 9)

Chlorite in Zone III often shows relatively strong pleochroism compared with that in Zones I and II. Chemical compositions of chlorite are plotted in Fig.21, showing no considerable difference in composition due to metamorphic

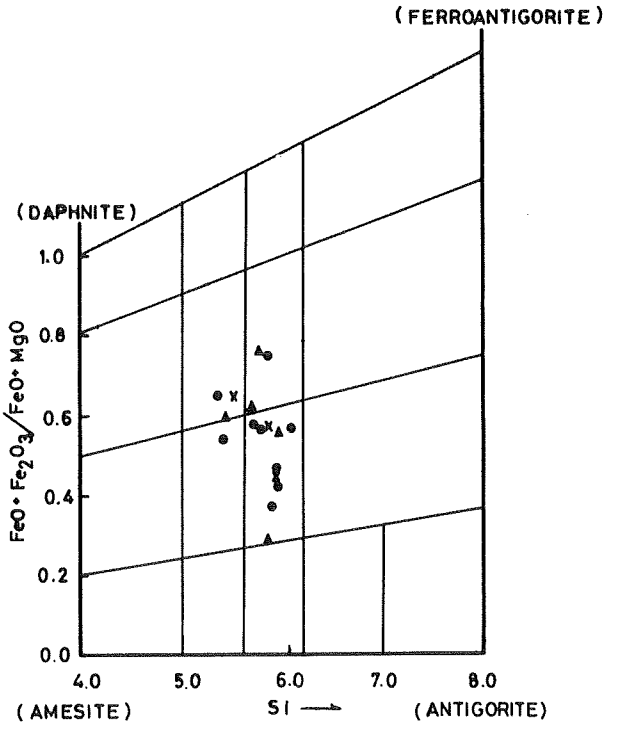

Fig. 21 Diagram showing composition of chlorite. Symbols are the same as in Fig.7. In addition to the analyses listed in Table 9 the analyses whose total values range from 98.00% to 101.49% are also plotted.

grade. SiO_2 content of the chlorite slightly decreases with increasing metamorphism (Table 9). However, there is no evidence which shows relation between metamorphic grade and the composition of the chlorite, because the two diffrent types of chlorite sometimes occur even in the same thin section. Compositional heterogeneity of chlorite is widely observed in the Sambagawa Belt (Kurata, 1972). MgO/(MgO+FeO) in chlorite does not have relation to metamorphic grade, but to the chemical composition of the host rocks.

Table 9 Representative chemical compositions of chlorite.

	1	2	3	4	5	6	7	8	9	10
	80105 (Zone I)	73007 (Zone I)	82912 (Zone I)	72811 (Zone II)	82011 (Zone III)	7072807 (Zone III)	7072807 (Zone III)	72931 (Zone III)	72910 (Zone III)	82003 (Zone III)
SiO_2	29.21	30.34	26.40	25.76	27.80	29.12	29.15	27.56	25.81	29.38
TiO_2	0.00	0.00	0.00	0.00	0.00	0.00	0.00	0.00	0.00	0.00
Al_2O_3	22.25	20.18	16.42	19.14	17.75	17.53	17.60	20.96	19.54	18.61
FeO	20.67	11.00	29.63	29.03	24.98	17.95	16.26	28.57	25.16	19.74
MnO	0.06	0.27	0.15	0.32	0.19	0.53	0.63	0.73	1.45	0.09
MgO	15.31	26.34	15.58	14.14	17.36	22.18	23.80	10.30	16.95	20.51
CaO	0.06	0.08	0.08	0.21	0.00	0.05	0.04	0.02	0.01	0.06
Na_2O	0.00	0.00	0.00	0.00	0.00	0.00	0.00	0.56	0.00	0.00
K_2O	0.00	0.00	0.00	0.00	0.00	0.00	0.00	0.00	0.00	0.00
H_2O (+)	11.82*	12.43	11.14	11.24	11.47	11.80	11.92	11.44	11.45	11.89
Total	99.38	100.64	99.40	99.84	99.55	99.16	99.40	100.15	100.37	100.28
Si	5.927	5.853	5.684	5.496	5.813	5.915	5.862	5.778	5.404	5.923
Al^{IV}	2.73	2.147	2.316	2.504	2.187	2.085	2.138	2.222	2.596	2.077
	8.000	8.000	8.000	8.000	8.000	8.000	8.000	8.000	8.000	8.000
Al^{VI}	3.249	2.442	1.851	2.312	2.188	2.115	2.032	2.957	2.227	2.345
Ti	0.000	0.000	0.000	0.000	0.000	0.000	0.000	0.000	0.000	0.000
Fe^{2+}	3.507	1.774	5.335	5.180	4.368	3.049	2.733	5.008	4.406	3.328
Mn	0.010	0.044	0.027	0.057	0.033	0.091	0.106	0.129	0.257	0.015
Mg	4.630	7.573	4.999	4.497	5.409	6.716	7.170	3.217	5.289	6.162
Ca	0.013	0.016	0.018	0.048	0.000	0.011	0.009	0.004	0.002	0.012
Na	0.000	0.000	0.000	0.000	0.000	0.000	0.000	0.227	0.000	0.000
K	0.000	0.000	0.000	0.000	0.000	0.000	0.000	0.000	0.000	0.000
	11.409	11.849	12.230	12.094	11.998	11.982	12.050	11.643	12.181	11.862

* not determined but calculated on the basis of mineral formula

Epidote (Table 10)

Epidote in Zone III shows distinct pleochroism (X = pale yellow) and that in Zones I and II shows weak pleochroism. Zonal structure is characteristic in epidote in Zones II and III and the margin is generally rich in Fe. Reverse zoning is sometimes found in Zone III. The Zonal structure of epidote is sometimes asymmetric.

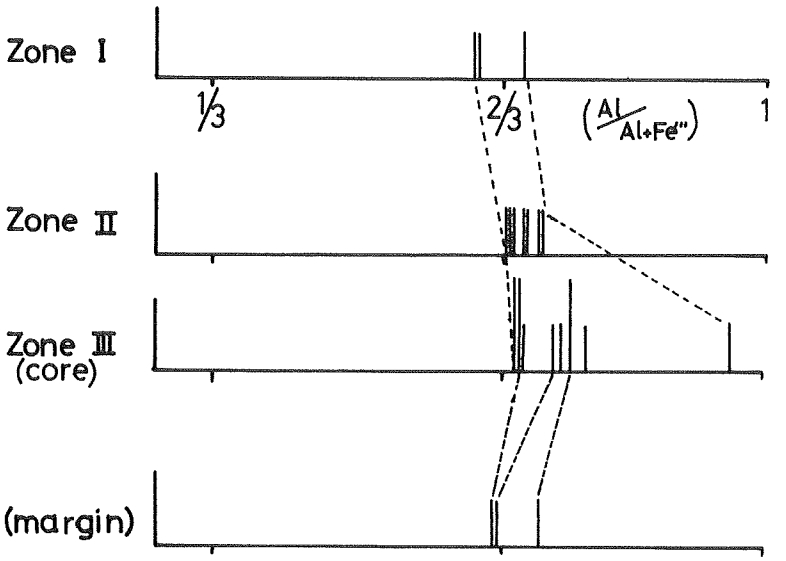

Fig. 22 Diagram showing $Al/(Al+Fe^{3+})$ ratio of epidote in the mafic rocks. In addition to the analyses listed in Table 10, the analyses whose total values range from 98.71% to 101.02% are also plotted.

$Al/(Al+Fe^{3+})$ of the epidote in each metamorphic zone is plotted in Fig.22. The Al content at the core of the epidote increases with metamorphic grade, especially from Zone II to Zone III. The change in composition of the epidote may be related to the disappearance of pumpellyite – epidote assemblage in the higher grade.

Actinolite (Table 11)

In Zone I, actinolite often occurs around relict Ca-pyroxene. In Zones II and III, occurrence of actinolite become more common than that in Zone I. Actinolite in Zone III shows the strongest pleochroism (X′ = colourless, Z′ = pale green). Composite amphibole grains composed of actinolite and Na-amphibole are sometimes observed. Compared with actinolites from Zones I and II, those from Zone III are high in Na/(Na+Ca) and slightly high in Mg/(Mg+Fe) (Fig.23). Actinolite from the Ohana-zawa block is slightly higher in Mg/(Mg+Fe) and Na/(Na+Ca) than that associated with Na-amphibole from the Tebiraki-zawa and the Torikura-yama blocks (Fig.23). Al_2O_3 content increases in Zones II and III compared with in Zone I, though no distinct difference in Al_2O_3 is found between Zones II and III (Fig.24a) except greenish actinolite mantling relict clinopyroxene and kaersutitic amphibole. In Shikoku and Kanto Mountains, Ca-amphibole in the high-grade metamorphic area where Na-amphibole is absent, is barroisite or barroisitic amphibole

Table 10 Chemical compositions of epidote.

	1	2	3	4	5	6	7	8	9	10	11	12	13	14	15	16	17
	82918	82912	801	72726	72726	72727	43001	71907	72811	72805 core	72805 margin	82217	72806 core	72806 margin	72906	82003	100607
	Zone I	Zone I	Zone II	Zone II	Zone II	Zone II	Zone II	Zone II	Zone II	Zone II	Zone II	Zone II	Zone III	Zone III	Zone III	Zone III	Zone III
SiO_2	36.77	36.73	36.57	37.81	37.16	38.84	36.85	38.43	36.33	37.52	36.70	35.94	38.88	36.99	37.94	38.13	36.82
TiO_2	0.00	0.00	0.00	0.00	0.00	0.00	0.00	0.00	0.00	0.00	0.00	0.00	0.00	0.00	0.00	0.00	0.00
Al_2O_3	20.77	22.49	20.57	22.47	22.18	22.40	21.05	21.38	27.31	23.82	21.89	22.41	23.77	23.58	23.45	21.83	22.68
Fe_2O_3	17.96	15.62	18.42	15.38	16.23	14.47	16.07	15.80	12.76	14.21	16.63	17.09	12.90	14.97	13.28	16.08	15.93
FeO	0.00	0.00	0.00	0.00	0.00	0.00	0.00	0.00	0.00	0.00	0.00	0.00	0.00	0.00	0.00	0.00	0.00
MnO	0.18	0.14	0.11	0.00	0.00	0.00	0.17	0.03	0.05	0.03	0.10	0.00	0.00	0.00	0.00	0.11	0.09
MgO	0.00	0.00	0.00	0.00	0.00	0.00	0.52	0.00	0.00	0.00	0.00	0.00	0.00	0.00	0.04	0.00	0.00
CaO	22.55	22.53	22.03	22.88	22.34	22.00	22.82	22.49	21.71	22.26	22.62	22.57	22.62	22.74	22.62	22.08	22.31
Na_2O	0.00	0.00	0.03	0.00	0.00	0.00	0.00	0.03	0.00	0.00	0.00	0.00	0.00	0.00	0.01	0.00	0.00
K_2O	0.00	0.00	0.01	0.00	0.00	0.00	0.00	0.01	0.00	0.00	0.00	0.00	0.00	0.00	0.00	0.00	0.00
H_2O (+)	1.85*	1.86	1.84	1.88	1.86	1.88	1.85	1.87	1.90	1.88	1.86	1.85	1.90	1.88	1.86	1.88	1.86
Total	100.08	99.37	99.58	100.42	99.77	99.59	99.33	100.09	99.95	99.72	99.80	99.86	100.07	100.16	99.20	100.11	99.69
Si	2.968	2.959	2.967	3.005	2.982	3.088	2.982	3.064	2.857	2.985	2.955	2.899	3.064	2.946	2.980	3.040	2.955
Al^{IV}	0.032	0.041	0.033	-	0.018	0.000	0.018	0.000	0.143	0.015	0.045	0.101	-	0.054	0.020	-	0.045
	3.000	3.000	3.000	3.005	3.000	3.088	3.000	3.064	3.000	3.000	3.000	3.000	3.064	3.000	3.000	3.040	3.000
Al^{VI}	1.943	2.096	1.935	2.105	2.079	2.099	1.990	2.010	2.397	2.212	2.032	2.030	2.208	2.160	2.151	2.052	2.101
Fe^{3+}	1.090	0.947	1.125	0.920	0.980	0.865	0.978	0.948	0.758	0.851	1.008	1.037	0.765	0.897	0.785	0.964	0.962
Ti	0.000	0.000	0.000	0.000	0.000	0.000	0.000	0.002	0.000	0.000	0.000	0.000	0.000	0.000	0.000	0.000	0.000
Fe^{2+}	0.000	0.000	0.000	0.000	0.000	0.000	0.000	0.000	0.000	0.000	0.000	0.000	0.000	0.000	0.000	0.000	0.000
Mn	0.012	0.009	0.007	0.000	0.000	0.000	0.011	0.002	0.003	0.002	0.006	0.000	0.000	0.000	0.000	0.007	0.006
Mg	0.000	0.000	0.000	0.000	0.000	0.000	0.062	0.000	0.000	0.000	0.000	0.000	0.000	0.000	0.004	0.000	0.000
	3.045	3.052	3.067	3.025	3.025	2.964	3.041	2.962	3.158	3.072	3.046	3.067	2.973	3.057	2.941	3.023	3.070
Ca	1.950	1.945	1.945	1.948	1.920	1.874	1.979	1.921	1.835	1.897	1.951	1.946	1.910	1.940	1.904	1.886	1.918
Na	0.000	0.000	0.004	0.000	0.000	0.000	0.000	0.000	0.000	0.000	0.000	0.000	0.000	0.000	0.001	0.000	0.000
K	0.000	0.000	0.001	0.000	0.000	0.000	0.000	0.000	0.000	0.000	0.000	0.000	0.000	0.000	0.000	0.000	0.000
	1.950	1.945	1.950	1.948	1.920	1.874	1.979	1.921	1.835	1.897	1.951	1.946	1.910	1.940	1.905	1.886	1.918

* not determined but calculated on the basis of mineral formula

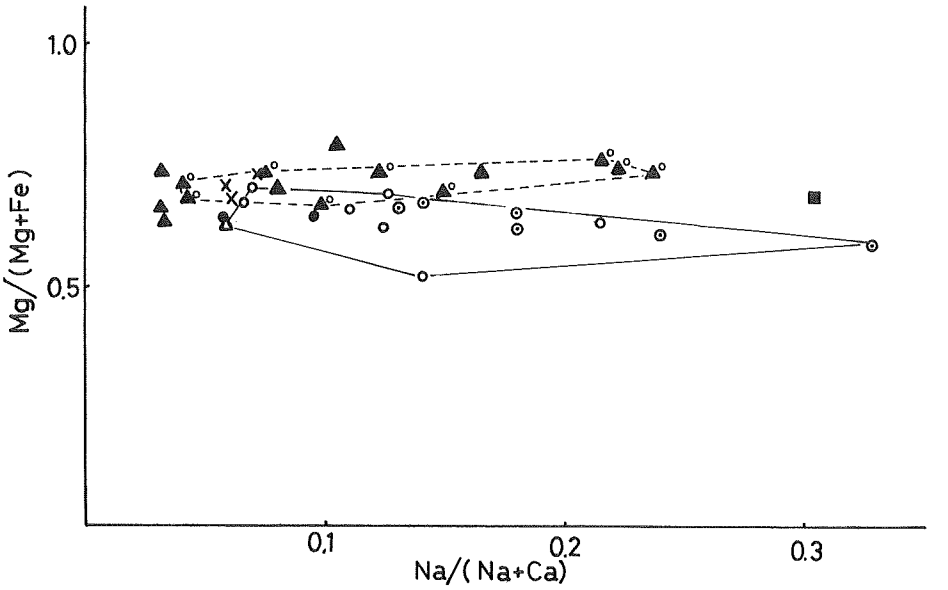

Fig. 23 Mg/(Mg+Fe) – Na/(Na+Ca) diagram of actinolite. solid circle: Zone I, cross: Zone II, solid triangle: Zone III (with O mark —— Ohana-zawa block), open circle: Zone II (coexisting with Na-amphibole), open triangle: Zone III (coexisting with Na-amphibole), open circle with dott: Kanto Mountains (coexisting with Na-amphibole (Toriumi, 1974)). solid squere: Koseto-gorge (coexisting with Ca-Na amphibole). enclosed area by solid line: actinolite coexisting with Na-amphibole in the Oshika district and Kanto Mountains. enclosed area by broken line: actinolite not coexisting with Na-amphibole in the Ohana-zawa block.

containing 2% Na_2O and 4% Al_2O_3 or more (Iwasaki, 1963; Banno, 1964; Ernst et al., 1970; Toriumi, 1975). Such Ca-amphibole is obviously different in composition from the actinolite in the Ohana-zawa block. The actinolite which contains less than 2% Na_2O and less than 4.5% Al_2O_3 can coexist with the Na-amphibole in the Sambagawa metamorphic belt. Therefore, decomposition of the Na-amphibole in the Ohana-zawa block is not expected.

The actinolite from this block which is rich in MgO, Na_2O, and Fe_2O_3/FeO (No.14 in Table 11), is magnesio-ribebeckitic rather than tremolitic in composition. The composition of the actinolite is not homogeneous. In a xenolith of gabbro at the Koshibu-gawa, two kinds of actinolite occur together with Na-amphibole in a composite grain (Fig.24b). The inner part and margin of the composite grain are occupied by actinolites and Na-amphibole is observed between two actinolites. The composition of the inner actinolite is lower in FeO, Na_2O, and CaO than that of the outer actinolite. The outer actinolite shows weak pleochroism (X′ = colourless, Z′ = faint bluish green). In a few cases, brown hornblende is preserved in the inner actinolite produced by breakdown of brown hornblende.

Table 11 Chemical compositions of actinolite. No.14 (sample No.72601) was analysed by wet chemical analysis (analyst M. Tagiri).

	1	2	3	4	5	6	7	8	9	10	11	12	13	14
	82912	92416	71909	72811	72811	72915	82003	82003	72601	72601	82217	82218	82218	72601
	Zone I	Zone II	Zone II	Zone II	Zone II	Zone III	Zone III	Zone III	Zone III	Zone III	Zone III	Zone III	Zone III	Zone III
SiO_2	53.73	53.26	53.45	53.80	54.36	55.53	54.84	53.99	57.23	54.87	55.27	57.30	54.11	52.48
TiO_2	0.00	0.46	0.00	0.20	1.12	0.00	0.00	0.00	0.03	0.13	0.02	0.01	0.00	0.62
Al_2O_3	0.72	3.55	2.01	2.90	0.91	1.98	1.46	2.49	0.60	1.77	1.47	0.66	1.65	3.01
Fe_2O_3	0.00	0.00	0.00	0.00	0.00	0.00	0.00	0.00	0.00	0.00	0.00	0.00	0.00	4.57
FeO	14.82	10.46	11.74	11.20	12.18	11.22	11.84	12.72	10.13	10.57	8.90	11.06	15.07	6.34
MnO	0.21	0.19	0.19	0.10	0.43	0.00	0.16	0.00	0.16	0.18	0.25	0.13	0.11	0.18
MgO	14.87	16.51	16.30	15.50	16.32	17.63	15.85	14.78	18.55	16.70	19.26	17.58	14.67	17.29
CaO	12.71	12.05	12.84	12.30	11.72	10.59	11.63	12.73	10.41	12.35	12.07	10.58	11.28	11.07
Na_2O	0.40	0.50	0.44	0.50	0.92	1.66	1.13	0.72	1.58	0.53	0.70	1.15	0.39	1.19
K_2O	0.04	0.04	0.03	0.00	0.03	0.00	0.05	0.00	0.04	0.06	0.02	0.06	0.00	0.05
H_2O (+)	1.99	2.09	2.12	2.07	2.07	2.13	2.07	2.07	2.14	2.09	2.12	2.13	2.06	3.13
Total	99.49	99.11	99.12	98.57	99.06	100.73	99.03	99.50	100.87	99.25	100.17	100.66	99.34	100.13
Si	7.845	7.635	7.665	7.770	7.871	7.810	7.907	7.790	8.000	7.851	7.787	8.044	7.868	7.506
Al^{IV}	0.124	0.365	0.335	0.230	0.129	0.190	0.093	0.210	-	0.149	0.213	-	0.132	0.494
	7.969	8.000	8.000	8.000	8.000	8.000	8.000	8.000	8.000	8.000	8.000	8.000	8.000	8.000
Al^{VI}	0.000	0.234	0.000	0.263	0.027	0.137	0.154	0.214	0.098	0.149	0.031	0.109	0.150	0.003
Fe^{3+}	0.000	0.000	0.000	0.000	0.013	0.000	0.000	0.000	0.000	0.000	0.000	0.000	0.000	0.491
Ti	0.000	0.049	0.000	0.021	0.000	0.000	0.000	0.000	0.003	0.013	0.002	0.001	0.000	0.067
Fe^{2+}	1.810	1.254	1.385	1.352	1.475	1.319	1.427	1.535	1.184	1.264	1.048	1.298	1.832	0.759
Mn	0.026	0.023	0.022	0.012	0.053	0.000	0.019	0.000	0.018	0.021	0.029	0.015	0.013	0.021
Mg	3.235	3.527	3.427	3.336	3.521	3.695	3.406	3.178	3.864	3.561	4.044	3.678	3.179	3.683
	5.071	5.087	4.834	4.984	5.088	5.188	5.006	4.927	5.167	5.008	5.154	5.101	5.174	5.024
Ca	1.988	1.851	2.000	1.903	1.819	1.595	1.796	1.968	1.559	1.893	1.822	1.591	1.757	1.696
Na	0.113	0.138	0.120	0.140	0.258	0.452	0.315	0.201	0.428	0.147	0.215	0.313	0.109	0.385
K	0.007	0.007	0.005	0.000	0.006	0.000	0.009	0.000	0.007	0.010	0.003	0.010	0.000	0.009
	2.108	1.996	2.125	2.043	2.082	2.061	2.120	2.169	1.994	2.050	2.041	1.914	1.866	2.090

* not determined but calculated on the basis of mineral formula except No.14.

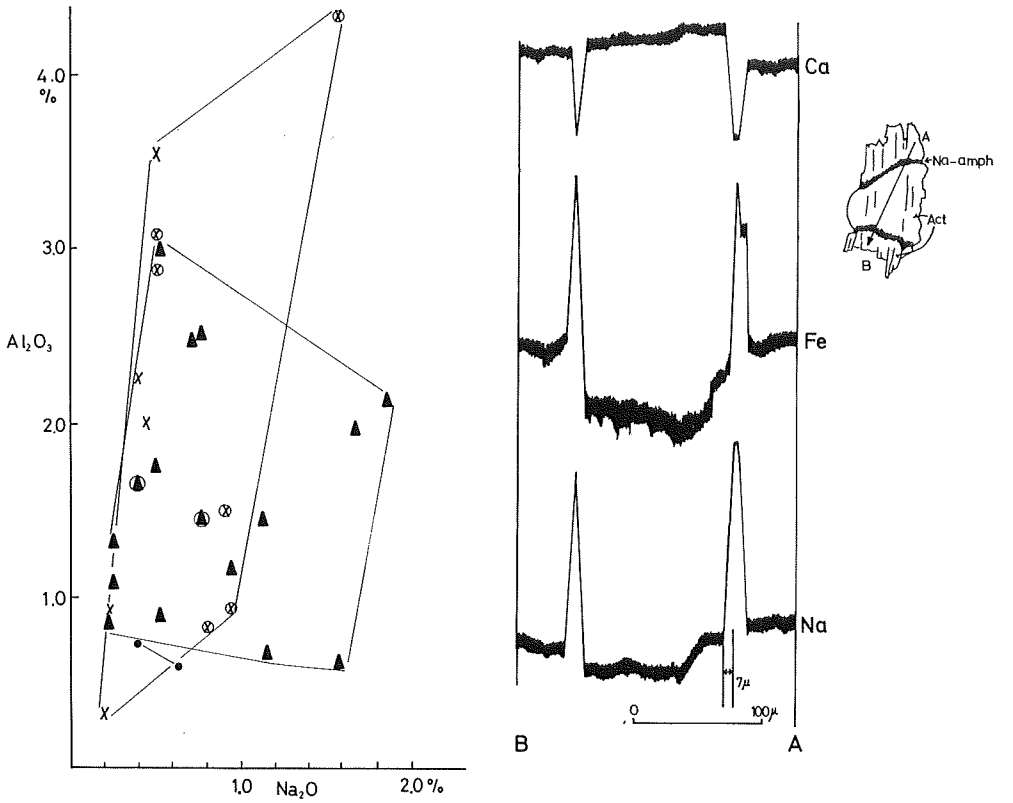

Fig. 24a (Left): Na_2O – Al_2O_3 diagram of actinolite solid circle: Zone I, cross: Zone II, solid triangle: Zone III, symbol with open circle: actinolite coexisting with Na-amphibole. In addition to the analyses listed in Table II, the analyses whose total values range from 98.04% to 101.81% are also plotted.

Fig. 24b (Right): Line scanning analysis of an amphibole composite-grain (Na-amphibole + actinolite) in sample No. 72811.

Na-amphibole (Table 12)

In Fig.25a the (310) peak position of X-ray diffraction and the relationship between 2V and refractive index of Na-amphibole are shown. In Table 12 the Fe^{3+} content of Na-amphibole is calculated as $Mg+Fe^{2+}$ content is 3.0 in Y site. The Na-amphiboles are scattered in the range from glaucophane to riebeckite (Fig.25b). The Na-amphiboles coexisting with actinolite fall near the field of magnesio-riebeckite. Within the same thin section, Na-amphibole show a variation in chemical composition, with a zonal structure whose marginal part is generally richer in the riebeckite molecule than the core.

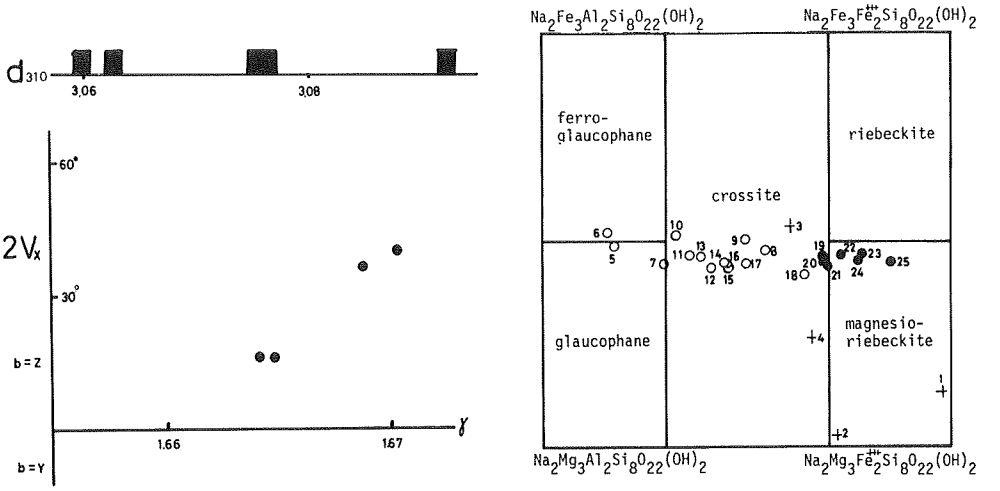

Fig. 25a (Left): d_{310} and 2V-γ of Na-amphibole in the mafic rocks.
Fig. 25b (Right): Diagram showing composition of Na-amphibole. Classification by Miyashiro (1957). Numbers correspond in Table 12. cross: Na-amphibole coexisting with actinolite, solid circle: marginal composition of zoned Na-amphibole in 72931. open circle: core composition of zoned Na-amphibole in 72931.

Pumpellyite (Table 13)

Pumpellyite in the rocks without epidote is poor in Fe, whereas that coexisting with epidote is rich in Fe. Pumpellyite of No.6 in Table 13 shows weak pleochroism (Z′ = very pale green, X′ = colourless), but others show strong pleochroism (Z′ = green, X′ = colourless). Generally speaking, the Fe content of pumpellyite seems to decrease with increasing metamorphic grade.

Biotite (No.7 in Table 13)

Biotite considered to occur in the highest grade metamorphic rocks of the Sambagawa Belt in central Shikoku (e.g. Hide, 1961; Kurata and Banno, 1971). But, recently, Tanaka and Fukuda (1974) reported that green and brown biotites occur widely in lower grade rocks such as spotted schists in the Kanto mountains, and used biotite as an index mineral in metamorphic zonation. In the Oshika district, green biotite occurs in the lower grade rocks, that is, in the non-spotted zone often associated with pyrite. In some cases, pools of biotite and pyrite cut the schistosity. The biotite is rich in the phlogopite molecule, and shows strong pleochroism (Z′ = green, X′ = very pale green).

Hornblende (Table 14)

Bluish green hornblende occurs sometimes around and along the cleavage of kaersutitic amphibole and some Ca-pyroxene. The hornblende also occurs in

Table 12 Chemical compositions of Na-amphibole.

	1 72811 Zone II	2 50801 Zone II	3 80905 Zone III	4 82218 Zone III	5 72931 Zone III	6 72931 Zone III	7 72931 Zone III	8 72931 Zone III	9 72931 Zone III	10 72931 Zone III	11 72931 Zone III	12 72931 Zone III	13 72931 Zone III	14 72931 Zone III
SiO_2	52.90	55.40	55.43	56.27	56.47	57.08	56.69	52.72	53.56	56.14	55.95	55.20	55.60	54.79
TiO_2	0.20	0.20	0.00	0.00	0.07	0.18	0.11	0.02	0.35	0.17	0.10	0.11	0.14	0.14
Al_2O_3	3.00	5.40	4.41	4.39	9.92	9.38	8.58	8.20	8.18	7.64	7.57	7.44	7.33	6.99
Fe_2O_3*	19.43	13.50	10.36	12.15	3.30	2.89	5.64	10.67	9.87	5.88	6.60	7.68	7.16	8.14
FeO	3.56	0.72	13.40	6.77	12.44	13.27	11.51	12.30	12.82	13.03	11.88	11.12	11.55	11.26
MnO	0.00	0.10	0.16	0.10	0.13	0.18	0.14	0.38	0.01	0.15	0.15	0.20	0.16	0.18
MgO	12.30	14.20	6.48	10.50	7.32	6.82	7.91	7.13	6.92	6.83	7.49	7.86	7.61	7.72
CaO	2.10	3.00	1.79	1.97	0.63	0.49	0.45	0.95	0.67	0.34	0.30	0.31	0.43	1.33
Na_2O	5.10	5.80	6.73	5.81	7.10	6.89	7.22	6.00	6.25	7.35	7.38	7.20	6.88	6.56
K_2O	0.00	0.00	0.04	0.00	0.04	0.02	0.02	0.01	0.01	0.04	0.02	0.02	0.03	0.05
$H_2O(+)$**	2.10	2.17	2.08	2.13	2.13	2.12	2.14	2.09	2.10	2.10	2.11	2.10	2.10	2.09
Total	100.49	100.49	100.88	100.06	99.55	99.32	100.41	100.47	100.73	99.67	99.55	99.24	99.05	99.25
Si	7.538	7.658	7.983	7.941	7.954	8.061	7.949	7.581	7.654	8.005	7.969	7.896	7.964	7.870
Al^{IV}	0.462	0.342	0.017	0.059	0.046	-	0.051	0.419	0.345	-	0.031	0.104	0.036	0.130
	8.000	8.000	8.000	8.000	8.000	8.061	8.000	8.000	8.000	8.005	8.000	8.000	8.000	8.000
Al^{VI}	0.042	0.538	0.732	0.671	1.602	1.562	1.368	0.971	1.033	1.285	1.240	1.515	1.201	1.054
Ti	0.022	0.021	0.000	0.000	0.007	0.019	0.011	0.002	0.038	0.018	0.011	0.012	0.015	0.016
Fe^{3+}	2.067	1.393	1.114	1.279	0.347	0.305	0.590	1.145	1.053	0.626	0.701	0.820	0.765	0.873
Fe^{2+}	0.388	0.075	1.608	0.792	1.463	1.566	1.346	1.472	1.526	1.550	1.410	1.325	1.378	1.347
Mn	0.000	0.012	0.020	0.012	0.015	0.021	0.017	0.046	0.001	0.018	0.018	0.025	0.019	0.022
Mg	2.612	2.925	1.392	2.208	1.537	1.434	1.654	1.528	1.474	1.450	1.590	1.675	1.622	1.653
	5.131	4.964	4.866	4.960	4.971	4.907	4.986	5.164	5.125	4.947	4.970	5.008	5.000	4.965
Ca	0.321	0.444	0.276	0.298	0.095	0.074	0.068	0.146	0.103	0.051	0.045	0.047	0.066	0.204
Na	1.409	1.555	1.880	1.590	1.942	1.886	1.962	1.673	1.732	2.031	2.039	1.997	1.908	1.828
K	0.000	0.000	0.007	0.000	0.007	0.004	0.003	0.002	0.002	0.007	0.003	0.004	0.005	0.010
	1.730	1.999	2.163	1.888	2.004	1.964	2.033	1.821	1.837	2.089	2.087	2.048	1.979	2.042

* Fe^{3+} is calculated as $Mg+Fe^{2+} = 3.000$ in Y site

** not determined but calculated on the basis of mineral formula

	15 72931 Zone III	16 72931 Zone III	17 72931 Zone III	18 72931 Zone III	19 72931 Zone III	20 72931 Zone III	21 72931 Zone III	22 72931 Zone III	23 72931 Zone III	24 72931 Zone III	25 72931 Zone III
SiO_2	55.86	55.79	55.66	54.19	55.35	54.63	55.06	55.52	54.48	55.38	54.33
TiO_2	0.11	0.19	0.13	0.20	0.06	0.13	0.01	0.05	0.02	0.00	0.04
Al_2O_3	6.47	6.37	5.98	4.86	3.76	3.73	3.29	3.05	2.69	2.50	2.15
Fe_2O_3	8.41	8.34	9.20	11.74	12.06	12.15	12.13	13.01	13.54	13.57	15.01
FeO	11.08	11.32	11.26	10.47	11.39	11.55	10.95	11.55	11.59	11.28	11.13
MnO	0.20	0.19	0.05	0.22	0.23	0.06	0.13	0.15	0.19	0.09	0.17
MgO	7.88	7.77	7.77	8.04	7.65	7.39	7.70	7.29	7.33	7.60	7.63
CaO	0.81	0.90	0.47	0.51	0.84	0.52	0.58	0.58	1.32	0.86	1.70
Na_2O	6.81	6.68	6.96	6.92	7.40	7.48	7.12	6.74	6.86	7.00	6.33
K_2O	0.02	0.08	0.02	0.04	0.01	0.03	0.04	0.03	0.03	0.02	0.03
$H_2O(+)$	2.10	2.10	2.09	2.07	2.09	2.06	2.06	2.04	2.06	2.07	2.06
Total	99.75	99.72	99.59	99.26	100.84	99.73	99.07	99.01	100.10	100.37	100.58
Si	7.950	7.963	7.969	7.860	7.953	7.945	8.028	7.996	7.949	8.023	7.907
Al^{IV}	0.050	0.036	0.031	0.140	0.047	0.054	-	0.004	0.051	-	0.093
	8.000	8.000	8.000	8.000	8.000	8.000	8.028	8.000	8.000	8.023	8.000
Al^{VI}	1.041	1.036	0.978	0.691	0.589	0.585	0.565	0.526	0.412	0.427	0.275
Ti	0.012	0.021	0.014	0.022	0.006	0.014	0.002	0.006	0.002	0.000	0.004
Fe^{3+}	0.898	0.888	0.983	1.271	1.294	1.319	1.320	1.424	1.475	1.456	1.630
Fe^{2+}	1.320	1.347	1.342	1.263	1.361	1.397	1.328	1.408	1.405	1.359	1.345
Mn	0.024	0.023	0.006	0.027	0.028	0.008	0.016	0.018	0.011	0.011	0.021
Mg	1.681	1.654	1.658	1.737	1.639	1.603	1.672	1.592	1.595	1.642	1.655
	4.976	4.969	4.981	5.011	4.917	4.926	4.903	4.972	4.900	4.895	4.930
Ca	0.124	0.138	0.072	0.079	0.129	0.081	0.090	0.091	0.206	0.133	0.265
Na	1.888	1.848	1.932	1.946	2.061	2.109	2.011	1.918	1.941	1.968	1.787
K	0.004	0.015	0.004	0.007	0.002	0.005	0.007	0.005	0.005	0.004	0.005
	2.016	2.001	2.008	2.032	2.192	2.195	2.108	2.014	2.162	2.105	2.057

Table 13 (Left): Chemical compositions of pumpellyite and biotite.
Table 14 (Center): Chemical compositions of bluish green hornblende.
Table 15 (Right): Chemical compositions of the blue amphibole of intermediate composition between Ca- and Na-amphiboles and the actinolite in contact with the blue amphibole (Koseto-Gorge, north of the Oshika district).

No.	1	2	3	4	5	6	7
	72902	72403	702	101602	100502	82011	82217
	Zone I	Zone I	Zone II	Zone II	Zone II	Zone III	Zone III
SiO_2	37.70	36.66	37.31	37.47	36.80	37.10	41.36
TiO_2	0.00	0.00	0.02	0.00	0.00	0.00	0.05
Al_2O_3	23.99	22.29	26.26	22.31	22.90	24.62	13.64
FeO	6.68	8.73	5.73	6.74	8.90	4.20	16.63
MnO	0.00	0.00	0.00	0.00	0.00	0.00	0.14
MgO	1.25	3.19	1.03	3.01	2.13	3.08	13.82
CaO	24.14	21.90	23.59	23.11	23.10	23.07	0.10
Na_2O	0.00	0.17	0.05	0.00	0.09	0.00	0.01
K_2O	0.00	0.00	0.00	0.00	0.02	0.00	9.72
H_2O (+)	6.17*	6.35	6.54	6.39	6.42	6.44	4.21
Total	99.93	99.29	100.53	99.03	100.36	98.51	99.50
Si	6.181	6.051	5.980	6.149	6.031	6.037	6.154
Al^{IV}	-	-	0.020	-	-	-	1.846
	6.181	6.051	6.000	6.149	6.031	6.037	8.000
Al^{VI}	4.636	4.337	4.942	4.316	4.424	4.723	0.547
Ti	0.000	0.000	0.002	0.000	0.000	0.000	0.006
Fe^{2+}	0.916	1.205	0.768	0.925	1.288	0.571	2.070
Mn	0.000	0.000	0.016	0.000	0.000	0.000	0.018
Mg	0.304	0.784	0.246	0.736	0.520	0.746	3.065
	5.856	6.326	5.974	5.977	6.232	6.040	5.704
Ca	4.240	3.873	4.051	4.064	4.056	4.022	0.016
Na	0.000	0.054	0.015	0.000	0.028	0.000	0.003
K	0.000	0.000	0.000	0.000	0.004	0.000	1.845
	4.240	3.927	4.066	4.064	4.088	4.022	1.864

* not determined but calculated on the basis of mineral formula.

	1	2
	72723	92416
SiO_2	42.40	47.74
TiO_2	0.50	1.11
Al_2O_3	13.08	5.97
FeO	18.01	15.18
MnO	0.25	0.23
MgO	10.12	14.76
CaO	10.31	10.52
Na_2O	2.70	1.99
K_2O	0.42	0.16
H_2O (+)	1.99*	2.03
Total	99.78	99.69
Si	6.375	7.044
Al	1.625	0.956
	8.000	8.000
Al	0.694	0.082
Ti	0.056	0.123
Fe	2.265	1.873
Mn	0.032	0.028
Mg	2.267	3.245
	5.314	5.351
Ca	1.661	1.664
Na	0.788	0.569
K	0.081	0.030
	2.530	2.263

* not determined but calculated on the basis of mineral formula

	Ca-Na amphibole	actino-lite
SiO_2	54.09	55.65
TiO_2	1.60	0.10
Al_2O_3	1.63	0.92
Fe_2O_3*	3.22	3.10
FeO	15.53	9.88
MnO	0.11	0.21
MgO	10.64	15.53
CaO	5.73	9.45
Na_2O	4.64	2.23
K_2O	0.04	0.10
H_2O(+)**	2.04	2.09
Total	99.27	99.26
Si	7.939	7.975
Al^{IV}	0.061	0.025
	8.000	8.000
Al^{VI}	0.221	0.130
Ti	0.177	0.011
Fe^{3+}	0.356	0.335
Fe^{2+}	1.906	1.184
Mn	0.014	0.025
Mg	2.328	3.316
	5.000	5.000
Ca	0.902	1.451
Na	1.320	0.620
K	0.007	0.018
	2.229	2.089

* Fe^{3+} is calculated as Y=5.000

** not determined but calculated on the basis of mineral formula

the cores of actinolite – hornblende composite grains. The hornblende shows distinct pleochroism (X′ = light green, Z′ = bluish green), and is rich in FeO (Fig.26). This hornblende has not always been produced during metamorphism, but might also have been produced by igneous activity. However, since the Ti content gradually decreases from kaersutitic amphibole to hornblende and the hornblende occurs as fine-grained elongate minerals, there is a possibility that the hornblende has been produced by removal of Ti from kaersutitic amphibole during metamorphism.

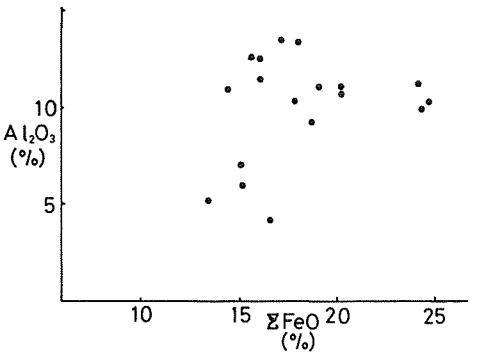

Fig. 26 Al_2O_3 – FeO diagram of bluish-green hornblende. Representative chemical compositions are listed in Table 14.

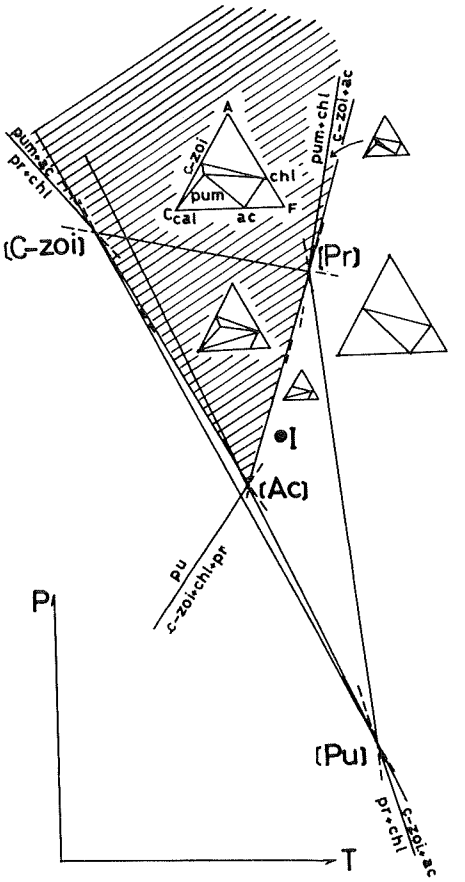

Fig. 27 Hypothetical P/T diagram for a part of three component-six phase (actinolite, pumpellyite, chlorite, clinozoisite, calcite, and prehnite) net work.
[Pr]: invariant point, prehnite absent.
[c-Zoi]: invariant point, clinozoisite absent
[Ac]: invariant point, actinolite absent
[Pu]: invariant point, pumpellyite absent
ac: actinolite, pum: pumpellyite, chl: chlorite, c-zoi: clinozoisite, cal: calcite, pr: prehnite, I: invariant point for four phase assemblage, actinolite, pumpellyite, chlorite, and clinozoisite at about 345°C, 2.5 kb (Nitsch, 1971).

Metamorphic Facies and Facies Series

Coexistence of actinolite and Na-amphibole

Na-amphibole and actinolite often occur in contact with each other in Zones II and III. Two pairs of this assemblage from Zones II and III (Sample Nos.82218 and 81905) were analysed. Values of K'_D : (Fe/Mg in Na-amphibole) / (Fe/Mg in Ca-amphibole) are 1.63 (Zone III) and 1.88 (Zone II) repectively, and shift to high Fe content in Na-amphibole compared with that of the Sambagawa Belt in Shikoku (Ernst et al., 1970).

Iwasaki (1963) and Coleman and Papike (1968) gave the range of the miscibility gap between Ca and Na amphiboles. Toriumi (1975) also examined the quarternary miscibility gap in the system of actinolite – glaucophane – magnesioriebeckite – tschermakite at 330°C and Toriumi (1974) suggested that the gap disappears at the temperature of the Kyanite – staurolite zone of Klein (1969). Katagas (1974) mentioned that the gap may disappear at higher temperatures than the glaucophanitic facies. On the other hand, Nakajima (1975) reported the occurrence of riebeckitic actinolite in the lower grade rocks of the pumpellyite – actinolite zone in the Sambagawa Belt, Shikoku, Therefore, the temperature at which the miscibility gap disappears still remains a problem.

Recently, blue amphiboles, intermediate composition between Ca- and Na-amphiboles, were found at the Koseto-gorge on the northern extension of the Shin'nagi-zawa block.The chemical compositions of the blue amphibole and the actinolite in contact with this blue amphobole are shown in Table 15. The ratio of Fe/Mg in the actinolite coexisting with this blue amphibole generally falls between the field of actinolites coexisting with Na-amphibole and those not coexisting with Na-amphibole, (Fig.31). This blue amphibole is riebeckitic in composition as Al_2O_3 is low. The miscibility gap between Ca-amphibole and riebeckite may disappear at the temperature of formation of the pumpellyite – actinolite zone.

Zonal structure and compositional heterogeneity of minerals

Zonal structure is often recognized in the epidote and the Na-amphibole. In the epidote, the marginal part is generally rich in FeO, though the reverse pattern is rarely recognized. FeO enrichment in the marginal zone of the epidote suggests that this part has been recrystallized under retrogressive conditions, as the Al content in epidote increases with increasing metamorphic grade. In the Na-amphibole, the marginal part is richer in FeO and poorer in Al_2O_3 ; it is well developed in the direction of the c-axis, but poorly developed in the directions of the a- and b-axes. If the assumption of Miyashiro and Banno (1958) is valid, it is likely that the decrease of load pressure causes the

decrease of Al_2O_3 in the marginal part.

Actinolite, chlorite, pumpellyite, phengite etc. are heterogeneous in composition. The heterogeneity seems to depend partly on differences in contact minerals. In sample 92416, the actinolite occurring around relict clinopyroxene is poor in Na_2O, FeO, and Al_2O_3 (SiO_2 53.26%, Al_2O_3 3.55, FeO 10.46, MgO 16.51, CaO 12.05, Na_2O 0.50), but that in contact with albite is rich in these components (SiO_2 52.23%, Al_2O_3 4.33, FeO 14.14, MgO 13.70, CaO 10.02, Na_2O 1.53). In Sample 82218, the actinolite in contact with Na-amphibole is also rich in FeO (about 4%) compared with other actinolite. These data may indicate that equilibrium was not attained in several mm. However, judging from the occurrence of pumpellyite with low Fe between chlorite and pumpellyite with high Fe (see p.657) the mineral assemblage may be in equilibrium within a distance of a few ten microns in mafic layers of mafic schist in the highest grade part of Zone I.

Metamorphic facies

Mineral assemblages in the mafic rocks consist of pumpellyite, actinolite, epidote, chlorite, Na-amphibole, calcite, sphene, albite, and quartz. Occurrences of the Na-amphibole and the pumpellyite are controlled by bulk compositions of host rock. These occurrences of the Na-amphibole and pumpellyite shows that Zones II and III belong to neither typical glaucophane schist facies nor typical pumpellyite – actinolite schist facies whereas Zone I may belong to pumpellyite – actinolite schist facies of Hashimoto (1966). Mineral assemblages corresponding to greenschist facies, such as actinolite – chlorite – epidote – albite – quartz, are common in this district. However, facies of the rocks being considered should not belong to greenschist facies because of the occurrence of Na-amphibole, but to the glaucophane schist facies if Miyashiro's (1973b) definition is followed. The higher grade part of Zone III may belong to the glaucophanitic greenschist facies proposed by Winkler (1965), whereas, Zones I and II belong to pumpellyite – actinolite facies proposed by Seki (1969). This facies does not correspond to the pumpellyite – actinolite schist facies proposed by Hashimoto (1966), in which Na-amphibole and jadeitic pyroxene are absent. It is more suitable that metamorphic facies in this district should belong to a transitional facies between typical glaucophane schist, pumpellyite – actinolite schist, and greenschist facies, than that this facies correspond to a defined facies.

Stability field of pumpellyite – actinolite assemblage

In Zones I and II, the following minerals are stable in the mafic rocks with low Fe_2O_3/FeO pumpellyite, actinolite, epidote, chlorite, calcite, sphene,

albite and quartz. Considering that SiO_2 is excess and TiO_2 is indifferent, the mole fraction of CO_2 in the fluid phase is fixed, and Fe_2O_3 enters into epidote, paragenetic relations of the above minerals can be plotted in the ACF diagram and treated as in three component systems. When prehnite is present in addition to the five minerals mentioned above, paragenetic relations of these minerals can be obtained from Schreinemakers' bundle of three component-six phase assemblages (Schreinemakers, 1915–25; Korzhinskii, 1958; Zen, 1966). Detailed discussion of this treatment has already been given by Watanabe (1974). The result is shown is shown in Fig.37, in which temperatures and pressures ($P_{solid} = P_{H_2O}$) are quoted from the basis of the experimental data by Nitsch (1971). The stability field of the pumpellyite – actinolite assemblage is shown by the hatched area in Fig.27.

The stability field of each mineral assemblage also depends strongly on the amount of H_2O and CO_2 in the fluid phase as well as pressure and temperature (Greenwood, 1962).

There are some difficult problems in the application of the results obtained by theoretical considerations and experiments on the natural rocks. Problems arise due to simplification of the natural rocks. Moreover, fluid pressure in nature has been greater than water pressure, because CO_2 was present in the fluid. Therefore the earlier discussion of Watanabe (1974) is open to question.

Presence or absence of other minerals gives also clues to the estimation of the metamorphic conditions producing the rocks. Absence of metamorphic aragonite shows that the pressure has been lower than that of the calcite-aragonite transformation. Judging from the presence of jadeite without quartz, the pressure seems to have been within the jadeite stability field (Robertson et al., 1957), or the pressure has been slightly lower, because the jadeite stability field decreases when acmitic and diopsidic molecules are contained in jadeite (Newton and Smith, 1967). The pressure must correspond to the stability field of lawsonite, because lawsonite occurs in the northern extension of the Oshika

Plate 1 a: Flat S_2 and vertical enveloping surface of S_1 at the Kuro-kawa in the Tebiraki-zawa block.
b: Close-packed pillow lava* at the Shin'nagi-zawa. *after Carlisle (1963).
c: Contact altered zone by serpentinite at the lower stream of Shio-kawa. Left side is the altered zone. Note that S_1 of the pelitic schist becomes obscure in the contact effect of serpentinite.
d: Hyaloclastic breccia at Shio-kawa.

Plate 1

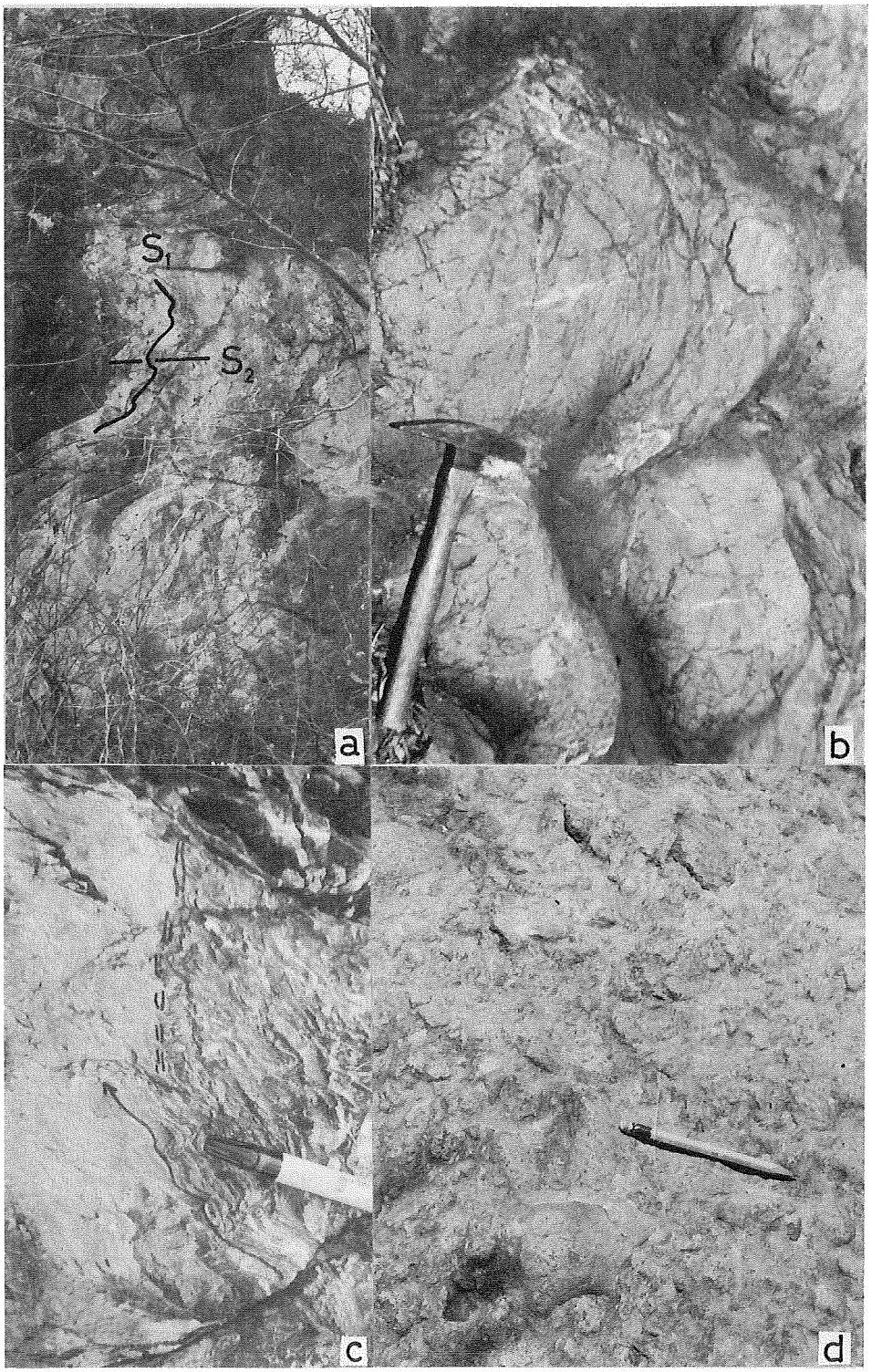

district (Hashimoto, 1960) and the Sambagawa metamorphic terrain of the Kanto Mountains, east of Oshika (Seki, 1957, 1958a). According to the discription by Seki (1957), lawsonite often occurs in the mafic rocks having peculiar composition, i.e. rocks of high CaO and low MgO and high

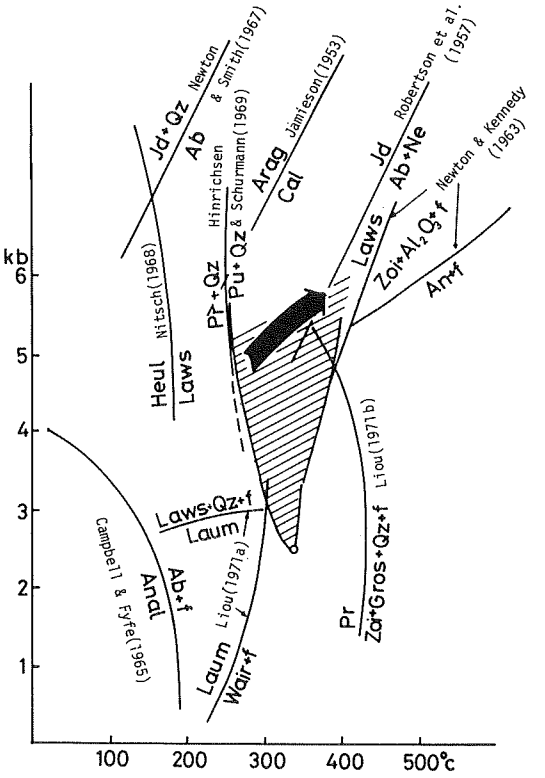

Fig. 28 Inferred P-T stability field ($P_{total} = P_{H_2O}$) of the mineral assemblage of the Sambagawa and Chichibu Belts in the Oshika district (arrow). Hatched area corresponds to that in Fig.37, showing stability field of pumpellyite-actinolite assemblage. Jd: jadeite, Qz: quartz, Ab: albite, Heul: heulandite, Laws: lawsonite, Pr: prehnite, Pu: pumpellyite, Arag: aragonite, Cal: calcite, Ne: nepheline, Zoi: zoisite, f: fluid phase, An: anorthite Gros: grossular, Laum: laumontite, Wair: wairakite, Anal: analcime.

Plate 2 a: Dendritic pyroxene in greenstones (sample No.90501). Scale is 0.1 mm.
b: Texture of hyaloclastite (sample No.101310). Scale is 0.1 mm.
c: Glass shard texture in meta-hyaloclastite (sample No.7180706). Scale is 0.1 mm.
d: Boundary between two different foliated structures. Scale is 0.1 mm.
e: Mafic shists intercalating thin siliceous schists (Si) at Kuro-kawa in the Tebiraki-zawa block.

Plate 2

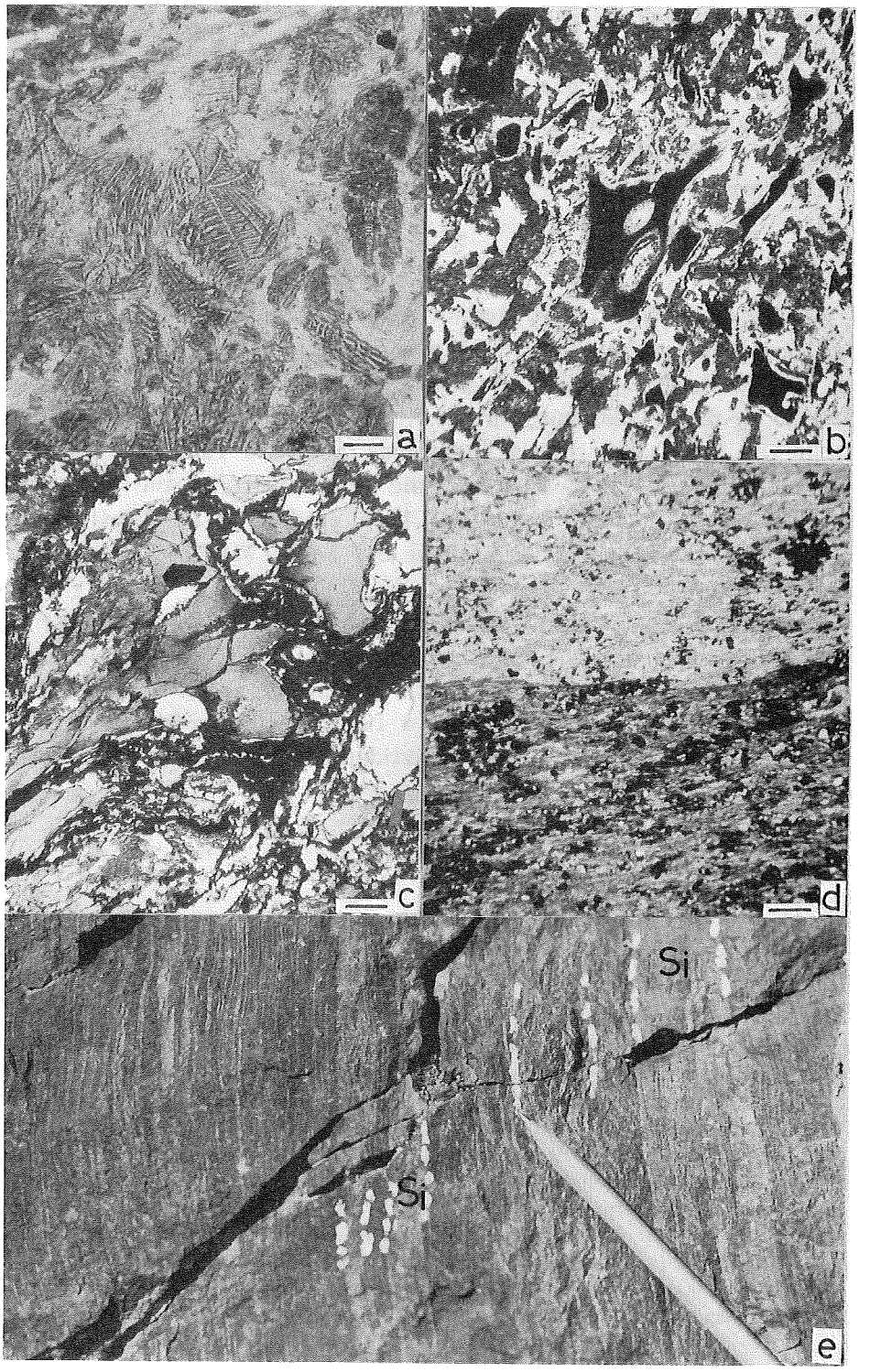

Fe_2O_3/FeO. Lack of lawsonite occurrences is considered to be due to the absence of rocks having such peculiar compositions.

The metamorphic conditions can be illustrated as in Fig.28. The estimated stability field is not contradictory to the assumption of the upper limit of the pumpellite-actinolite facies by Liou (1971). Taking the estimated stability field of crossite – actinolite paragenesis by Dobretsov et al. (1974) into consideration, the pressure may shift to the higher pressure side.

Age of the Metamorphism

The age of the Sambagawa metamorphism has been considered to lie in the range from Late Permian to Early Cretaceous (Minato et al. ed., 1965; Ichikawa et al. ed., 1970; Miyashiro, 1973a; Minato, 1973). The upper limit of the age is estimated by the pebbles and grains derived from the Sambagawa and Chichibu Belts in the Arita series, Lower Cretaceous (Seki and Takizawa, 1965; Seki, 1965; This paper). These facts indicate that a part of the rocks of the Sambagawa and Chichibu Belts have been eroded, at the latest, in Early Cretaceous. A Rb-Sr age by Yamaguchi and Yanagi (1970), 110×10^6 m.y., may show the erosion age.

Metamorphic minerals and schists derived from the Sambagawa are often reported from the rocks of Late Cretaceous (e.g. Takei, 1964; Teraoka, 1970). This age coincides with the younger radio-isotope age i.e. $85 - 94 \times 10^6$ m.y. (Hayase and Ishizaka, 1967), $82 - 93 \times 10^6$ m.y. (Banno and Miller, 1965). Consequently, the Sambagawa Belt is considered to have widely eroded in Late Cretaceous.

Plate 3 a: Micro-grading structure shown by change in grain size of relict clinopyroxene and its alternation products (dark grains), (sample No.72932). Scale is 1 mm.
b: Asymmetrical texture of mafic layer in mafic schist (sample No.51506). Amount of actinolite decrease and amount of epidote and sphene increase to the upward side in the layer. Scale is 0.1 mm.
c: Asymmetrical foliated layer in the mafic schist (sample No.82015). The light layer is mainly composed of quartz and albite. The dark layer is mainly composed of chlorite, epidote, and sphene. Scale is 1 mm.
d: F_1-a fold in semi-schist from Shio-kawa. Note the partial arrangement of chlorite (dark part) along the axial plane cleavage of F_1-a fold (arrow sign). Scale is 1 mm.

Plate 3

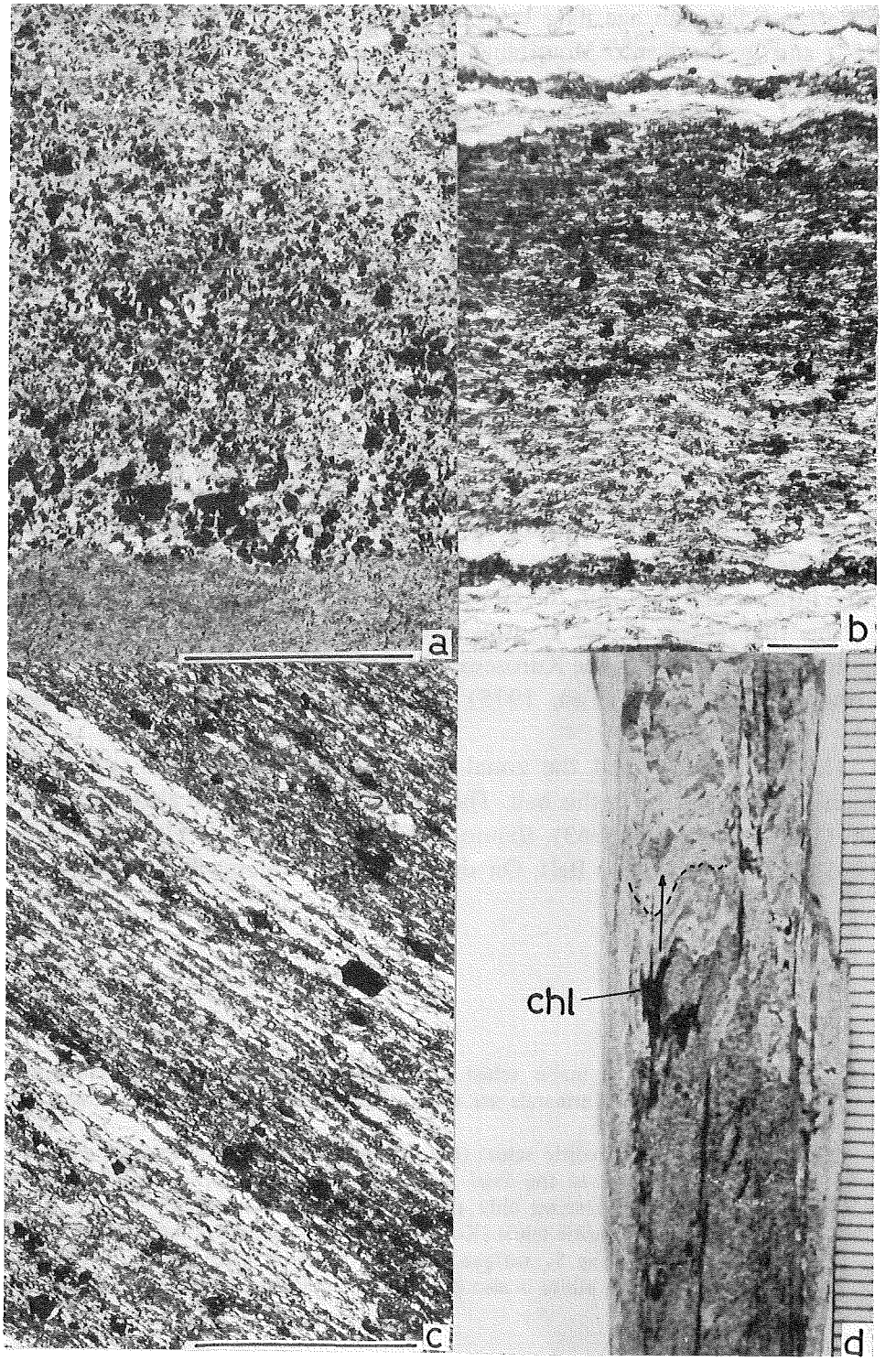

In some weakly metamorphosed rocks of the Chichibu Belt, fossils indicating a Permian age have been discovered in central Shikoku (Ishii et al. 1957) and in the Kanto Mountains (Chichibu Research Group, 1961; Okubo and Horiguchi, 1969). Therefore, the Permian rocks have suffered the Sambagawa metamorphism. Triassic rocks occur in the southern extention of the Chichibu Belt in the Oshika district (Sakamoto, 1976). Judging from the data for the metamorphism in this district, the Triassic rocks seem to have weakly suffered the Sambagawa metamorphism. However, in the area including the Kurosegawa Tectonic zone in the Chichibu Belt, such as in Shikoku, the Chichibu terrain has suffered a diastrophism going rise to the Sakashu unconformity before the Upper Triassic (Ichikawa et al., 1953). In this area, continuous prograde metamorphism from the southern margin of the Chichibu Belt, where Triassic rocks may be contained, to the Sambagawa Belt is not recognized (Ishii et al., 1957; Banno, 1964; Suzuki, 1971).

Yao (1975, p.141) mentioned the geologic history from Late Paleozoic to Mesozoic of southwest Japan as follows: "During the Late Permian and the Early Triassic, the Late Paelozoic geosyncline site underwent a diastrophism (First stage of the Honshu orogeny) — through the end of the Late Triassic – Early Jurassic diastrophism, the Honshu Geosyncline become extinct as whole" If "the first stage of the Honshu Orogeny" had not been related to the Sambagawa Belt, but to the Kurosegawa Tectonic Zone, "Late Triassic – Early Jurassic diastrophism" (Yao, 1975) might have prevailed in the Sambagawa Belt.

The author described the zonal structure of Na-amphibole and epidote, which is characteristic in this belt. These zonal structure were also described by Seki (1958b), Iwasaki (1963), Banno (1964), Ernst et al. (1970), and Toriumi (1975) in the Sambagawa Belt. On the basis of mesoscopic structure in schists,

Plate 4 a: F_1-b1 fold in a mafic schist (Kosibu-gawa). Needle like minerals are Na-amphibole, other minerals are quartz. lift: polarizer only, right: crossed polars (enlarged).

b: F_1-b2 fold in a pelitic schist (Shio-kawa). Elongated minerals are white mica which lie parallel to the axial plane. Texture of quartz is nearly granoblastic polygonal. lift: polarizer only, right: crossed polars (enlarged).

c: F_1-b3 fold in a pelitic schist (Koshibu-gawa). Elongated minerals are white mica which lie along the S_1 surface. Texture of quartz grain is nearly granoblastic polygonal. Minor albite is also present. lift: polarizer only, right: crossed polars (enlarged).

Plate 4

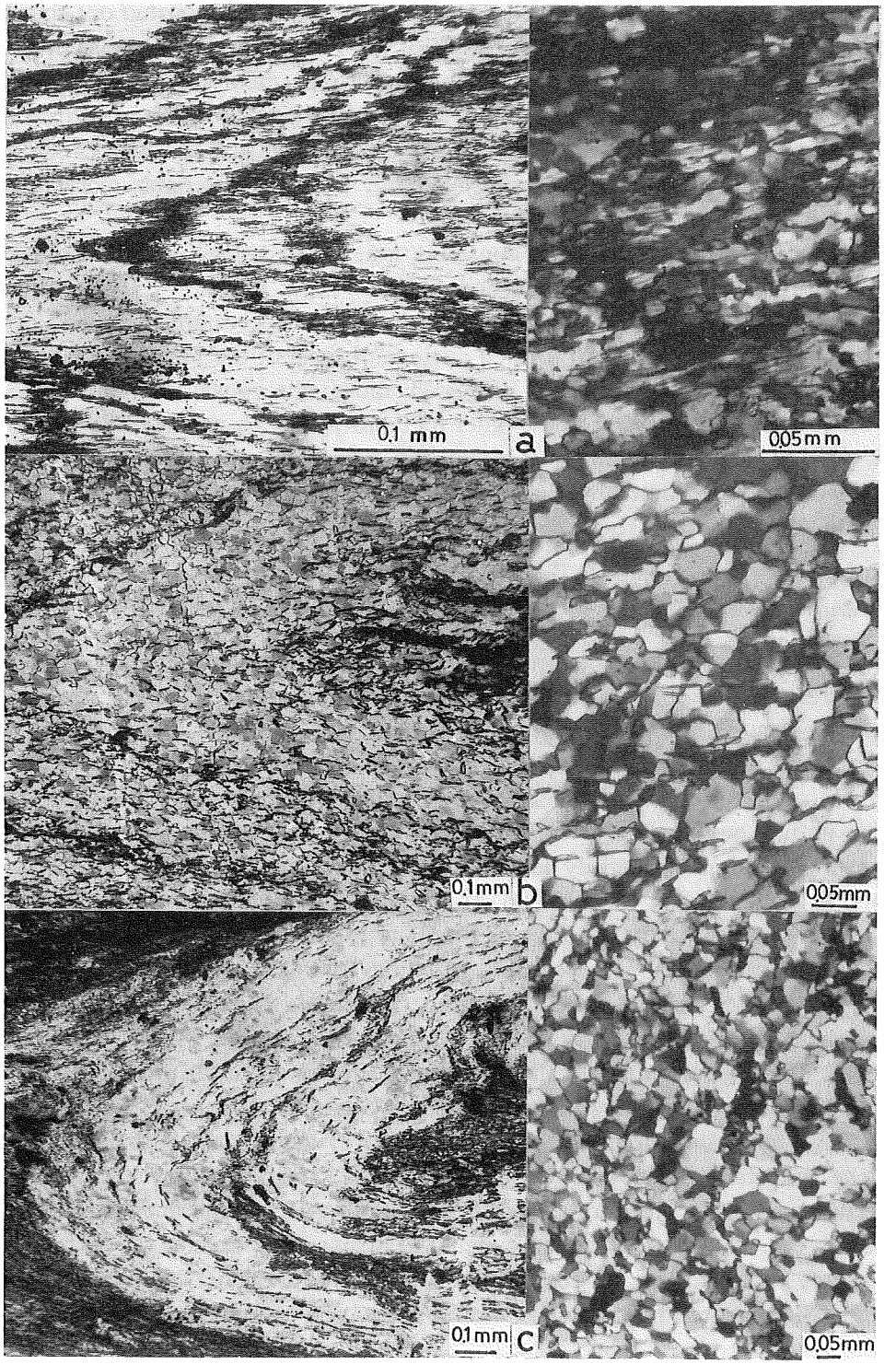

the formation of these zonal structures are not related to the F_2 folding and the later foldings, but to the F_1 folding. Higashino (1975) pointed out that the mineral assemblage "muscovite + chlorite + biotite" was considered to recrystallized in a later stage of the Sambagawa metamorphism in central Shikoku, the assemblage is favored by the decrease of load pressure. The occurrence of the zonal structure of the Na-amphibole and the epidote and the biotite mentioned above suggest speculatively a long and variable recrystallization periods.

Inferred from the geological consideration, the first stage of the Sambagawa metamorphism may have proceeded before "Late Triassic – Early Jurassic diastrophism". F_2 folding with retrogressive partial recrystallization and other later folding may have been formed during upheaval of the Sambagawa Belt. In addition to the metamorphism discussed above, the rocks of granulite facies which seem to have suffered the older metamorphism are reported by Banno et al. (1976) and Yokoyama (1976) in the Sambagawa Belt in Shikoku. The genissose rocks reported by Murai, Takei, and Hirano (1976) may be equivalent to the above granulite rocks.

Acknowledgements

The author wishes to express his cordial thanks to Professor Y. Katsui and Emeritus Professor T. Ishikawa of Hokkaido University for their continuing guidance and encouragement. He would also like to acknowledge the continuing guidance of Dr. Y. Kawachi of Otago University and the advice of Professors M. Hunahashi, K. Yagi and S. Hashimoto of Hokkaido University. The author has benefited from the discussion and assistance of the following persons, which are gratefully acknowledged: Dr. Y. Oba (Yamagata University), Drs. K. Okumura, Y. Soya, S. Igi, M. Yuasa (Geological Survey of Japan), the members of the Reserch Group of the Akaishi Mountainlands, Dr. T. Yamada (Shinshu University), Mr. M. Sekine (Nissaku Co., Ltd) and Dr. M. Matsushima (Tenryu middle school). Dr. S. Banno (Kanazawa University) gave valuable comments and Dr. N. Stevens (Queensland University) and Dr. K. Onuma (Hokkaido University) critically read the paper in manuscript. Dr. M. Tagiri (Ibaraki University) analysed an actinolite. Graduate students (Department of Geology and Mineralogy, Hokkaido University) and Dr. S. Sayama (Government Industrial Development Laboratory, Hokkaido) helped the author. Mr. Ikeda and Mr. Matsuura and their families kindly helped the author during the field work. Mrs. S. Yokoyama typed the manuscript. Thanks are also due to these persons. Part of the cost for the present study was defrayed by Grant for Scientific Research from the Ministry of Education of Japan.

Appendix Locality map of analysed samples

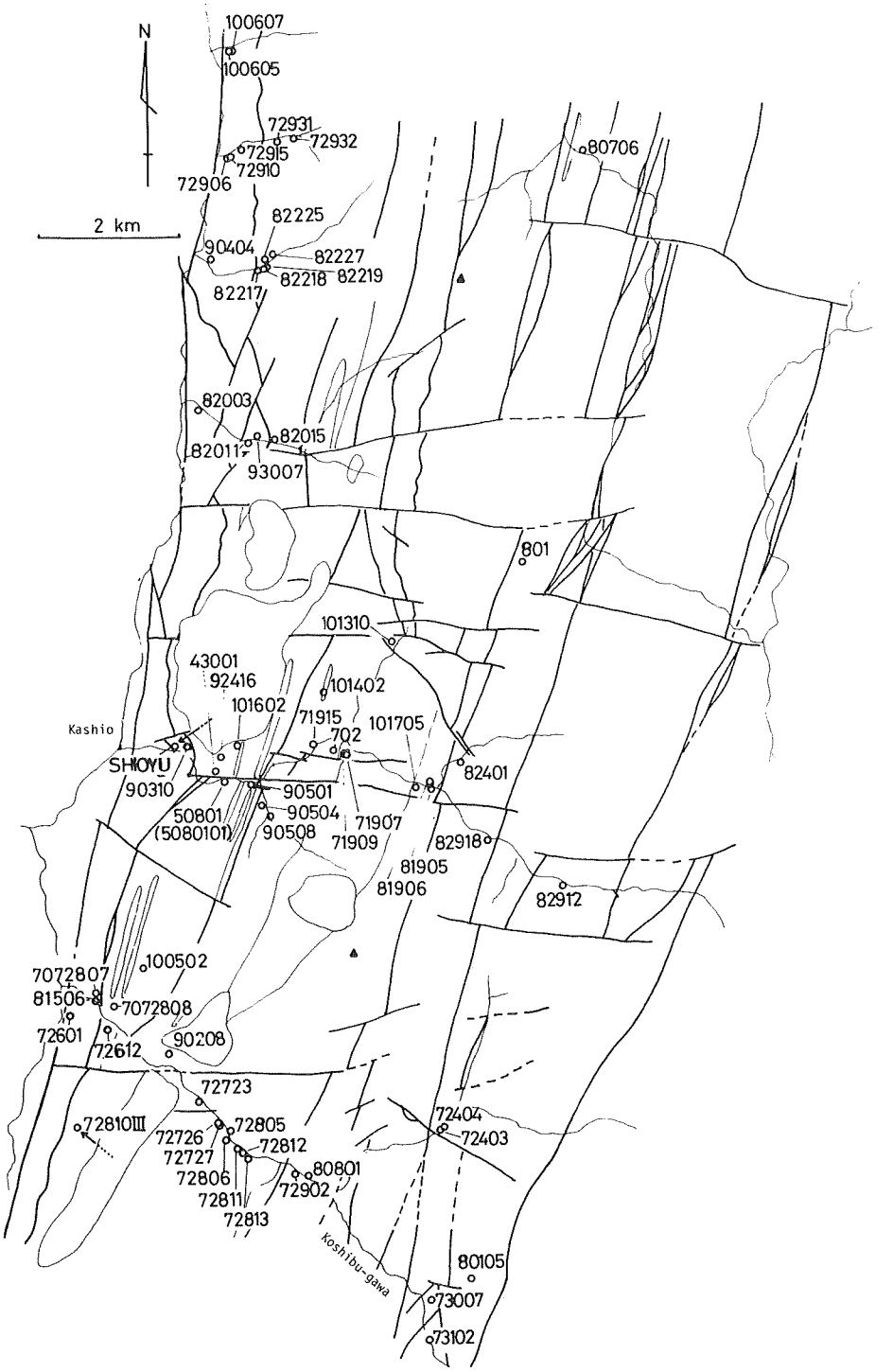

References

Banno, S., Petrologic studies on Sanbagawa crystalline schists in the Bessi – Ino district, central Sikoku, Japan. *Jour. Fac. Sci. Tokyo Univ.*, section II, 15: 203-319.

Banno, A. and Miller, A., 1965. Additional data on the age of metamorphism of the Ryoke-Abukuma and Sanbagawa metamorphic belts, Japan. *Jap. Jour. Geol. Geogr.*, 36: 17-22.

Banno, S., Yokoyama, K., Iwata, O., and Terashima, S., 1976. Genesis of epidote amphibolite masses in the Sanbagawa metamorphic belt of central Shikoku. *Jour. Geol. Soc. Japan*, 82: 199-210 (in Japanese with English abstract).

Bence, A.E. and Albee, A.L., 1968. Empirical correction factors for the electron microanalysis of silicates and oxides. *Jour. Geol.*, 76: 382-403.

Cambell, A.S. and Fyfe, W.S., 1955. Analcine-albite equilibria. *Am. Jour. Sci.*, 263: 807-816.

Carlisle, D., 1963. Pillow breccias and their aquagene tuffs, Quadra island, British Columbia. *Jour. Geol.*, 71: 48-71.

Carter, N.L., Christie, J.M. and Griggs, D.T., 1964. Experimental deformation and recrystallization of quartz. *Jour. Geol.*, 72: 687-733.

Chichibu Research Group 1961. On the Palaeozoic formations and geologic structure of the Kanna-gawa district. *Earth Science (Chikyu Kagaku)*, 57: 1-11 (in Japanese with English abstract).

Clark, S.P., 1957. A note on calcite-aragonite equilibrium. *Amer. Mineral.*, 42: 454-456.

Coleman, R.G. and Papike, J.J., 1968. Alkali amphiboles from the blueschists of Cazadero, California. *Jour. Petrol.*, 9: 105-122.

de Sitter, L.V., 1956. *Structural geology*. McGraw-Hill, New York 552 pp.

Dobretsov, N.L., Sobolev, V.S., Sobolev, N.V., and Khlestov, V.V. (translated by Brown, D.A., 1975), *The facies of regional metamorphism at high pressures*. Australian National University, Canbera, 363 pp.

Ernst, W.G., Seki, Y., Onuki, H. and Gilbert, M.C., 1970. Comparative study of low-grade metamorphism in the California coast Ranges and the Outer metamorphic belt of Japan. *Mem. Geol. Soc. Am.*, 124: 276 pp.

Essene, E.J. and Fyfe, W.S., 1967. Omphacite in California metamorphic rocks. Contr. Mineral, and Petrol., 15: 1-23.

Fleuty, M.J., 1964. The description of folds. *Proc. Geologists Ass.*, 75: 461-472.

Green, H.W., Griggs, D.T. and Christie, J.M., 1970. Syntectonic and annealing recrystallization of the fine-grained quartz aggregates In: H.W. Green, D.T. Griggs and J.M. Christie (editors) *Experimental and Natural Rock Deformation*. Springer, Berlin, pp. 272-335.

Greenwood, H.J., 1962. Metamorphic reactions involving two volatile components. *Carnegie Inst. Wash. Yearb.*, 61: 82-85.

Griggs, D.T., Turner, F.J., and Head, H.C., 1960. Deformation of rocks at 500 – 800°C. *Geol. Soc. Am. Memoir*, 79: 39-104.

Hara, I., 1966. Movement picture in confined incompetent leyers in flexural folding deformation of heterogeneously layered rocks in flexural folding (1). *Jour. Geol. Soc. Japan*, 72: 363-369.

Hara, I., 1971. An ultimate steady-state pattern of C-axis fabric of quartz in metamorphic tectonites. *Geol. Rundschau*, 60: 1142-1173.

Hara, I., 1974. Geological deformation of the crustal material, In: S. Ueda (editor), *Flow of solid (Kotai no Ryudo)*, Tokai University Press, Tokyo, pp. 29-52 (in Japanese).

Hara, I. and Paulitsch, P., 1971. C-axis fabrics of quartz in buckled quartz veins. *Neues Jahrb. Miner. Abh.*, 115: 31-53.

Hashimoto, M., 1960. Metamorphic rocks of the Hase district, Nagano prefecture, Japan. *Bull. National Science Museum.,* 5: 104-115 (in Japanese with English abstract).

Hashimoto, M., 1966. On the prehnite-pumpellyite metagreywacke facies. *Jour. Geol. Soc. Japan.,* 72: 253-265 (in Japanese with English abstract).

Hayase, I., and Ishizaka, K., 1967. Rb-Sr dating on the rocks in Japan, I. *Jour. Jap. Assoc. Mineral. Petrol. and Econ. Geol.,* 58: 201-211 (in Japanese with English abstract).

Hide, K., 1961. Geologic structure and metamorphism of the Sambagawa crystalline schists of the Bessi-Shirataki district in Shikoku, Southwest Japan. *Geol. Rept. Hiroshima Univ.,* 9: 1-87 (in Japanese with English abstract).

Hide, K., 1972. Significance of the finding of two recumbent folds in the Sambagawa metamorphic belt of the Nagahama-Ozu district, west Shikoku. —— Re-examination of the Besshi recumbent fold (1) —— *Memoir Fac. General Education, Horoshima Univ.* III, 5: 35-51 (in Japanese with English abstract).

Higashino, T., 1975. Biotite zone of Sanbagawa metamorphic terrain in the Siragayama area, central Sikoku, Japan. *Jour. Geol. Soc. Japan.* 81: 653-670 (in Japanese with English abstract).

Hinrichsen, von T. and Schürmann, K., 1969. Untersuchungen zur stabilität von Pumpellyit. *Neues Jahrb. Mineral. Monatsch.,* 10: 441-445.

Horikoshi, G., 1934. On the aegirine bearing green metamorphosed rock in the Kannagawa area of Kozuke. *Jour. Geol. Soc. Japan,* 41: 731-737 (in Japanese).

Ichikawa, K., Ishii, K., Nakagawa, C., Suyari, K., and Yamashita, N., 1953. On Sakashu uncomformity. *Jour. Gakugei Tokushima Univ. Nat. Sci.,* 3: 61-74 (in Japanese with English abstract).

Ichikawa, K., Fujita, Y., and Shimazu, M. ed., 1970. *The geologic development of the Japanese islands.* Tsukuji-Shokan, 232pp. (in Japanese).

Iizumi, S., 1968. The Ogawara ultrabasic intrusion, Nagano prefecture, in central Japan (part I). *Earth Science (Chikyu Kagaku),* 22: 267-273.

Iizumi, S., 1972. Rb and Sr concentrations and Sr isotopic compositions of some mafic and ultramafic rocks from Ogawara body, Nagano prefecture, central Japan. *Jour. Jap. Assoc. Mineral. Petrol. and Econ. Geol.,* 67: 203-208 (in Japanese with English abstract).

Ishii, K., Ueda, Y., and Shimazu, M., 1953. Geology and petrology of the Akaishi mountain range, Nagano prefecture. *Jour. Jap. Assoc. Mineral. Petrol. and Econ. Geol.,* 37: 123-130 (in Japanese with English abstract).

Ishii, K., Ichikawa, K. Katto, J., Yoshida, H. and Kojima, G., 1957. Geology of the Chichibu terrain along the highway from Kamiyakawa to Ino, Shikoku. *Jour. Geol. Soc. Japan,* 63: 449-454 (in Japanese with English abstract).

Ishikawa, T., 1971. Minor folds and metamorphism of Sambagawa crystalline schist in the Tenryu district, central Japan. *Jour. Earth Sci. Nagoya Univ.,* 19: 39-66.

Iwasaki, M., 1963. Metamorphic rocks of the Kotu-Bizan area. eastern Sikoku. *Jour. Fac. Sci. Tokyo Univ.,* sec. II. 15: 1-90.

Iwasaki, M., 1969. The basic metamorphic rocks at the boundary between the Sambagawa metamorphic belt and the Chichibu unmetamorphosed Paleozoic sediments. *Memoir Geol. Soc. Japan,* 4: 41-50 (in Japanese with English abstract).

Jamisesson, J.C., 1953. Phase equilibria in the system calcite-aragonite. *Jour. Chem. Phys.,* 21: 1389-1390.

Kano, H., 1961. Granite bearing conglomerate in the Todai formation of Akaishi mountains and its problem. *Jour. Geol. Soc. Japan.,* 67: 362 (in Japanese).

Katagas, C., 1974. Alkali amphiboles intermediate in composition between actinolite and riebeckite. *Contr. Mineral. and Petrol.,* 46: 257-264.

Kawachi, Y., 1970. Geology and metamorphism near the head of Lake Wakatipu. *Ph. D. Thesis, Univ. of Otago,* New Zealand, 204pp.

Kawachi, Y., and Kwanke, E., 1968. The shortening of the Akaishi axial zone in the Shimanto terrain deduced from concentrically folded quartz veins. *Jour. Geol. Soc. Japan,* 74: 9-20 (in Japanese with English abstract).

Kawachi, Y., and Okumura, K., 1972. Quantitative analyses of silicates by on-line controlled electronprobe. *Magma,* 31: 2-6 (in Japanese).

Kawachi, Y. and Watanabe, T., 1972. Relic clinopyroxene in the Sambagawa and Chichibu belts of the Oshika district, Nagano prefecture. *Jour. Jap. Assoc. Mineral. Petrol. and Econ. Geol.,* 67: 110 (in Japanese).

Kawachi, Y. and Watanabe, T., 1974. Identification of stable mineral parageneses in metamorphic rocks by phases in mutual contact and the metamorphic zonation defined by univariant reactions. *(Earth Science), Chikyu Kagaku,* 28: 1-10 (in Japanese with English abstract).

Kawachi, Y., Landis, C.A., and Watanabe, T., 1973. Pillow lava, agglutinate and associated volcanogenic rocks in spotted greenschists, blueschists and epidote-amphibolites of the Sambagawa Belt, central Shikoku, Japan. *Jour. Geol. Soc. Japan,* 79: 745-753 (in Japanesw with English abstract).

Kawachi, Y., Landis, C.A., and Watanabe, T., 1976. Hyaloclastite – a critical review. *Jour. Geol. Soc. Japan,* 82: 355-366 (in Japanese with English abstract).

Kobayashi, K., 1973. *Nihon Alps no Shizen (Nature of Japanese Alps)* Tsukiji-shokan 258pp (in Japanese).

Kojima, G., 1951. Stratigraphy and geological structure of the crystalline schist region in central Sikoku. *Jour. Geol. Soc. Japan,* 57: 177-190 (in Japanese with English abstract).

Kojima, G., 1958. The Sambagawa metamorphic zone, In: T. Ishikawa (editor), Jubilee publication in *the commemoration of Professor Jun Suzuki, M.J.A. sistieth birthday,* Commemorative Society of sixtieth birthday Professor Jun Suzuki, Sapporo pp. 988-100 (in Japanese with English abstract).

Kojima, G. and Hide, K., 1958. Kinematic interpretation of the quartz fabric of tectonites from Besshi, central Shikoku, Japan. *Jour. Sci. Hiroshima Univ.* series C, 2: 195-226.

Kojima, G. and Suzuki, T., 1958. Rock structure and quartz fabric in a thrusting shear zone: Kiyomizu tectonic zone in Shikoku, Japan. *Jour. Sci. Hiroshima Univ.* series C, 2: 173-194.

Korzhinskii, D.S., 1958. *Physico-chemical basis of the analysis of the paragenesis of minerals.* Consultants Bereau. New York., 143pp. (Japanese traslation –– Kobayashi, H. and Hayama, Y. (1968)).

Klein, C. Jr., 1969. Two amphibole assemblages in the system actinolite-hornblende-glaucophane. *Am. Mineral.,* 54: 212-237.

Kuno, H., 1968. Differentiation of basalt magma in *Basalt.* 2: 623-688.

Kurata, H., 1972. Local chemical heterogeneity of chlorites in Sanbagawa pelitic schists from Sazare area, central Shikoku. *Jour. Geol. Soc. Japan,* 73: 652-657.

Kumazawa, M., Yamazaki, T., and Tsukahara, H., 1971. Theory of stable fabric under the condition of high temperature, high pressure and non-hydrostatic stage. *Regime of lectures of scientific party of 5 society of Earth Science,* 265 (in Japanese).

Liou, J.G., 1971a. P-T stabilities of laumontite, wairakite, lawsonite, and related minerals in the system $CaAl_2Si_2O_8 - SiO_2 - H_2O$. *Jour. Petrol.,* 12: 379-411.

Liou, J.G., 1971b. Synthesis and stability relations of prehnite, $Ca_2Al_2Si_3O_{10}(OH)_2$. *Am. Mineral.,* 56: 507-531.

Maeda, S. and Kitamura, K., 1965. On the stratigraphy and geologic structure of the Todai formation in the western part of the Akaishi mountain range, central Japan. *Jour. Fac. Lit. & Sci. Univ. Chiba,* 4: 323-332 (in Japanese).

Maruyama, S., 1976. Chemical natures of the Sawadani Greenstone complex in Chichibu Belt, eastern Shikoku. *Jour. Geol. Soc. Japan.* 82: 183-197 (in Japanese with English abstract).

Matsuda, M. and Kizaki, K., 1971. Experimental deformation of polycrystalline ice with special reference to internal deformation. *Jour. Geol. Soc. Japan,* 77: 771-778 (in Japanese with English abstract).

Matsushima, N., Kamei, S., Iwai, S., Yoshida, Y., and Tachigi, S., 1957. On the Todai formation. *Jour. Geol. Soc. Japan,* 63: 416 (in Japanese).

Matsushima N., 1973. The Median Tectonic line in the Akaishi Mountains, In: R. Sugiyama -(editor), *Median Tectonic Line,* Tokai University Press, Tokyo, pp.9-27 (in Japanese with English abstract).

Minato, M., Gorai, M., and Hunahashi, M., ed., 1965. *The geologic development of the Japanese Islands.,* Tsukiji-shokan, Tokyo, 442pp

Minato, M., 1973. *Chiso-gaku,* Iwanami-shoten, Tokyo, 396pp (in Japanese).

Miyashiro, A., 1957. The chemistry, optics and genesis of the alkali-amphiboles. *Jour. Fac. Sci. Tokyo Univ.,* sec. 311: 57-83.

Miyashiro, A., 1965. *Metamorphic rock and metamorphic belts.* Iwanami-shoten, Tokyo, 458pp (in Japanese).

Miyashiro, A., 1973a. Paired and unpaired metamorphic belts. *Tectonophysics,* 17: 241-254.

Miyashiro, A., 1973b. *Metamorphism and metamorphic belts.* George Allen & Unwin Ltd, London, 492pp

Miyashiro, A. Shido, F. and Ewing, M., 1971. Metamorphism in the Mid-allantic Ridge near 24° and 30°N, *Phil. Trans. Roy. Soc. London,* A268: 589-603.

Miyashiro, A. and Banno, S., 1958. Nature of glaucophanitic metamorphism. *Am. Jour. Sci.,* 256: 97-110.

Moore, J.G., 1975. Mechanism of formation of pillow lava. *American Scientist,* 63: 269-277.

Nagano Prefectural Geological Society ed., 1962. *Geological map of Nagano prefecture* (1/200,000), Naigai-Chizu Co. Ltd., Tokyo (in Japanese).

Murai, T., Takei, K. and Hirano, H., 1976. Geological structure and metamorphic rocks around the Yoshimi Hills, eastern Kanto Mountains. *Toko-kiban (Basement of island arc),* 3, 71-72 (in Japanese).

Nakayama, I., 1950. Petrofabric study of the Oboke phyllitic sandstone. *Jour. Geol. Soc. Japan,* 56: 433-438 (in Japanese with English abstract).

Nakayama, I., 1952. On the foliation plane of the Sanbagawa crystalline schist in the Tenryu river basin. *Mem. Coll. Sci. Univ. Kyoto,* series B, 20: 47-54.

Nakayama, I., 1960. The tectonic movement and the rock structure of the Sambagawa metamorphic zone, Japan. *Monograph No.10, the association for the geological collaboration in Japan,* 40pp (in Japanese with English abstract).

Nakajima, T., 1975. Paragenesis of high temperature part of pumpellyite-actinolite facies in the Sambagawa Belt, central Shikoku. *Jour. Jap. Assoc. Mineral. Petrol. Eco. Geol.,* 70: 131 (in Japanese).

Newton, R.C. and Kennedy, G.C., 1963. Some equilibrium reactions in the join $CaAl_2Si_2O_8$-H_2O. *Jour. Geophys. Res.,* 68: 2967-2983.

Newton, R.C. and Smith, J.V., 1967. Investigation concerning the breakdown of albite at depth in the earth. *Jour. Geol.,* 75: 268-286.

Nishimura, Y., 1971. Chemical composition of basic schists from the Sangun metamorphic terrain in the Nishiki-cho district, Yamaguchi Pref. Japan. *Jour. Sci. Hiroshima Univ.,* series C, 6: 171-202.

Nitsch, K.H., 1968. Die Stabilität von Lawsonit. *Naturwissenschaften, 55: 388.*

Nitsch, K.H., 1971. Stabilitätsberziehungen von Prehnit- und Pumpellyithaltigen Paragenesen. *Contr. Mineral. Petrol.* 30: 240-260.

Okubo, M. and Horiguchi, M., 1969. *Geology of the Mamba district, Quardrangle series, scale 1:50,000.* Tokyo (8), 26:66p. Geological Survey Japan. (in Japanese with English abstract).

Okumura, K., Soya, T. and Kawachi Y., 1974. A note on the Quantitative silicate analysis by electron-probe microanalyser in *Progress of X-Ray Analysis* IV, 45-53 (in Japanese with English abstract).

Okumura, K. and Soya, T., 1976. Quantitative analysis of silicate minerals by automated electron probe microanalyser. *Jour. Mineral. Soc. Japan,* 12: 116-124 (in Japanese).

Oyagi, N., 1964. Structural analysis of the Sambagawa crystalline schists of the Sazare mining district, central Shikoku. *Jour. Sci. Hiroshima Univ.,* ser. C, 4: 271-332.

Research Group for the Crystalline Schist of Southwest Japan, 1953. On the relation between Sambagawa metamorphic rocks and non-metamorphosed Chichibu system, near Futamata town, Iwata-gun, Shizuoka prefecture. (Earth Science) Chikyu kagaku., *13: 5-6 (in Japanese).*

Robertson, E.C., Birch, F., and MacDonald, G.J.F., 1957. Experimental determination of jadeite stability relation to 25,000 bars. *Am. Jour. Sci.,* 255: 115-135.

Robertson, A.H.F. and Hudson, J.D., 1973. Cyprus umbers: chemical precipitates on a Tethyan ocean ridge. *Earth and Planetary Sci. Letters,* 18: 93-101.

Sakamoto, M., 1976. Discovery of conodonts in the Chichibu terrain, the Shimoina district, Nagano Prefecture. *Jour. Geol. Soc. Japan,* 82: 553-554 (in Japanese).

Sander, B., 1966. *An introduction to the study of fabrics of geological bodies.* (translation by F.C. Phillips and G Windson) Pergamon Press, Oxford, 641p.

Schreinemakers, F.A.H., 1951-25. *In-, mono-, and divariant equilibria:* Koninkl. Akad. Wetenschappen Te Amsterdam Proc., English edition., 18-28: (29 separate articles in the series).

Seki, Y., 1957. Lawsonite from the eastern part of the Kanto mountainland. *Jour. Jap. Assoc. Mineral. Petrol. and Econ. Geol.,* 41: 155-163 (in Japanese with English abstract).

Seki, Y., 1958a. Glaucophanitic regional metamorphism in the Kanto mountains, central Japan. *Jap. Jour. Geol. Geogr.,* 29: 234-258.

Seki, Y., 1958b. Alkali-amphiboles in the eastern part of the Kanto mountains. *Jour. Jap. Assoc. Mineral. Petrol. and Econ. Geol.,* 42: 128-135 (in Japanese with English abstract).

Seki, Y., 1960a. Distribution and mineral assemblages of jadeite-bearing metamorphic rocks in Sambagawa metamorphic terrains of central Japan. *Sci. Rep. Saitama Univ.,* ser. B, 3: 313-320.

Seki, Y., 1960b. Jadeite in Sanbagawa crystalline schists of central Japan. *Amer. Jour. Sci.,* 258: 705-715.

Seki, Y., 1961. Geology and metamorphism of Sanbagawa crystalline schists in the Tenryu district, central Japan. *Sci. Rep. Saitama Univ.,* ser. B. 4: 75-92.

Seki, Y., 1965. Jadeitic pyroxene found as pebbles in lower Cretaceous formation of the Kanto Mountains, central Japan. *Jour. Jap. Assoc. Mineral. Petral. and Econ. Geol.,* 53: 165-168 (in Japanese with English abstract).

Seki, Y., 1969. Facies series in low-grade metamorphism. *Jour. Geol. Soc. Japan,* 75: 255-266.

Seki, Y. and Shido, F., 1959. Finding of jadeite from the Sanbagawa and Kamuikotan metamorphic belts, Japan. *Proc. Japan Academy,* 35: 137-138.

Seki, Y., Aiba, M. and Kato, C., 1960. Jadeite and associated minerals in meta-gabbroic rocks of the Shibukawa district, central Japan. *Am. Mineral,* 45: 668-679.

Seki, Y. and Takizawa, H., 1965. Finding of pebbles of lawsonite- and pumpellyite-bearing rocks in a lower Cretaceous formation of the Kanto mountains, central Japan. *Jap. Jour. Geol. Geogr.,* 386: 81-87.

Shimazu, M., 1956. Ultramafic and mafic rocks of Shimo-Ina district,Nagano prefecture. *Jour. Jap. Assoc. Mineral. Petrol. and Econ. Geol.,* 40: 207-216 (in Japanese with English abstract).

Spry, A., 1969. *Metamorphic texture.* Pergamon Press, Oxford, 350p.

Suzuki, T., 1970. Röntgenographische Gefügeonalyse mit dem Zahlrohl-Texturgoniometer von Quarzschiefer aus Zentral Shikoku, Japan In: H.W. Green, DiT. Griggs and J.M. Christie (editors), *Experimental and Natural Rock Deformation.* 1-18, Springer, Berlin.

Suzuki, T., 1972. Volcanism and metamorphism of the Mikabu green-rocks in central and western Shikoku. *Research Reports Kochi Univ.,* 21: 39-62 (in Japanese with English abstract).

Suzuki, T., Sugisaki, R., and Tanaka, T., 1971. Geosynclinal igneous activity of the Mikabu green rocks of Ozu city, Ehime prefecture. *Memoirs Geol. Soc. Japan,* 6: 121-136 (in Japanese with English abstract).

Suzuki, T., Kashima, N., Hada, S. and Umemura, H., 1972. Geosyncline volcanism of the Mikabu green-rocks in the Okuki area, western Shikoku, Japan. *Jour. Jap. Assoc. Mineral. Petrol. and Econ. Geol.,* 67: 177-192.

Sweatman, T.R. and Long, J.V.P., 1969. Quantitative Electronprobe Microanalysis of rock-forming minerals. *Jour. Petrol.* 10: 332-379.

Takei, K., 1964. On lawsonite from the so-called Atokura formation. *Earth Science (Chikyu Kagaku),* 72: 36-37 (in Japanese).

Tanaka, K. and Fukuda, M., 1974. Geologic structure and metamorphic zoning of the northern extremity of the Sanbagawa Metamorphic Terrain in the Kanto Mountains – with special reference to the occurrence of biotites. *Jour. Jap. Assoc. Mineral. Petrol. and Econ. Geol.,* 69: 313-323.

Teraoka, Y., 1970. Cretaceous formations in the Onogawa basin and its vicinity, Kyushu, southwest Japan. *Geol. Sur. Japan. Rep.,* 237: 1-87.

Toriumi, M., 1974. Actinolite – alkali amphibole miscibility gap in an amphibole composite-grain in a glaucophane schist facies rocks, Kanto Mountains, Japan. *Jour. Geol. Soc. Japan.,* 80: 75-80.

Toriumi, M., 1975a. Petrological study of the Sambagawa metamorphic rocks –– The Kanto mountains, central Japan ––. *Bull. Univ. Museum, Univ. Tokyo,* 9: 99pp

Turner, F.J. and Weiss, L.E., 1963. *Structural analysis of metamorphic tectonites.* McGraw-Hill, New York, 545p.

Uchida, N., 1967. Chemical composition of basic tuff in the Mikabu and Mamba formations. *Seikei Ronso,* 6: 206-220 (in Japanese with English abstract).

Vallance, T.G., 1965. On the chemistry of pillow lavas and the origin of spilites. *Mineral. Mag.,* 34: 471-481.

Watanabe, T., 1970. Geology and structure of the Sambagawa metamorphic belt and the Chichibu belt in the Oshika district, Nagano Prefecture, Japan. *Jour. Geol. Soc. Japan,* 76: 373-388 (in Japanese with English abstract).

Watanabe, T., 1974. Some consideration on mechanism of formation of micro-folding in the Sambagawa and Chichibu belts in the Oshika district, central Japan. *Jour. Geol. Soc. Japan.,* 80: 225-238 (in Japanese with English abstract).

Watanabe, T., 1975. Aegirine-augite and sodic augite from the Sambagawa and the Chichibu Belts in the Oshika district, central Japan, with special reference to Na-metasomatism. *Jour. Fac. Sci., Hokkaido Univ.,* ser.IV, 16: 519-532.

Watanabe, T. and Kwanke, I., 1974. Multiple deformation in the Sambagawa metamorphic belt, Ina district, Nagano prefecture, central Japan. *Jour. Geol. Soc. Japan,* 80: 17-30 (in Japanese with English abstract).

Watanabe, T. and Kawachi, Y., 1975. Some aspects on the nature of original rocks, structure and metamorphism of the Sambagawa Belt in Problem on geosyncline in Japan. *Ass. Geol. Collab. Japan Monograph* 19: 81-87 (in Japanese with English abstract).

Watanabe, T., Yuasa, M., and Makimoto, H., 1976. "Mikabu" greenstones and ultramafic rocks in Ina district, Nagano prefecture. *Ryokushokuganrui (greenstones),* 1: 3-10 (in Japanese).

Watanabe, T. and Kawachi, Y. Sambagawa metamorphism in the Ina district, Nagano prefecture, central Japan. Jubilee publication in the commemoration of Professor George Kojima, sixtieth birthday (in Press).

Winkler, H.G.F., 1965. *Petrogenesis of metamorphis rocks,* Springer-Verlag, Berlin (English translation by N.D. Chatterjee), 220pp.

Yamaguchi, M. and Yanagi, T., 1970. Geochronology of some metamorphic rocks in Japan. *Eclogae Geol. Helvetiae,* 63: 371-388.

Yamazaki, T., Tsukahara, H. and Kumazawa, M., 1971. Fabric analysis of chert by X-ray recrystallized under the condition of high temperature, high pressure and non-hydrostatic state and application for metamorphic rocks. *Regime of lectures of scientific party of 5 society of Earth Science,* 385 (in Japanese).

Yao, A., 1975. Transition from the Honshu geosynoline to the Shimanto geosyncline in Problems on geosyncline in Japan. *Ass. Geol. Collab. in Japan, Monograph* 19: 131-141 (in Japanese with English abstract).

Zen, E. an, 1966. Construction of pressure-temperature diagrams for multicomponent systems after the method of Schreinemakers —— a geometric approach. *U.S. Geol. Survey Bull.,* 1225: 56pp.

(Received on May 28, 1977)